

**DEBRIS FLOW RUNOUT SIMULATION BASED ON  
EMPIRICAL AND CONTINUUM MODELLING APPROACHES**

by

**© ARIJIT BISWAS ARGHYA**

A thesis submitted to the

School of Graduate Studies

in partial fulfillment of the requirements for the degree of

**Master of Engineering (Civil)**

**Faculty of Engineering and Applied Science**

Memorial University of Newfoundland

**February 2024**

St. John's

Newfoundland and Labrador

Canada

## ABSTRACT

Debris flow is an extremely rapid flow type of landslide that consists of a mixture of materials, including soil, mud, rock, and water, which flows down a slope. A debris flow might be initiated due to rapid rainfall, logging, snowmelt, or sudden changes in the landscape. It has a relatively higher potential to cause loss of lives and damage to the infrastructure due to its higher velocity, huge impact force, and longer runout. Therefore, predicting the extent and impacts of debris flow is important. Several computer programs are available for simulating debris flows. These programs have been developed based on some simplified models due to the challenges of encompassing the complexities of the mechanisms of such a large event. This study uses three simulation tools—DebrisFlow Predictor, Flow-R, and RAMMS—to simulate actual debris flow events at three different sites. Each site is characterized by unique features. (e.g., channelized/unchannelized, granular/muddy flow, topography, soil type, etc.). The underlying features (e.g., displacement of debris) of each program are also different. By comparing the simulation results with satellite images, it is shown that all three numerical programs can simulate the debris flows if appropriate model parameters are selected. The erosion of the channel bed during downslope displacement of debris can significantly affect simulation results. RAMMS has the capability of simulating the erosion effects if the erosion properties and erosion zone are defined properly. Defining the erosion zone without having post-event data is challenging. Therefore, the authors suggest using DebrisFlow Predictor, which can be used to identify the zones of erosion and deposition based on statistical approaches. Flow-R can be advantageous for preliminary assessments of runout extent over a large area which is based on fewer input parameters and limited information about the initiation of debris flow.

***This Thesis is dedicated to my parents***

For their unconditional love, endless support, and encouragement

## **ACKNOWLEDGMENTS**

First, I would like to express my sincere gratitude and appreciation to my thesis supervisors, Dr. Bipul Hawlader, Dr. Richard Guthrie, and Dr. Joseph Daraio, for their invaluable guidance, advice, and support throughout this journey. Their supervision, mentorship, and encouragement have helped me to shape my research. I would also like to thank Dr. Ripon Karmaker, Graham Knibbs, Dr. Thad Wasklewicz, and Dr. Rajib Dey for their valuable advice, suggestions, and time that accelerated the progress of my research.

I gratefully acknowledge the financial support provided by the School of Graduate Studies of Memorial University of Newfoundland, Natural Sciences and Engineering Research Council of Canada (NSERC), and Equinor Research Chair. I would also like to thank Stantec, WSL Institute for Snow and Avalanche Research SLF, Risk Analysis group of the Institute of Earth Science of the University of Lausanne for providing DebrisFlow Predictor, RAAMS, and Flow-R software, respectively, for conducting this research. I would also like to thank Ankan Mahajan, Sudipta Bhowmick, Piash Saha, Pritam Kundu, Shishir Amit, and my other colleagues in our research group, with whom I spent some memorable years in my life.

Lastly, I would like to express my deepest gratitude to my parents, sister, and family members for their unwavering support and encouragement throughout my academic journey. Their sacrifices and tireless efforts have made it possible for me to pursue this Master's degree.

## TABLE OF CONTENTS

<b>ABSTRACT</b> .....	<b>ii</b>
<b>ACKNOWLEDGMENTS</b> .....	<b>iv</b>
<b>LIST OF FIGURES</b> .....	<b>viii</b>
<b>LIST OF TABLES</b> .....	<b>x</b>
<b>Chapter 1: Introduction</b> .....	<b>1</b>
1.1 Background.....	1
1.2 Rationale.....	4
1.3 Objectives.....	5
1.4 Outline of the thesis.....	5
<b>Chapter 2: Literature Review</b> .....	<b>7</b>
2.1 General.....	7
2.2 Constituents and Forms of Debris Flow.....	7
2.3 Debris Flow Hazard Assessment.....	9
2.4 Debris Flow Modelling.....	10
2.4.1 Empirical Modelling.....	12
2.4.2 Physical Modelling.....	13
2.4.3 Dynamic Modelling.....	13
2.5 Simulation Tools.....	16

2.5.1 DebrisFlow Predictor .....	17
2.5.2 RAMMS.....	20
2.5.3 Flow-R .....	29
2.5.3.1 Source Area Identification .....	29
2.5.3.2 Assessment of Propagation.....	30
2.6 Summary .....	32
<b>Chapter 3: A Comparative Study of Three Computer Programs for Debris Flow Runout Simulation.....</b>	<b>34</b>
3.1 Abstract.....	34
3.2 Introduction.....	35
3.3 Study Areas.....	38
3.3.1 Site 1: Highway 7, Hope-Agassiz.....	39
3.3.2 Site 2: Klanawa Watershed.....	40
3.3.2 Site 3: Solalex-Anzeindaz.....	43
3.4 Simulation Tools.....	45
3.4.1 DebrisFlow Predictor .....	45
3.4.2 RAMMS.....	49
3.4.2.1 Erosion Module (RAMMS).....	51
3.4.3 Flow-R .....	53
3.5 Results.....	56

3.5.1 Site 1: Highway 7, Hope-Agassiz.....	56
3.5.1.1 Effects of erosion .....	58
3.5.2 Site 2: Klanawa Watershed.....	61
3.5.3 Site 3: Solalex-Anzeindaz.....	62
3.6 Conclusions.....	71
<b>Chapter 4: Conclusions and Future Recommendations .....</b>	<b>73</b>
4.1 Conclusions.....	73
4.2 Future Recommendations .....	74
<b>REFERENCES.....</b>	<b>76</b>
<b>Appendix I: A comparison of two runout programs for debris flow assessment at the Solalex-Anzeindaz region of Switzerland.....</b>	<b>97</b>
<b>Appendix II: Simulation of some debris flows in Klanawa watershed in Vancouver, British Columbia.....</b>	<b>106</b>
<b>Appendix III .....</b>	<b>113</b>

## LIST OF FIGURES

<b>Fig. 1.1.</b> A diagram representing a fully developed debris flow surge (Hungr 2001).....	2
<b>Fig. 1.2.</b> Range of velocities for different flow-type landslides (Hungr 2001) .....	4
<b>Fig. 2.1.</b> Type debris flow: (a) hillslope debris flow; (b) channelized debris flow (Nettleton 2005) .....	9
<b>Fig. 2.2.</b> Methods of predicting runout extent (after Chen and Lee 2004) .....	11
<b>Fig. 2.3.</b> Runout analysis methods (after McDougall 2017).....	11
<b>Fig. 2.4.</b> Flow diagram of agent's lifetime (after Guthrie 2007).....	19
<b>Fig. 3.1.</b> Debris flow at Highway 7 between Hope to Agassiz, BC, Canada (Site 1): (a) entire view, (b) view along the highway, (c) view at the toe; Source: Google Earth and BC Ministry of Transport & Infrastructure .....	41
<b>Fig. 3.2.</b> An unchannelized (AA') and a channelized (BB') flow at Site 2 (Inset map, Guthrie et al. 2008) .....	42
<b>Fig. 3.4.</b> Simulated runout at Site 1: (a) DebrisFlow Predictor; (b) Flow-R; and (c) RAMMS flood height without erosion; (d) RAMMS final deposition height without erosion.....	63
<b>Fig. 3.5.</b> Simulated scour and deposition depths at Site 1 using DebrisFlow Predictor.....	64
<b>Fig. 3.6.</b> Effects of erosion in RAMMS: (a) flood height; (b) final deposition depth; (c) variation of flow height with time at three locations shown in Figs. 3.4(d) and 3.6(b).....	65
<b>Fig. 3.7.</b> Ground elevation and deposition height near the toe: (a) ground elevation before the event; (b) debris thickness obtained from DebrisFlow Predictor; (c) final deposition height from RAMMS with erosion module.....	66
<b>Fig. 3.8.</b> Thickness of debris in polygon X.....	67
<b>Fig. 3.9.</b> Maximum velocity and maximum pressure map at Site 1 generated by RAMMS.....	67

**Fig. 3.10.** Channelized and unchannelized debris flow at Site 2: (a) DebrisFlow Predictor; (b) Flow-R; (c) RAMMS without erosion..... 69

**Fig. 3.11.** Simulation results for Site 3: (a) DebrisFlow Predictor; (b) Flow-R; (c) RAMMS without erosion..... 70

(e.g., flow height), DebrisFlow Predictor and RAMMS could be used in conjunction with Flow-R..... 71

## LIST OF TABLES

<b>Table 1.1.</b> Classification of flow-type landslides (Hungar 2001) .....	3
<b>Table 2.1.</b> Typical values of basic physical properties of debris flow mixtures (Iverson 1997) ...	8
<b>Table 2.2.</b> Available numerical models to simulate debris flow (revised from McDougall 2017) .....	15
<b>Table 2.3.</b> Overview of previous debris flow modelling using RAMMS (modified from Dash et al. 2019) .....	21
<b>Table 2.4.</b> Review of debris flow modelling using RAMMS .....	26
<b>Table 2.5.</b> Best calibrated values for $\mu$ and $\xi$ as obtained from previous studies on debris flows (revised from Mikoš and Bezak 2021).....	27
<b>Table 2.6.</b> Studies that incorporated Flow-R.....	31
<b>Table 3.1.</b> Key information about the sites considered in this study .....	44
<b>Table 3.2.</b> Parameters used in DebrisFlow Predictor .....	49
<b>Table 3.3.</b> Best fit material parameters used in RAMMS .....	51
<b>Table 3.4.</b> Erosion parameters used in RAMMS for Site 1.....	52
<b>Table 3.5.</b> Algorithms and parameters used in Flow-R.....	55

# Chapter 1: Introduction

## 1.1 Background

Debris flow could be one of the most dangerous and disastrous components of a landslide. Many studies focused on the analysis of slope failure and developed analytical and numerical modelling techniques using limit equilibrium (LE) and finite element (FE) methods. These types of analyses give the factor of safety of the slope and the deformation if FE method is used. Global failure is expected if the factor of safety is less than one. After failure, the failed soil mass might travel a long distance. Attempts have also been taken to model the downslope movement of soil mass using different numerical modelling techniques, including the Eulerian-based finite element method (Dey et al. 2015), computational fluid dynamics approach (Clark 2018), and material point method (Abe and Konagai 2016). An appropriate soil model is required in these types of numerical modelling, which is difficult to define for debris that contains a wide range of materials, and the analyses are limited to relatively slow-moving failed soil mass. Most of the analyses were conducted for two-dimensional plane strain conditions or used a thin section in the out-of-plane direction because these large-deformation analyses are computationally very expensive. The debris changes direction during downslope movement at high velocity over a three-dimensional terrain, and therefore the above-mentioned advanced numerical modelling techniques in two-dimensional conditions cannot be used for debris flow simulation. The debris is composed of soil, mud, rock, and water. While flowing, the debris could create significantly large shear stress on the basal layer (Costa and Fleisher 1984). This shear stress can erode some materials from the basal layer, and the eroded soil enters into the debris. This implies that the debris contains materials not only from the

initiation zone but also those materials that enter during downslope movement and form a complex mixture of different types of materials. Figure 1.1 shows schematically some of the components of the debris flow that contains a wide range of materials, including slurry to boulders.

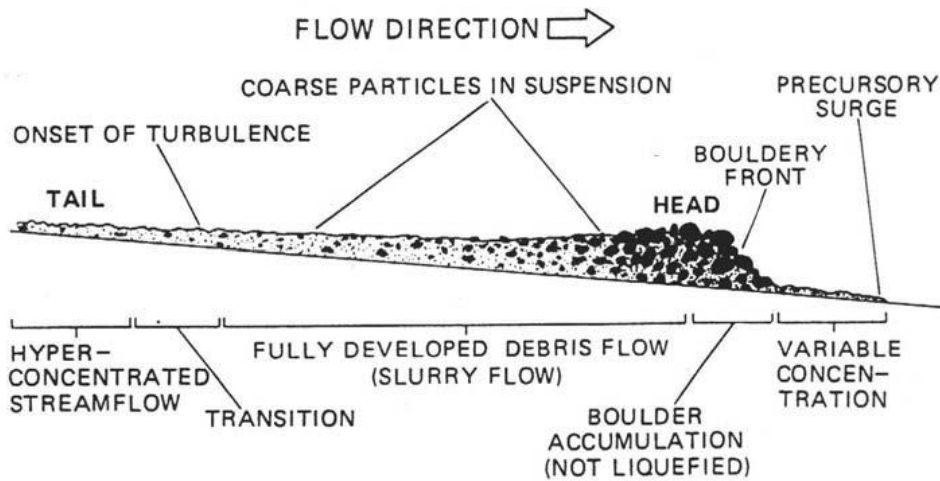


**Fig. 1.1.** A diagram representing a fully developed debris flow surge (Hungar 2001)

Debris flow falls under the category of flow-type landslides (Varnes 1978). Table 1.1 shows the materials involved and the conditions required for typical debris flow (Hungar 2001). Extremely rapid flow (velocity 1–20 m/s) occurs in debris flow (Table. 1.1 and Fig. 1.2).

Generally, the debris flow is associated with high velocities, long runout distances, larger inundation areas, and high impact forces on infrastructure (Naqvi 2020). It could be initiated by many triggering factors, including heavy rainfall and wildfire, and could affect the infrastructure, communities, resources, lives, and the environment at a considerable distance from the source. Therefore, accurate prediction of runout extent and other intensity parameters (e.g., velocity, impact pressure, and depth) can help assess the hazard in the potentially affected areas. However,

it is a very challenging task because of several reasons: (i) significant uncertainties in modelling material behaviour, as it contains a wide range of particles of varying size (clay to boulders), (ii) estimating initiation zone, (iii) estimating basal erosion, and (iv) computational costs of numerical simulations. Therefore, most of the available approaches simplified the problem using some assumptions and then conducted numerical analysis.

**Table 1.1.** Classification of flow-type landslides (Hungar 2001)

Material	Water Content <sup>1</sup>	Special Condition	Velocity	Name
Silt, Sand, Gravel, Debris (talus)	dry, moist or saturated	- no excess pore-pressure, - limited volume	various	Non-liquefied sand (silt, gravel, debris) flow
Silt, Sand, Debris, Weak rock <sup>2</sup>	saturated at rupture surface content	- liquefiable material <sup>3</sup> , - constant water	Ex. Rapid	Sand (silt, debris, rock) flow slide
Sensitive clay	at or above liquid limit	- liquefaction <i>in situ</i> , <sup>3</sup> - constant water content <sup>4</sup>	Ex. Rapid	Clay flow slide
Peat	saturated	- excess pore-pressure	Slow to very rapid	Peat flow
Clay or Earth	near plastic limit	- slow movements, - plug flow (sliding)	< Rapid	Earth flow
Debris	saturated	- established channel <sup>5</sup> , - increased water content <sup>4</sup>	Ex. Rapid	Debris flow
Mud	at or above liquid limit	- fine-grained debris flow	> Very rapid	Mud flow
Debris	free water present	- flood <sup>6</sup>	Ex. Rapid	Debris flood
Debris	partly or fully saturated	- no established channel <sup>5</sup> , - relatively shallow, steep source	Ex. Rapid	Debris avalanche
Fragmented Rock	various, mainly dry	- intact rock at source, - large volume <sup>7</sup>	Ex. Rapid	Rock avalanche

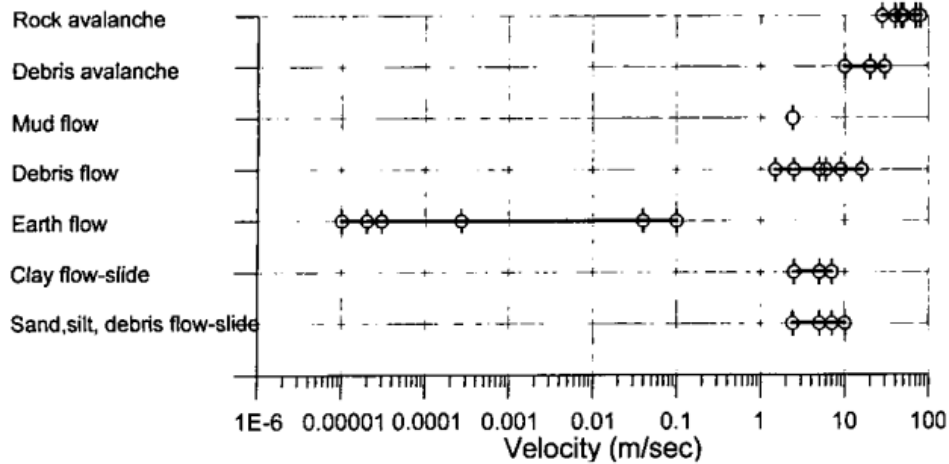


**Fig. 1.2.** Range of velocities for different flow-type landslides (Hungr 2001)

## 1.2 Rationale

Several numerical techniques have been developed to understand the mechanisms and extent of debris flow. All these techniques have been developed by simplifying the problems from different angles, and varying algorithms are used to calculate the flow. The analysis also requires a varying range of input parameters. Also, the numerical simulations using different programs give different outputs. For example, some programs give susceptibility maps while others provide the values for impact assessment parameters (e.g., flow depth and pressure). The available computer programs have been developed using different mathematical frameworks. For example, some used empirical/statistical approaches to calculate the flow path, while others used mechanical models (yet simplified) and implemented in more intensive numerical programs. Finally, the performance of these programs depends on site conditions, including topography, soil conditions, existing channels, and frequency of events. Therefore, site-specific parameterization and calibration of the model are needed to understand the characteristics of a debris flow. The above-mentioned simplified approaches are computationally efficient. However, the main challenge is the

calibration of the model using field data from different sites. Such calibration would increase the confidence in using the model results and identify appropriate soil parameters.

### **1.3 Objectives**

The focus of the present study is to assess the runout of debris flows in three different geological settings. Three computer programs are used to simulate some of the reported debris flow at these three sites. The objectives of the research include:

- Examine selected debris flows at these sites and evaluate the characteristics of the flow (e.g., initiation zones, spreading, and runout);
- Simulate those debris flows using the computer programs, compare with field observation, and identify the set of parameters that model best the field observation (parameterization);
- Compare the simulation results with the three programs and identify the suitability of the programs to simulate the debris at these sites and
- Examine whether the simulation results obtained from one program could be used in conjunction with the results of another program for a better evaluation of the process.

### **1.4 Outline of the thesis**

The thesis consists of four chapters and two appendixes.

**Chapter 1** highlights the background, rationale, and objectives of the study.

**Chapter 2** contains a literature review. As the thesis is presented in manuscript format, sufficient literature review is provided in the manuscript in Chapter 3 and conference papers (Appendixes I and II). However, an additional literature review is presented in this chapter.

**Chapter 3** is written in the format of a manuscript. This chapter presents a comparative study of three debris flow computer programs. In this study, debris flows at three different sites were

modeled using empirical and numerical approaches. A comparison of the simulation results and applicability of the three programs is also discussed. A part of the work presented in Chapter 3 has been published earlier as two conference papers (Arghya et al. 2022a, Appendix-I; Arghya et al. 2022b, Appendix-II).

**Chapter 4** provides some general conclusions and limitations of the present study. The recommendations for future research are also discussed in this chapter.

## **Chapter 2: Literature Review**

### **2.1 General**

Debris flow initiates as a consequence of slope failure. Once initiated, the debris might travel over a large distance in the downslope direction. It is difficult to prevent the event itself because they initiate from upslope steep terrain that is far from the affected areas in the downslope direction, which might even be non-accessible. Therefore, the best approach to counteract or avoid the impact of debris flow is through modelling the landslide runout and better predicting relevant intensity parameters, such as area of spreading, flow depth, flow velocity, and impact pressure (McDougall 2017; Teetzmann 2020). Several approaches have been developed to predict debris flow impact. Among them, numerical tools provide more information. Three numerical tools are used in the present study. Therefore, the literature review presented in this chapter primarily concentrated on numerical techniques. However, some additional information (e.g., debris behaviour, classification, and other methods of prediction) is also provided briefly for completeness.

### **2.2 Constituents and Forms of Debris Flow**

In general, debris contains a mixture of coarse-grained (e.g., rock, gravel, and sand) and fine-grained materials (i.e., silt and clay-sized particles) in water (Costa 1984; Iverson 1997; Takahashi). These heterogeneous materials have been described in different ways. For example, Takahashi (2007) considered the debris as a mix of mud, water, and debris, where the particles are dispersed in a slurry. Davies (1990) described debris as a heterogeneous fluid that is formed by water and solids without distinct separation of the phases. In many cases, debris flows very rapidly to extremely rapidly (Hung et al. 2001). It is very difficult to measure the properties of the debris

as it contains a mixture of a wide range of materials (from fines to boulders). Table 2.1 shows some basic properties of the materials in debris flow (Iverson 1997).

**Table 2.1.** Typical values of basic physical properties of debris flow mixtures (Iverson 1997)

<i>Property and Unit</i>	<i>Symbol</i>	<i>Typical Values</i>
<i>Solid Grain Properties</i>		
Mass density, kg/m <sup>3</sup>	$\rho_s$	2500–3000
Mean diameter, m	$\delta$	10 <sup>-5</sup> –10
Friction angle, deg	$\phi_g$	25–45
Restitution coefficient	$e$	0.1–0.5
<i>Pore Fluid Properties</i>		
Mass density, kg/m <sup>3</sup>	$\rho_f$	1000–1200
Viscosity, Pa s	$\mu$	0.001–0.1
<i>Mixture Properties</i>		
Solid volume fraction	$v_s$	0.4–0.8
Fluid volume fraction	$v_f$	0.2–0.6
Hydraulic permeability, m <sup>2</sup>	$k$	10 <sup>-13</sup> –10 <sup>-9</sup>
Hydraulic conductivity, m/s	$K$	10 <sup>-7</sup> –10 <sup>-2</sup>
Compressive stiffness, Pa	$E$	10 <sup>3</sup> –10 <sup>5</sup>
Friction angle, deg	$\phi$	25–45

As the debris is a two-phase material (solid and fluid), the interaction between these two phases plays a major role. Although challenging, several attempts have been made to understand the characteristics of the mixture’s interaction. For simplicity, in most of the mechanics-based approaches, the behaviour of debris has been idealized as non-Newtonian fluid. The idealized fluid properties depend on fluid and solid contents and their interaction, which is related to speeds and shear rates (Iverson 1997). Therefore, numerical simulations have been performed for a wide range of properties (Mikoš and Bezak 2021).

According to Nettleton (2005), there are two forms of debris flows: (i) hillslope/open slope (i.e., unchannelized) flow and (ii) channelized debris flow (Fig. 2.1). Hillslope forms their own path while flowing down the slope, just like tracks or sheets, before depositing the entrained material

at a lower slope gradient. In contrast, in channelized flow, the debris follows existing gullies, valleys, depressions, and hollows. In the present study, numerical simulations are performed for both types of debris flow.

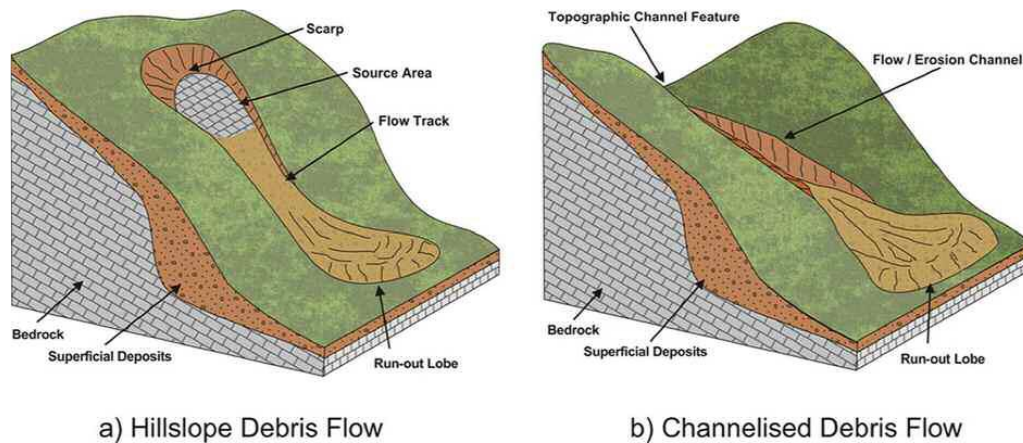


**Fig. 2.1.** Type debris flow: (a) hillslope debris flow; (b) channelized debris flow (Nettleton 2005)

### 2.3 Debris Flow Hazard Assessment

Rickenmann (1999) stated that assessing debris flow hazards in a specific catchment involves two steps: determining the likelihood or probability of debris flows occurring on a torrent and quantitatively estimating important parameters for hazard assessment. Both are equally important. The former provides overall information which could be used for estimating the likelihood of occurrence such that appropriate measures could be taken (e.g., avoiding new development of critical structures in an area of major debris flow). The latter one is used for detailed calculations of debris flow impact.

The likelihood or probability of debris flow occurrence can be assessed either by measuring the physical characteristics of the catchment or by statistical analysis. Besides, it is possible to identify

the pattern of debris flow frequency and debris flow volume of a specific catchment if we have information on the historical debris flow events. According to Zimmermann et al. (1997), this pattern is dependent on the sediment availability and lithology of the catchment.

For quantitative debris flow hazard assessment, empirical relationships for debris flow volume, peak discharge, front velocity, flow cross-section, total travel distance, and runout distance on the fan may be used to determine the endangered area. These parameters could also be determined using numerical simulation programs.

## **2.4 Debris Flow Modelling**

Several approaches have been proposed to model the debris flow. The available methods have also been classified in different ways. Chen and Lee (2004) divided the available approaches into the following three major categories: empirical, physical, and dynamic modelling (Fig. 2.2). Empirical analysis and physical modelling were the only options in the early days. However, with the advancement of computational power in the last several decades, a number of numerical modelling tools have been developed which can simulate debris flow phenomena more accurately and provide additional information for hazard analysis.

McDougall (2017) classified the available runout analysis methods into two broad categories: empirical-statistical and analytical methods (Fig. 2.3). The red dashed line indicates a subcategory of hybrid “semi-empirical” numerical models that require parameter calibration. The available analytical methods have been divided into several sub-groups (Fig. 2.3).

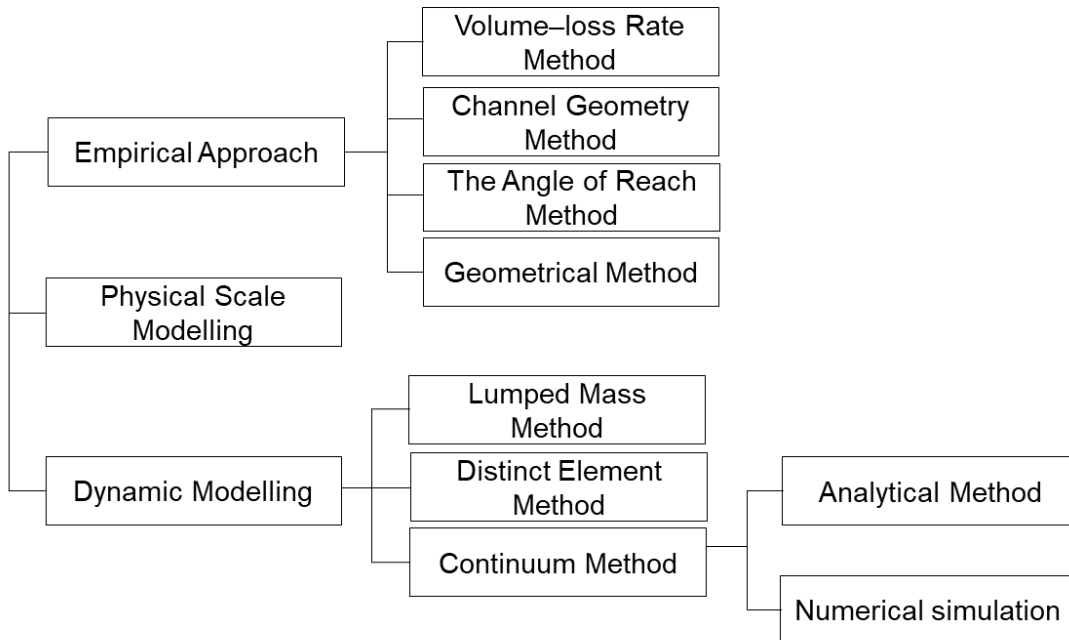


**Fig. 2.2.** Methods of predicting runout extent (after Chen and Lee 2004)

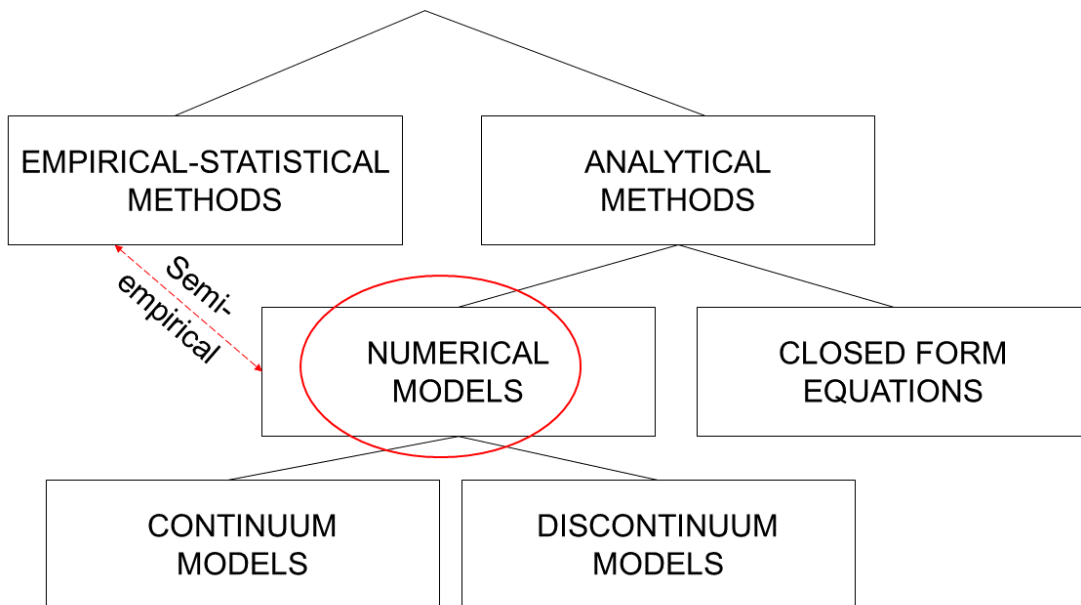


**Fig. 2.3.** Runout analysis methods (after McDougall 2017)

### ***2.4.1 Empirical Modelling***

Empirical relationships are simpler and can be used to estimate the parameters, including the volume, peak discharge, mean flow velocity, total travel, and runout distances of a debris flow. Rickenmaan (1999) developed some empirical relationships based on a large amount of historical data. Empirical relationships are generally site-specific and may not be applicable to new locations unless calibrated. Also, these approaches do not consider the material behaviour (rheology), which may not be the same at different sites. Moreover, it does not provide some key information (e.g., flow depth, flood height, impact pressure) which is required for engineering design. Despite their limitations, empirical models play a crucial role in hazard assessment and are widely used (Hürlimann 2008).

Some well-known empirical approaches for debris flow modelling are: (i) Angle of Reach Method (Corominas 1996), (ii) Volume-Change Rate Method (Fannin and Wise 2001), (iii) Channel Geometry Method (Benda and Cundy 1990), and (iv) Geometrical Method (Lucia 1981). Guthrie (2009) divided the empirical models into two categories. The first category of models was developed using the initial volume of the debris (Corominas 1996; Rickenmann 1999). However, several researchers have observed that debris flow volume depends not only on the initial volumes but also on the materials entrained during flow (Benda and Cundy 1990; Guthrie et al. 2008). This entrained volume along the path could surpass the initial volume (Benda and Cundy 1990). Therefore, empirical relationships based on the initial volume only might be questionable (Hungry et al. 2008). Therefore, the second category of models also considered the entrained volume components and is known as the “sediment balance approach” (Benda and Cundy 1990; Fannin and Wise 2001). In this approach, debris starts to flow with a known volume of debris. It also evaluates the change in volume based on morphological and geometrical variables along with the

incoming flow volume. The process continues until the volume or mass of the event reaches zero. While the second one is a better approach, it requires detailed channel information.

#### ***2.4.2 Physical Modelling***

This approach involves physical simulation of debris flow in laboratory settings, such as flume experiments or reduced scale model tests, to study the behaviours and dynamics of debris flow. The goal of this type of modelling is to improve the understanding of the complex process of debris flow. The data from the physical models can be used to improve the accuracy of numerical modelling for predicting and mitigating hazards (Turnbull 2015). However, it is an intricate task to recreate the natural debris flow in a laboratory setup as significant uncertainties are involved in debris flow in the field where the debris displaces over a large distance. A scaled-down physical model may behave differently compared to that in the field. Besides, complex geological formations, sediment properties, and vegetation effects may not be fully captured in physical models. Therefore, the results obtained from physical models can limit the direct applicability to real-world situations.

#### ***2.4.3 Dynamic Modelling***

Dynamic modelling of debris flows involves simulating the movement of the debris flow over time and predicting its behaviour as it moves downslope. It is mainly subdivided into three categories: lumped mass model, distinct element model, and continuum model.

Lumped mass models, also known as discontinuum models, simplify the movement of a flow by representing it as a single point (Perla et al.1980; Hutchinson 1986). However, this approach does not account for internal deformation (Naqvi 2020). While these models can provide a basic approximation to the movements of the center of gravity of the sliding mass, they cannot simulate

the motion of the flow front (Hungri 1995). The flow front is the most important part of runout analysis as it is the most dynamic and rapidly changing part of the flow. Although simplicity is an advantage of the lumped mass model, this approach cannot capture complex failure patterns or internal deformation of the sliding mass.

Distinct Element Model (DEM) is a numerical technique to investigate the mechanical characteristics of granular flows. In this method, the interaction among the flow particles is investigated using a collection of regular-shaped particles (e.g., discs and spheres). Equilibrium states are achieved when the internal forces within the flow particles are balanced. This method is effective in comprehending segregation and deposition in granular flows. However, this approach of modelling applies to micro-scale modelling, as the simulations are computationally expensive. While modelling debris flows, it is important to capture the macro-scale behaviours quantitatively. The continuum method generally incorporates mass and momentum conservation equations to describe the dynamic behaviour of debris flows. It can be used with an appropriate rheological model, and the required parameters of it can be determined either by laboratory experiments or through back analysis of historical events. This type of approach provides detailed information for landslide hazard assessment. The continuum method is subdivided into two categories: analytical solution and numerical simulation. The analytical solution relies on several simplifying assumptions. These assumptions are made to make the mathematical analysis more tractable and to simplify the complexities of the real-world behaviour of debris flows. As a result, the analytical solution represents an idealized or simplified version of the actual behaviour observed in the field or in physical models. On the other hand, numerical simulation models are based on Eulerian or Lagrangian reference frames. In numerical simulation, friction parameters are used to explain the

roughness and turbulence of debris flow (Rickenmann 1999). Therefore, it is essential to choose the proper rheology and friction parameters, which require careful calibration.

A number of numerical programs have been developed to simulate runout. Some notable programs are (i) Flow-R, where the friction loss function can be calculated by the angle of reach method proposed by Corominas (1996) (Horton et al. 2013); (ii) DebrisFlow Predictor (Guthrie and Befus 2021), which incorporates a mass balance approach similar to the work of Fannin and Wise (2001). Some other prominent numerical programs are DAN (Hungr 1995) and DAN3D (Hungr and McDougall 2009), FLO-2D (O'Brien et al. 1993), r.avalow (Mergili et al. 2017), TITAN2D (Pitman 2003), RAMMS (Christen et al. 2010), which are based on rheological models. Table 2.2 shows a list of numerical models available for debris flow simulation.

**Table 2.2.** Available numerical models to simulate debris flow (revised from McDougall 2017)

<b>Model</b>	<b>Type</b>	<b>Selected References</b>
3dDMM	3D, Continuum	Kwan and Sun (2007)
DAN	2D, Continuum	Hungr (1995)
DAN3D	3D, Continuum	McDougall (2006)
FLATModel	3D, Continuum	Medina et al. (2008)
FLO-2D	3D, Continuum	FLO-2 D Software Inc. (2007)
Flow-R	3D, Spreading Algorithm	Horton et al. (2013)
GeoFlow-SPH	3D, Continuum	Pastor et al. (2009b)
D-Claw	3D, Continuum	Iverson and George (2014)
MADFLOW	3D, Continuum	Chen and Lee (2000)

**Table 2.2.** (Continued)

<b>Model</b>	<b>Type</b>	<b>Selected References</b>
MassMov2D	3D, continuum	Beguiria et al. (2009)
PFC	3D, Discontinuum	Poisel and Preh (2008)
RAMMS	3D, Continuum	Christen et al. (2010)
RASH3D	3D, Continuum	Pirulli (2005)
r.avalanche	3D, Continuum	Mergili et al. (2012)
r.avaflow	3D, Continuum	Mergili et al. (2017)
Sassa-Wang	3D, Continuum	Wang and Sassa (2002)
SCIDDICA S3-hex	3D, Cellular Automata	D'Ambrosio et al. (2003)
SHALTOP-2D	3D, Continuum	Mangeny-Castelnau et al. (2003)
TITAN2D	3D, Continuum	Pitman et al. (2003)
TOCHNOG	3D, Continuum	Roddeman (2002)
VolcFlow	3D, Continuum	Kelfoun and Druitt (2005)
Wang	2D, Continuum	Wang (2008)

## 2.5 Simulation Tools

In this study, the following three computer programs are used to simulate debris flow: (i) DebrisFlow Predictor, (ii) RAMMS, and (iii) Flow-R. The key features of these programs have been provided in Chapter 3. However, some additional details are provided in the following sections. All three programs solve the process numerically; however, the modelling of the flow of material from one cell to another is different. DebrisFlow Predictor and Flow-R were developed using some empirical models/algorithms, while RAMMS is based on three-dimensional continuum modelling that simulates the flow process with time increment.

### ***2.5.1 DebrisFlow Predictor***

DebrisFlow Predictor, formerly known as LABS (Landslides: Agent Based Simulation), is a computer program for simulating landslide runout, scour, and deposition. It was developed by Guthrie and Befus (2021) and is based on a cellular automata approach. In the cellular automata model for debris flow, the topographic surface is divided into a grid of small cells, similar to pixels on an image. Each cell in the grid represents a small portion of the terrain and has its own state, which can either be empty or filled with debris. The simulation starts with an initial configuration where some cells are filled with debris, and others are empty. As time progresses, the model updates the states of these cells based on predefined rules that govern how debris interacts with their neighbouring cells. These rules can be quite simple or highly complex, depending on the specific characteristics of the debris flow being simulated. For instance, they might take into account factors such as slope, soil properties, etc. The rules could define how debris propagates, erodes, deposits, and accumulates in certain areas. Details about the concept of CA and its application in debris flow modelling can be found in Han et al. (2017). In DebrisFlow Predictor, debris flow consists of a set of agents or autonomous subroutines that each occupy a single cell on the grid at a given time step and represent a variable mass of material moving from cell to cell down a slope. Agents are spawned and terminated as necessary to simulate landslide spread and decay according to the set of rules. Agents' lifetime is illustrated in Fig. 2.4. Scour and deposition at each time step depend on the topography and the probabilistic rules assigned to the agents. Guthrie and Befus (2021) defined independent probability distribution rules for 12 slope classes (bins). Further details of this program can be found in Guthrie and Befus (2021).

DebrisFlow Predictor has been used in previous studies for runout modelling. Using DebrisFlow Predictor, probability maps were developed to assess the hazard components of risk to the residents

of the North Shore of Cowichan Lake in Vancouver Island, British Columbia, due to debris flow and debris avalanche (Stantec 2021). Wasklewicz et al. (2022) evaluated the performance of an agent-based probabilistic model (DebrisFlow Predictor) by simulating the Black Hollow debris flow that occurred in Larimer County, Colorado, USA. Using DebrisFlow Predictor, Wasklewicz et al. (2023) simulated debris flow at three active wildfire locations in Colorado. They also compared the performance of DebrisFlow Predictor with the most utilized tool for assessment of postfire debris flow hazards in the USA (USGS Model) and showed that USGS calculated a higher volume of debris and thereby represented more conservative measures. Knibbs et al. (2023) showed that the agent-based model (e.g., DebrisFlow Predictor) can be used in conjunction with geographic information software (GIS) for quantification of geohazards over a large area (i.e., on a regional scale) to assess the impact on linear infrastructure, such as rail, highways, and pipelines. Grasso et al. (2022) identified vulnerable zones using DebrisFlow Predictor in North Ogden, Utah, and Laramie County, Colorado, USA, that could be impacted by debris flow. North Ogden already experienced a large debris flow known as the “1991 Cameron Cove debris flow”. As the urban area extends towards the Cameron Cove subdivision, and if a similar type of event takes place, it will be impacted by debris flow. In the case of Laramie County, which recently experienced a wildfire in December 2022. As the vegetation is burnt due to the wildfire, it is more exposed to rainfall, which might result in debris flow. Their prediction model indicates that 44 homes will be impacted by the debris flows, and the probability of being impacted is higher for the houses located near the apex and middle part of the alluvial fans.

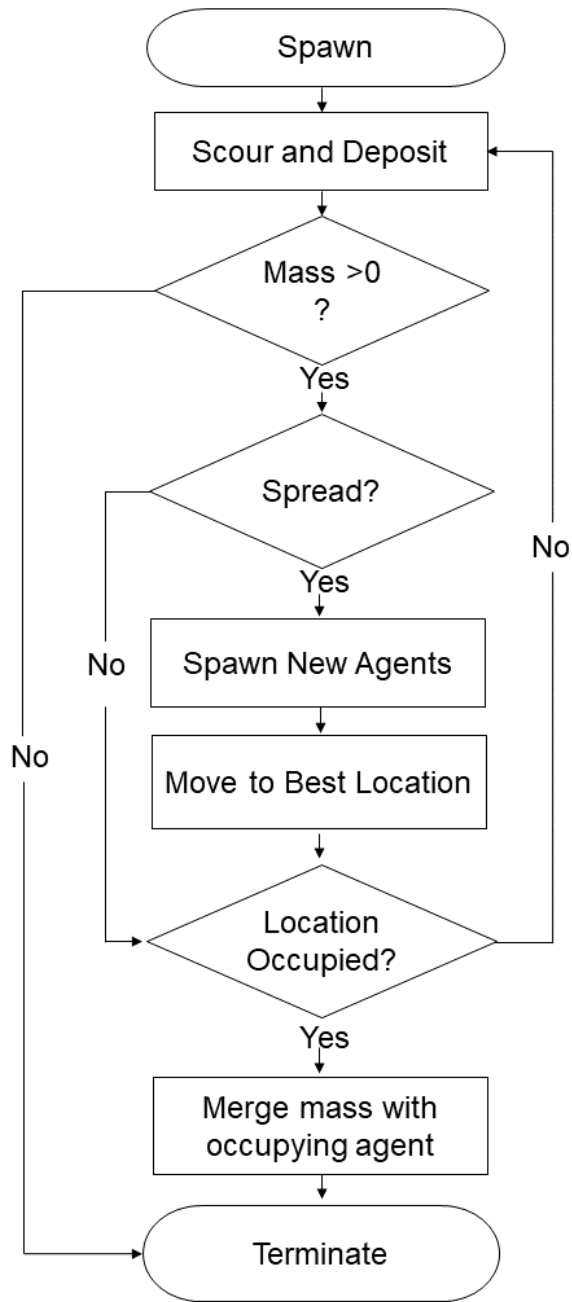


**Fig. 2.4.** Flow diagram of agent's lifetime (after Guthrie 2007)

### **2.5.2 RAMMS**

RAMMS::DEBRISFLOW is one of the three components of Rapid mass movement system (RAMMS) software. This component has been developed to simulate fast-moving materials like debris. RAMMS has been developed using some fundamental properties of the debris. The downslope movement is governed by gravitational force, which is related to density. Generally, the debris contains a wide range of materials. Previous studies showed an assumed density of 2000 kg/m<sup>3</sup> would be a good estimate (Costa and Fleisher 1984; Iverson 1997; Iverson and Denlinger 1987).

The RAMMS was developed using 2-D depth-averaged shallow water equations. It incorporates the Voellmy-Salm fluid model to describe the rheology of the flowing debris (Christen et al. 2010; Frank et al. 2015, 2017; Abraham et al. 2020; Gardezi et al. 2021). The frictional behaviour of the flow is described by the velocity-independent dry-Coulomb friction coefficient ( $\mu$ ) and the velocity-dependent turbulent friction coefficient ( $\xi$ ). The program can calculate the flow path, flow velocities, flow heights, and impact pressures. Further details on mathematical formulations are available in Christen et al. (2010). Dash et al. (2021) provided a list of studies where successful simulations of debris flows and calibration of model parameters were done using RAMMS (Table 2.3). A brief summary of some additional studies using RAMMS are also provided in Table 2.4. Table 2.5 shows the ranges of  $\mu$  and  $\xi$  used to simulate different types of debris flows across the world.

**Table 2.3.** Overview of previous debris flow modelling using RAMMS (modified from Dash et al. 2019)

<b>Authors</b>	<b>Study Area</b>	<b>Flow Type and Methods</b>	<b>Major Findings</b>
Cesca and D'Agostino (2008)	Italy (Belluno)	Type: N/A Release Type: Block Model Calibration: Yes Sensitivity Analysis: No Model Validation: No Entrainment: No	Surface detention has a large influence on runout distances and maximum lateral dispersions.
Simoni et al. (2012)	Eastern Italian Alps	Type: N/A Release Type: Block Model Calibration: Yes Sensitivity Analysis: Yes Model Validation: No Entrainment: No	Flow velocity is influenced by both parameters but mostly by the turbulent coefficient, which affects the peak flow velocity along the diverse channel and the rate of deceleration that increases with $\xi$ .

**Table 2.3. (Continued)**

<b>Authors</b>	<b>Study Area</b>	<b>Flow Type and Methods</b>	<b>Major Findings</b>
Hussin et al. (2012)	Southern French Alps (Barcelonnette Basin)	Type: Channelized Release Type: Block Model Calibration: Yes Sensitivity Analysis: Yes Model Validation: No Entrainment: Yes	Runout distance is most sensitive to the friction coefficient ( $\mu$ ). Velocities of the flows were most sensitive to Voellmy turbulent coefficient ( $\xi$ ). Total deposition volume and debris flow heights were most sensitive to the RAMMS entrainment coefficient (K).
Klaus et al. (2015)	Austria	Type: N/A Release Type: Block Model Calibration: Yes Sensitivity Analysis: Yes Model Validation: No Entrainment: No	Friction parameter $\mu$ has a stronger influence on the runout distances of the simulated debris flows.

**Table 2.3. (Continued)**

<b>Authors</b>	<b>Study Area</b>	<b>Flow Type and Methods</b>	<b>Major Findings</b>
Schraml et al. (2015)	Austria	Type: N/A Release Type: Block Model Calibration: Yes Sensitivity Analysis: Yes Model Validation: Yes Entrainment: No	Deposition patterns showed a significant sensitivity to variation in $\mu$ and event volume.
Frank et al. (2017)	Switzerland (Bondasca and Meretschibach Catchment)	Type: N/A Release Type: Block Model Calibration: Yes Sensitivity Analysis: Yes Model Validation: No Entrainment: Yes	Model results can be quite sensitive to the volume of the initial block release in the model, which corresponds to the initial landslide volume.

**Table 2.3. (Continued)**

<b>Authors</b>	<b>Study Area</b>	<b>Flow Type and Methods</b>	<b>Major Findings</b>
Chattoraj et al. (2018)	India (Malin Landslide)	Type: Unchannelized Release type: Block Model Calibration: Yes Sensitivity Analysis: No Model Validation: No Entrainment: No	An increase in the friction coefficient $\mu$ causes a decrease in the runout distance due to an increase in the basal friction of the flow. Change in the value of $\xi$ did not affect the runout distance significantly.
Krušić et al. (2018)	Selanac	Type: N/A Release Type: Block Model Calibration: Yes Sensitivity Analysis: Yes Model Validation: No Entrainment: No	Calibration of frictional parameters is difficult to verify without good field observation.

**Table 2.3. (Continued)**

<b>Authors</b>	<b>Study Area</b>	<b>Flow Type and Methods</b>	<b>Major Findings</b>
Chattoraj et al. (2019)	India (Varunavat, Ukhimath, Kedarnath, Maithana Landslide)	Type: Channelized and Unchannelized Release type: Block Model Calibration: Yes Sensitivity Analysis: No Model Validation: No Entrainment: No	Shear strength parameters used for a numerical simulation model can be validated by laboratory instrumentation techniques.

**Table 2.4.** Review of debris flow modelling using RAMMS

<b>Authors</b>	<b>Remarks</b>
Abraham et al. (2020)	Back calculated the runout extent of Kurichermala debris flow in Kerala, India. Effects of soil type and shear strength parameters were investigated to understand the flow behaviour.
Huang et al. (2017)	Simulated possible runouts before and after the engineering treatment (installment of slide-resisting piles) for the Tazhiping landslide in Sichuan Province, China. They showed that after engineering treatment, the area of high-hazard zones could be reduced by two-thirds.
Bezak et al. (2019)	Selected an actual debris fan from Slovenia and an artificially created fan with a constant slope to see the impact of a random debris flow sequence on debris fan formation. They found that a random sequence of debris flow events has a minor effect on the debris fan formation after varying Voellmy's rheological parameters in a wide range.
Gardezi et al. (2021)	Back calculated Attabad landslide in Pakistan using two numerical programs named DAN3D and RAMMS::DF. Both programs provided similar runout extent and volume estimation (44.9 Mm <sup>3</sup> ) compared to the actual event (45 Mm <sup>3</sup> ).

**Table 2.5.** Best calibrated values for  $\mu$  and  $\xi$  as obtained from previous studies on debris flows  
(revised from Mikoš and Bezak 2021)

<b>Authors</b>	<b><math>\mu</math></b>	<b><math>\xi</math> ( m/s<sup>2</sup>)</b>
Cesca and D'Agostino (2008)	0.18–0.45	15–1000
Hauser (2011)	0.20	10
Hussin (2011)	0.06	500
Scheuner et al. (2011)	0.1–0.15	125–200
Berger et al. (2012)	0.07	400
Hussin et al. (2012)	0.06	500
Scheidl et al. (2013)	0.08–0.18	300–350
Schneider et al. (2014)	0.01–0.16	500
Frank et al. (2015)	0.05	1200
Schraml et al. (2015)	0.07–0.23	200–300
Fischer et al. (2016)	0.09–0.27	150–200
De Finis et al. (2017a)	0.11–0.12	500–600
De Finis et al. (2017b)	0.05–0.2	300–650
Frank et al. (2017)	0.3–0.6	200–400
Kang et al. (2017)	0.1–0.2	800–950
RAMMS (2017)	0.05–0.4	1–2000
Chung et al. (2018)	0.42	2000
De Finis et al. (2018)	0.05–0.2	200–600
Frey et al. (2018)	0.04–0.08	500

**Table 2.5.** (Continued)

<b>Authors</b>	<b><math>\mu</math></b>	<b><math>\xi</math> ( m/s<sup>2</sup>)</b>
Anacona et al. (2018)	0.001	500
Kaltak (2018)	0.075	200
Krušić et al. (2018), (2019)	0.05–0.11	500
Tsao et al. (2018)	0.225	150
Bezak et al. (2019)	0.1–0.5	100–1500
Dietrich and Krautblatter (2019)	0.16	200
dos Santos Corrêa et al. (2019)	0.05	100–200
Gan and Zhang (2019)	0.07	1500
Nam et al. (2019)	0.1	950
Rodríguez-Morata et al. (2019)	0.1–0.2	200–400
Tsao et al. (2019)	0.24	300
Abraham et al. (2020)	0.01	100
Bezak et al. (2020)	0.13–0.2	400–900
Calista et al. (2020)	0.17	150
Franco-Ramos et al. (2020)	0.15	400
Zimmermann et al. (2020)	0.05–0.49	200–1250

### **2.5.3 Flow-R**

Flow-R is a numerical simulation tool based on empirical models for debris flow susceptibility assessment. It requires two sets of parameters; the first set of parameters is for identifying the source/initiation zone, and the second set is for propagation.

#### *2.5.3.1 Source Area Identification*

Identifying the initiation zone for runout analysis is an intricate task for debris flow modelling. In most of the debris flow simulation programs, users have to define the initiation zones. It is difficult to determine the initiation zone without high-resolution satellite images. However, Flow-R has the capability of identifying the initiation zones only by applying some conditions to selected topographic (e.g., slope gradient, aspect, and curvature) and hydrological (e.g., upslope contributing area) factors. These factors could be derived from DEM using GIS software. These factors are site-specific—for example, the majority of debris flows in the Swiss Alps originated from the terrain with slope gradients greater than  $15^\circ$  (Rickenmann and Zimmermann 1993). Upslope contributing area is also a critical factor for considering debris flow initiation. It refers to the area of the land that contributes water and sediment to a specific location where debris flow might start. Horton et al. (2013) determined  $0.01 \text{ km}^2$  as the appropriate threshold for the upslope contributing area for identifying the debris flow initiation zones in the Central Alps, Switzerland. Fischer (2012) found a lower value of upslope contributing area (0.3–1.0 ha) for Norway. Curvature is another morphological factor that measures the shape of the terrain surface and can be considered for identifying debris flow initiation zones. Debris flows tend to be concentrated in slope concavities (i.e., gullies rather than ridges) (Delmonaco et al. 2003; Wieczorek et al. 1997). Horton et al. (2013) suggested the plan curvature value of  $-2/100 \text{ m}^{-1}$  for a 10-m DEM of the

Solalex-Anzeindaz region by analyzing the orthophotographs,. Also, Fischer et al. (2012) found the curvature value  $-1.5/100 \text{ m}^{-1}$  to  $-0.5/100 \text{ m}^{-1}$  for Norway.

#### *2.5.3.2 Assessment of Propagation*

Propagation of debris flow is controlled by two algorithms: spreading algorithm and runout distance algorithm. The spreading algorithms have two sub-algorithms, namely the flow direction algorithm and the inertial algorithm (persistence function). Flow-R incorporates several direction algorithms that give the user the flexibility to select the most appropriate one for their analysis. For inertial algorithms, two options are available, which are weight and direction memory.

The runout distance algorithm is based on simple frictional laws (Horton 2013, Federico and Cesali 2015), where the friction loss can be calculated by either Perla et al. (1980) or the Simplified Friction Limited Model (SFLM) (Corominas 1996). Additional details of these algorithms can be found in (Paudel 2019; Jaboyedoff et al. 2011; Horton 2013).

Flow-R has been applied for runout assessments of debris flows in different countries, including Switzerland (Horton et al. 2008; Horton et al. 2013), France (Kappes et al. 2011), Italy (Blahut et al. 2010), Norway (Fischer et al. 2012), and Argentina (Baumann et al. 2011). Table 2.6 shows some successful studies that incorporated Flow-R for debris flow susceptibility assessment.

**Table 2.6.** Studies that incorporated Flow-R

<b>Authors</b>	<b>Remarks</b>
Kang et al. (2018)	Determined debris flows runout in the central region of South Korea. All available algorithms in Flow-R were tested to get the best simulation results. Besides, statistical analysis was performed to determine the efficiency and sensitivity of each algorithm.
Do et al. (2020)	Assessed the susceptibility of landslides in Ha Giang City, Vietnam, and its surrounding regions by combining the outcomes of Flow-R with three separate statistical models for better predictability of landslides.
Sturzenegger et al. (2021)	Proposed stream segments method by Holm (2016) for delineating debris flow and debris flood initiation zones rather than using the source identification step in Flow-R. Also, compared the simulation results of Flow-R with a numerical model (FLO-2D) and highlighted that Flow-R does not provide such parameters which are required for designing mitigation structures. Therefore, it is suitable for preliminary hazard assessment only.
Jiang et al. (2021)	Combined the results from the Flow-R model with other spatial information to form a debris flow hazard level map of the Karakoram highway in China. Their analysis indicated that the highway segment spanning 4.33 km falls under a “very high hazard level” category.

**Table 2.6.** (Continued)

<b>Authors</b>	<b>Remarks</b>
Blais-Stevens and Behnia et al. (2016)	Employed qualitative and quantitative methods to assess debris flow susceptibility in the Yukon Alaska highway in Canada. The qualitative approach utilized geological data and expert opinion, while the quantitative approach used Flow-R model to calculate the source areas and area of spreading of documented historical debris flow events. Flow-R model results in overgeneralization for a large area of varied topography. However, they suggested both methods should only be used for initial hazard assessment.

## 2.6 Summary

This chapter provides an overview of debris flow modelling approaches for hazard assessment. Debris flow modelling can be classified into three broad categories: empirical, physical, and dynamic modelling. Empirical modelling relies on simple relationships based on historical data and does not account for the rheology or kinematic parameters of the materials. Examples of empirical approaches include the angle of reach method, volume change rate method, and channel geometry method. Physical modelling involves laboratory tests to study debris flow behaviour. The major limitation of physical modelling is its application to real-world problems as it is scaled down to accommodate in a laboratory setup, and many field conditions may not be properly captured. Dynamic modelling simulates the movement of debris with time, which can be subdivided into lumped mass, distinct element, and continuum models. Continuum models provide

detailed information; however, the simulation results are highly affected by the rheological parameters used to model the debris.

Among the available methods, numerical approaches could provide better results. Still, these simulation tools are based on some simplified approaches. Therefore, proper calibration of the model parameters based on field data is necessary, which is done in the present study. This chapter introduces three computer programs, namely DebrisFlow Predictor, RAMMS, and Flow-R, which have been used for debris flow runout assessment. DebrisFlow Predictor and Flow-R have been developed based on some empirical models, while RAMMS is a 3D continuum numerical model. The DebrisFlow Predictor utilizes a cellular automata approach to simulate landslide runout, scour, and deposition information along the path. RAMMS uses the Voellmy-Salm fluid continuum model and incorporates depth-averaged equations for predicting runout, flow heights, velocities, and impact pressure. Finally, Flow-R can identify initiation zones based on topographic and hydrological factors and assess the propagation using spreading and runout distance algorithms. The present study identifies appropriate values of the parameters for these three computer programs by comparing the simulation results with field observations.

## **Chapter 3: A Comparative Study of Three Computer Programs for Debris Flow Runout Simulation**

**Co-Authorship:** This chapter is prepared as a manuscript for publication in a journal as: Arghya, A. B., Hawlader, B., Guthrie, R., Knibbs, G., and Wasklewicz, T., “A comparative study of three computer programs for debris flow runout simulation.” Most of the research presented in this chapter has been conducted by the first author. He also prepared the draft manuscript. The other authors mainly supervised the research and reviewed the manuscript.

### **3.1 Abstract**

Debris flows represent a large displacement of a wide variety of materials, including soil, mud, rock, and water. The extent and impact of debris flow depend on many factors, including the material type, topography, flow pattern, and amount of debris. Several computer programs are available for debris flow simulations. However, these programs have been developed based on some simplified models because capturing the complexities of the mechanisms and modelling such a large extent of the problem is challenging. In the present study, three simulation tools—namely DebrisFlow Predictor, Flow-R, and RAMMS—are used to simulate debris flow. Simulations are performed for three different sites where debris flows occurred. The characteristics of the sites differ in several aspects, including relief, geology, and soil type. Consequently, the debris flows on these sites exhibit varying characteristics such as runout extent, single/multiple flows, and channelized/unchannelized flows. Comparing the simulation results with field observations shows that all three numerical programs can simulate the debris flows if the appropriate model parameters are selected. Channel bed erosion during downslope displacement of debris can play a major role

in runout. RAMMS can simulate the erosion effects if the erosion properties and erosion zone are defined properly. DebrisFlow Predictor can be used to identify the zones of erosion and deposition based on statistical flow patterns over a given topography. Flow-R provides similar runout extent, in terms of susceptibility (0–1), as in DebrisFlow Predictor and RAMMS.

### **3.2 Introduction**

Debris flow is a gravity-driven moving mass of soil, mud, rock, and water, which might travel hundreds of meters in some cases (Takahashi 1981; Iverson 1997). Typically, debris travels at high velocity, which could exceed 15 m/s (Highland and Bobrowsky 2013) and create a large impact force on the infrastructure (Jakob and Hungr 2005; Naqvi 2020). A debris flow might be initiated when the failure of slope occurs at higher elevations due to several causes, including heavy rainfall (Anderson and Sitar 1995; Fiorillo and Wilson 2004; Guzzetti 2008), rapid snowmelt (Decaulne et al. 2005; Chiarle et al. 2007; Vergara et al. 2020; Hatchett et al. 2023), and wildfire (Nyman et al. 2011; Parise and Canon 2012; Rengers et al. 2016; McGuire et al. 2018; Staley et al. 2018).

Proper modelling of debris flow requires solving the mass and momentum balance equations incorporating appropriate constitutive behaviour of debris. However, it is an extremely challenging task because the process involves many complex phenomena such as spreading, erosion at the base, deposition, avulsions, change in flow path depending upon surface profile, and the effects of vegetation. In addition, while constitutive models are available for soil (e.g., sand and clay) for geotechnical engineering applications, such models cannot be directly used for debris that constitutes a wide range of particles of varying sizes. Therefore, the numerical programs for debris flow were developed using simplified approaches (Hungr and McDougall 2009).

A detailed discussion on the mechanisms and existing techniques for modelling debris flow is available in Hungr et al. (2005). McDougall (2017) classified the available runout analysis methods into two broad categories: (i) empirical-statistical methods and (ii) analytical methods (including numerical approaches). Based on field observation and characteristics of the landslide, several empirical methods were developed for estimating travel distance/runout and velocity of debris as a function of slope angle, elevation difference between the initiation and deposition points, volume of the material released, degree of confinement of the path (e.g., Ikeya 1981; Vandre 1985; Corominas 1996; Iverson 1997; Rickenmann 1999; Bianco and Franzini 2000; Hunter and Fell 2003; Guthrie et al. 2010).

Several computer programs were developed to model debris flow. Horton et al. (2013) presented an approach for developing debris flow susceptibility maps at a regional scale using a computer program called 'Flow-R.' This program used simplified empirical models for spreading and runout algorithms. Flow-R was used in several studies for regional-scale assessment of debris flow at different sites—for example, an ~125,000 km<sup>2</sup> area in southern British Columbia, Canada (Sturzenegger et al. 2021), 36 sites in the central region of Korea (Kang and Lee 2017); Yukon Alaska Highway Corridor, Canada (Blais-Stevens and Behnia 2016), Ha Giang city and the surrounding areas in Vietnam (Do et al. 2020). Simplicity and less number of input parameters are the main advantages of Flow-R; however, this program could be used for preliminary assessment (Sturzenegger et al. 2021) but does not provide sufficient information for decision-making and requires further assessment.

Another computer program called “DebrisFlow Predictor” was also developed based on an empirical-statistical approach (Guthrie et al. 2008; Guthrie and Befus 2021). This program was also successfully used to simulate several debris flow events—for example, North Shore Cowichan

Lake, Canada (Guthrie 2021), Black Hollow drainage basin in Colorado, USA (Wasklewicz et al. 2022), North Ogden, Utah, and Larimer County, Colorado, USA (Grasso et al. 2022). Guthrie and Befus (2021) provided some calibrated model parameters for DebrisFlow Predictor by analyzing data from several debris flows. The main advantage of this program is that it provides some additional information compared to Flow-R, which includes erosion and deposition zones and the thickness of debris. However, this program does not provide some key information for hazard assessment, such as the velocity of debris.

Mechanics-based numerical modelling techniques were also developed where simplified constitutive behaviour of debris was implemented. When the debris is saturated and flows at high velocity, the debris could be viewed as a fluidized material (Hung and McDougall 2009). For numerical modelling purposes, the complex heterogeneous materials are therefore replaced by an 'equivalent fluid' that provides resistance to downslope movement from two sources: (i) frictional resistance at the base and (ii) velocity-dependent viscous resistance. Using the simplified models that consider these two resistances, computer programs were developed to simulate time-dependent debris flow, which include DAN3D (Hung and McDougall 2009), RAMMS (Christen et al. 2010) and FLO-2D (O'Brien et al. 1993). Note that equivalent fluid properties cannot be measured in the laboratory but could be back-calculated by simulating field cases, as performed in previous studies (Mikoš and Bezak 2021). For example, RAMMS was successfully used to simulate a debris flow event in Dolomites in Belluno, Italy (Cesca and D'Agostino 2008), Tazhiping landslide in colluvial soil in China (Huang et al. 2017), and the debris flows in the Swiss Alps, Switzerland (Frank et al. 2015). Some studies also compared the performance of mechanics-based models; for example, FLO-2D and RAMMS (Cesca and D'Agostino 2008), DAN3D and RAMMS (Schraml et al. 2015; Gardezi et al. 2021).

In recent years, computer programs were developed to simulate the large displacement of failed soil mass, which include Smooth Particles Hydrodynamics method (Bui et al. 2011), Eulerian based finite element modelling (Dey et al. 2015), and Material Point Method (Soga et al. 2016). However, the use of these advanced numerical methods is not suggested at this moment because the constitutive behaviour of heterogeneous debris is not known, and three-dimensional simulation of debris flow problems will be computationally very expensive.

In summary, the existing numerical studies primarily simulated a single event or analyzed regional scale debris flow using a numerical program or programs of similar type (e.g., two mechanics-based programs, Gardezi et al. 2021). However, the following key questions still remain unanswered: (i) whether the computer programs based on empirical/statistical approaches could be used with mechanics-based programs for a better assessment of debris flow, and (ii) if so, how the parameterization could be done as these programs require very different sets of input parameters. The aim of the present study is to answer these questions from the simulations of debris flow at three different sites using three computer programs.

### **3.3 Study Areas**

Three debris flow sites are considered in this study. Each site has some unique characteristics. At Site 1, a single unchannelized debris flow occurred due to excessive rainfall near the highway. Site 2 is a watershed area where many debris flows have been observed for decades. Among them, one channelized and one unchannelized flow are considered. Site 1 and Site 2 are in British Columbia, Canada, where typically muddy or clastic type of debris flow occurs. Finally, Site 3 is selected from a large debris flow (granular type) fan in the Swiss Alps region in Switzerland.

All three programs used in the present study require a Digital Elevation Model (DEM) and the initiation zones from where the flow initiates. For Sites 1 and 2, 1 m × 1 m DEM was collected from LidarBC–open LiDAR data Portal. For Site 3, 0.5 m × 0.5 m DEM was downloaded from the Federal Office of Topography database (swissALTI3D). The simulation results might vary substantially with DEM resolutions; however, a 10-m pixel resolution was considered to be appropriate for regional debris flow susceptible mapping (Horton et al. 2013). In recent years, the computational power has increased rapidly; therefore, simulations could be performed even for smaller pixels. Guthrie and Befus (2021) suggested that a 5-m DEM strikes a balance of processing power and provides reasonable results. Therefore, all the simulations in this study are performed using 5 m × 5 m DEM.

There are several ways to identify the debris flow initiation zones. The most popular methods include: i) comparing the elevation changes before and after the event using LiDAR-derived DEM and ii) interpreting after-event high-resolution satellite images. In this study, initiation zones are determined using the following satellite images. For Sites 1 and 2, Google Earth Pro images were available before and after the event. For Site 3, high-resolution satellite images (10 cm × 10 cm) are publicly available at the Federal Office of Topography Swisstopo database.

### ***3.3.1 Site 1: Highway 7, Hope-Agassiz***

In mid-November 2021, a significant amount of rainfall occurred in southern British Columbia (BC), Canada. The rainfall was very intense on November 13–15 and was more than 100 mm on November 14 (Hansen 2021). The rainfall caused several slope failures in this area, resulting in flooding, mudslides, and debris flows. Among them, a debris flow that hit Highway 7 between Hope to Agassiz on November 14 was a major one. Several vehicles were swept off the highway

where a number of people were trapped, and luckily, no fatalities occurred. The runout length of this event was ~1,360 m. A closer examination of Google Earth Pro images for pre- and post-slide conditions shows that the failure of ~3,350 m<sup>2</sup> area was initiated ~580 m above the level of Highway 7. After initiating, the debris diverges into three flow channels and converges into a single flow channel near Highway 7 (Fig. 3.1). Large amount of debris accumulates behind the highway (Figs. 3.1(b) & 3.1(c)). Some debris flowed over the highway, spreading over a large area of thinner layers. In the present study, although the simulations are performed for the whole debris flow, more attention is provided to the accumulated debris behind the highway as the dynamics of this thick layer was the critical factor that could impact the highway. Figure 3.1(a) shows the preliminary interpretation of this catastrophic event based on satellite images. The yellow polygon near the toe represents the area where the deposition of the major amount of debris occurred. Some deposition also occurred in the upslope areas near the initiation zone, as shown by the yellow polygon near the initiation zone. When failure occurred, a majority portion of the failed material came down from the two corners of the initiation zone and followed the gullies. The pink polygon enclosed by a dashed line shows the entrainment zone, while the black polygon at the top represents a complex entrainment area where both deposition and entrainment might have occurred. Typically, erosion occurs in the entrainment zone; therefore, identifying the entrainment zone is essential for more accurate modelling, as discussed in the later sections.

### ***3.3.2 Site 2: Klanawa Watershed***

The Klanawa watershed on Vancouver Island, British Columbia, is approximately 240 km<sup>2</sup> in size and is located on the southwest coast side of the island. The floodplain is made up of glaciofluvial and alluvial sediments. Mid and upper slopes consist of glacially over-steepened morainal till or



**Fig. 3.1.** Debris flow at Highway 7 between Hope to Agassiz, BC, Canada (Site 1): (a) entire view, (b) view along the highway, (c) view at the toe; Source: Google Earth and BC Ministry of

Transport & Infrastructure

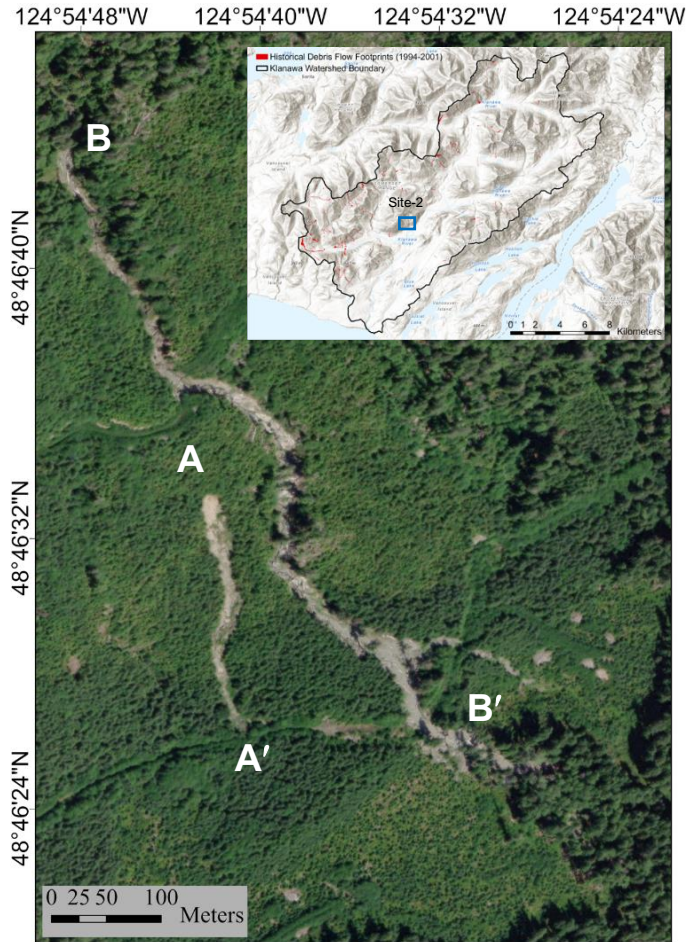


**Fig. 3.2.** An unchannelized (AA') and a channelized (BB') flow at Site 2 (Inset map, Guthrie et al. 2008)

gravelly colluvium veneers that frequently show signs of instability in the form of open slope and channelized debris flows (Morgan 2001). Slopes steeper than 30° and presence of gullied terrain have much higher landslide likelihood in this area (Rollerson et al. 2002). The watershed is also critical for the aquatic habitats, which are sensitive to peak flow disturbances and are affected by erosion and bedload sediment. Guthrie et al. (2008) reported 331 debris flows over 500 m<sup>2</sup> in the Klanawa watershed from the available 1994–2001 air photograph record (inset of Fig. 3.2). The

present study considered one channelized and one unchannelized debris flow from this site, which occurred between April 2021 and October 2021 (Fig. 3.2).

### 3.3.2 Site 3: Solalex-Anzeindaz

Solalex is a small village of Canton de Vaud, Switzerland, situated at an altitude of 1,460 m on the south side of Diablerets Mountain. It is connected with Anzeindaz village (400 m higher than Solalex) by a private road. The present study focused on a debris flow fan located between Solalex and Anzeindaz. These fans are very active because the upper part consists of folded limestone with marl layers, which creates steep, small, impervious catchments that are highly productive in rock fragments (Badoux and Gabus 1990). This study used a subset of this region ( $\sim 4 \text{ km}^2$ ) from where 10 debris flows are simulated to show the performance of these three programs in regional-scale modelling while maintaining clarity in presentation and computational efficiency (Fig. 3.3). The red spots in Fig. 3.3 represent the initiation zones, which were identified from the satellite image. Additional details of these debris flows are shown in Table 3.1.

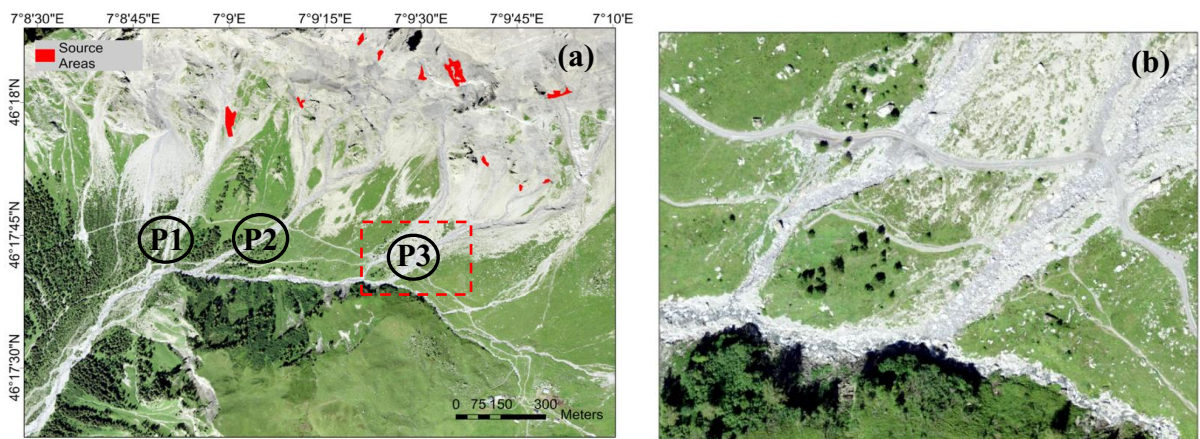


**Fig. 3.3.** Debris flow in Site 3 (Solalex-Anzeindaz region, Switzerland): (a) flow paths; (b) accumulation of materials around point P3 in Fig. 3.3(a)

**Table 3.1.** Key information about the sites considered in this study

<b>Parameters</b>	<b>Site 1 Highway 7, Hope- Agassiz</b>	<b>Site 2 Klanawa Watershed</b>	<b>Site 3 Solalex- Anzeindaz</b>
Runout length	~1,360 m	~285 m in open slope & ~870 m channelized zone	~1100–2400 m
Elevation difference between initiation zone to final deposition	~585 m	~96 m in open slope & ~248 m in channelized zone	~640 m
Entrained Material	Mostly finer & less granular; trees 	Finer materials; trees 	Granular & Boulders 
Failure Reason	Extreme rainfall	Rainfall, logging	Permafrost degradation, rainfall
Flow type	Open slope	Both open slope and channelized	Open slope
Geological Unit	Granodioritic intrusive rocks	Glacially over-steepened morainal till or gravelly colluvium veneers	Folded limestone with marl layers
Annual Precipitation	~1,755 mm at Agassiz (Thomas et al. 2019)	2,876 mm–3,102 mm at Klanawa watershed (Rollerson et al. 2004)	~2,600 mm–3000 mm at Anzeindaz region (Randin et al. 2009)

### **3.4 Simulation Tools**

Three debris flow programs named DebrisFlow Predictor (Guthrie and Befus 2021), RAMMS (Rapid Mass Movement Simulation) (Christen et al. 2010), and Flow-R (Horton et al. 2013) were used in the present study to simulate debris flow at the three different sites. Details of these programs are available in previous studies, including those mentioned above. However, a brief description is provided below.

#### ***3.4.1 DebrisFlow Predictor***

DebrisFlow Predictor is a computer program for simulating landslide runout developed by Guthrie and Befus (2021), which is based on a cellular automata (Wolfram 1884; Von Neumann 1996) method. Cellular automata (CA) has been deployed in several studies to model complex natural phenomena, including debris flows (Iovine et al. 2003; Guthrie et al. 2008), snow avalanches (Barpi et al. 2007), and lava flows (Spataro et al. 2004). Several studies showed successful applications of the cellular automata model for debris flow runout simulations (D'Ambrosio et al. 2003(a); D'Ambrosio et al. 2003(b); Guthrie et al. 2008; Han et al. 2017; Guthrie and Befus 2021). Further details on CA and its application in debris flow modelling are available in Han et al. (2017). In the DebrisFlow Predictor program, the flowing materials are represented by agents that occupy cells on a raster grid at a specific time step on which a set of simple rules for scour, deposition, path selection, and spread were applied. These rules were developed empirically based on the observations of debris flows in coastal areas of British Columbia and follow the probability distributions for 12 slope classes. These probabilities are based on the fieldwork conducted by Wise (1997), Guthrie et al. (2008), and Guthrie and Befus (2021).

The program requires the following input parameters. Firstly, it requires the digital elevation model (DEM) of the area with a resolution of 5 m × 5 m. Secondly, the user has to identify the initiation zones of the debris either by selecting within the program or importing shapefiles. When the DEM is imported into the program, each cell in the working grid collects the basic information from the DEM, including elevation, position, slope, and aspect. Each activated cell (i.e., the cell selected manually or by the computer model to generate an agent) contains an agent—an autonomous subroutine that interacts with the surface model and other agents. Scour and deposition are calculated for each time step, and the difference between these two gives the net mass. The mass is shed to the new cells by spawning additional agents. Each agent continues to move downslope until its mass balance is zero. The direction of movement is identified by a Moore Neighbourhood algorithm, where the elevations of the surrounding eight cells around the central cell are obtained. The materials flow toward the unoccupied cells at lower elevations. In the case where cells are not unoccupied or where three cells have the same elevation, the flow direction is a combination of random chance and the preservation of momentum. The redistribution of mass or spreading is described by a probability density function defining the standard deviation ( $\sigma$ ) as

$$\sigma = \left( \frac{m_{max} - m}{m_{max}} \right)^n (\sigma_L - \sigma_s) + \sigma_s \quad (3.1)$$

where  $m_{max}$  is the "fan maximum slope" to limit spreading above the selected slope value,  $m$  represents the DEM slope,  $n$  is a skew coefficient,  $\sigma_L$  is a low slope coefficient, and  $\sigma_s$  is steep slope coefficient.

The parameters used in this study for DebrisFlow Predictor are listed in Table 3.2. These parameters can be calibrated iteratively within the model, and the results can be compared to

known (observable) events or landforms. All these parameters in Table 3.2 were selected based on a critical review of the existing literature where the DebrisFlow Predictor was used to simulate field observations (Guthrie and Befus 2021; Guthrie 2021). The type and nature of spreading is primarily governed by the first four parameters ( $m_{\max}$ ,  $\sigma_S$ ,  $\sigma_L$ , and  $n$ ) in Table 3.2. The parameter  $m_{\max}$  limits spreading to slopes flatter than the selected value. Guthrie and Befus (2021) recommended using  $m_{\max} = 27^\circ$ , where additional information is not available. The parameters  $n$ ,  $\sigma_L$  and  $\sigma_S$  control the amount of spread by the creation of new agents redistributed to surrounding cells. With an increase in the value of  $\sigma_L$  and  $\sigma_S$ , spreading increases in the low and steep slope areas, respectively. Further details of these parameters can be found in Guthrie and Befus (2021). An increase in the number of maximum spawns allowed ( $N_{\max}$ ) widens the flow and reduces the runout length. The actual number of spawns is less than or equal to  $N_{\max}$ . Therefore, for the channelized flow in Site 2, a smaller value of  $N_{\max}$  (= 4) is used as the flow was through a confined path constrained by steep side slopes. Field evidence shows an increase in travel distance with a degree of confinement by the side slopes of a gully or small valley (Hunter and Fell 2003).  $N_{\max} = 100$  was used for the other simulations as the post-slide observations show the spreading of debris over a wider area. Note, however, that the simulation results do not change significantly for  $N_{\max} > 15$  for the cases simulated in this study.

Agent mass is a critical part of the DebrisFlow Predictor. The agent continues to move downslope and terminates when mass is zero, following probabilistic rules for scour and deposition based on the underlying slope of the debris. The probability curves were developed from approximately 1,700 field observations (Wise 1997; Guthrie et al. 2008, 2010). Nonetheless, the variations in local geomorphology may necessitate adjustments to scour or deposition depth. These are achieved using the deposition and erosion multipliers (Table 3.2) that are independently applied to the agent

mass after calculation in each time step. An increase in erosion multiplier increases the amount of debris and, thereby, the spreading and runout; however, the deposition multiplier gives opposite results.

The material can move from the central cell to any of the eight surrounding cells in the grid. The center of these surrounding cells are at  $45^\circ$  angular distance from the central cell. Therefore, in DebrisFlow Predictor, the loss of mass carried by the agents during the flow of the materials to these eight cells is defined by loss per  $45^\circ$  turn. As will be shown later, a major amount of debris flows through some gullies; therefore, a lower amount of mass loss is expected as the flow path is bounded by the slopes of the gullies. In this study, a mass loss of 5% per  $45^\circ$  turn is used, except for the unchannelized flow in Site 2, where the debris spread over a wider area.

Finally, the program requires a minimum scour depth ( $d_m$ ), which can be multiplied by the area of the initiation zone to find the release volume ( $V_{\text{release}}$ ). As the slide is very large,  $d_m = 5.0$  is used for Site 1, which gives  $V_{\text{release}} \sim 20,000 \text{ m}^3$ . The slides were relatively small for the two cases in Site 2; therefore,  $d_m = 2.0$  ( $V_{\text{release}} \sim 3,000 \text{ m}^3$ ) and  $d_m = 1.0$  ( $V_{\text{release}} \sim 2,200 \text{ m}^3$ ) are used for channelized and unchannelized cases. As the initiation zone of Site 3 contains rock,  $d_m = 1.0$  m is used, which gives  $V_{\text{release}} = 220 \text{ m}^3$ – $3,300 \text{ m}^3$ , depending upon the size of the initiation zone of the 10 cases considered in this study. Similar release volumes are used in the simulations with RAMMS.

Because the results are probabilistic, no two runs are identical; therefore, multiple runs are recommended to determine the potential cumulative footprint of a debris flow path and to calculate the probability that any location within the cumulative footprint will be occupied by an event. The simulation of runout with this program provides landslide pathways and sediment volume (scour and deposition) along the flow path.

**Table 3.2.** Parameters used in DebrisFlow Predictor

Parameters	Site 1	Site 2	Site 3
Fan maximum slope ( $m_{\max}$ )	27°	34°	27°
Steep slope coefficient ( $\sigma_S$ )	0.35	0.35	0.35
Low slope coefficient ( $\sigma_L$ )	1.35	1.35	1.35
Skew coefficient ( $n$ )	1.1	1.1	1.1
Maximum spawns allowed ( $N_{\max}$ )	100	4(100)	100
Deposition multiplier ( $\times$ )	0.4	0.5(1.0)	0.3
Erosion multiplier ( $\times$ )	0.8	0.7	0.5
Mass loss per 45° turn (%)	5	5(20)	5
Minimum initiation depth, $d_m$ (m)	5	2 (1)	1
Number of model runs	50	50	50

\* For Site 2, the numbers in parenthesis are for unchannelized, and without parenthesis for channelized flow

### 3.4.2 RAMMS

RAMMS software package was used by several researchers to simulate debris flow (Cesca and D'Agostino 2008; Frank et al. 2015; Frank et al. 2017). While debris involves a wide range of materials, the program was developed using depth-average shallow water equations of single-phase material. The Voellmy-Fluid model was used to model the material behaviour. The Voellmy-Fluid model does not consider the shear deformation; therefore, the debris moves at a constant velocity ( $u$ ) over the depth of the debris at a given location and time. That means the

deceleration of debris flow occurs only by the basal friction ( $S_f$ ) between the bottom of the debris and the slope, which was calculated as:

$$S_f = \mu(\rho gh \cos(\varphi)) + \frac{\rho g u^2}{\xi} \quad (3.2)$$

where  $\mu$  is dry Coulomb-type friction coefficient;  $\rho gh \cos(\varphi)$  is the normal stress on the slope caused by the weight of debris;  $\rho$  is the bulk mass density of debris;  $g$  is the gravitational acceleration;  $h$  is the flow height of the debris;  $\varphi$  is the channel slope angle;  $\xi$  is the viscous-turbulent friction coefficient of the flow.

While the model (Eq. (3.2)) is relatively simple, the estimation of the two model parameters ( $\mu$  and  $\xi$ ) is challenging. The parameters  $\mu$  and  $\xi$  depend on local debris flow characteristics such as topographical properties, rheological behaviour, and hydro-meteorological conditions. Calibrating the simulation results with field observations for various debris flows, previous studies reported a wide range of variation of these parameters (Cesca and D'Agostino 2008; Hussin 2011; Frank et al. 2015; Frey et al. 2016; Schraml et al. 2015; Frank et al. 2017; Franco-Ramos et al. 2020; Zhuang et al. 2021). While a wide range of  $\mu$  ( $= 0.001-0.7$ ) was reported,  $\mu$  of  $0.1-0.2$  was most commonly used (Anaconda et al. 2018; Mikoš and Bezak 2021). Typically used  $\xi$  lies between  $200 \text{ m/s}^2$  and  $500 \text{ m/s}^2$ , although it ranges from  $10 \text{ m/s}^2-2,000 \text{ m/s}^2$ . RAMMS user manual recommends  $\xi = 100 \text{ m/s}^2-200 \text{ m/s}^2$  for granular flow, and  $\xi$  could be more than  $1,000 \text{ m/s}^2$  if the debris contains more fluid. Gan and Zhang (2019) found  $\xi = 1500 \text{ m/s}^2$  simulates better a debris flow in the Luzhuang gully. Therefore, site-specific calibration of these model parameters is necessary. In the present study, simulations are performed for different combinations of  $\mu$  ( $= 0.05-0.3$ ) and  $\xi = 200 \text{ m/s}^2-2000 \text{ m/s}^2$ , and the best-matched simulations of the imagery footprint are found for  $\mu$  and  $\xi$  listed in Table 3.3. As the debris was muddy in Site 1 and Site 2, higher  $\xi$  and lower  $\mu$  values are required

to match the field observation. Relatively rigid and dry masses of broken rocks flow in Site 3, which are expected to have higher dry friction and lower viscous resistance. Therefore,  $\mu = 0.2$  and  $\xi = 200 \text{ m/s}^2$  are used for this site.

**Table 3.3.** Best fit material parameters used in RAMMS

Parameters	Site 1	Site 2	Site 3
Bulk mass density of debris, $\rho$ (kg/m <sup>3</sup> )	2,000	2,000	2,000
Dry Coulomb-type friction coefficient, $\mu$	0.1	0.1	0.2
Viscous-turbulent friction coefficient, $\xi$ (m/s <sup>2</sup> )	400	500	200

In addition to the above material model parameters, RAMMS requires a DEM and release information to run a simulation. Release information can be given either one/multiple block release or input hydrograph option. The block release method is suitable for unchannelized debris flow, while the hydrograph option appears to be more suitable for channelized debris flow. In the block release option, the program calculates the release volume from the release height and release area. The release area can be determined from high-resolution satellite images. However, the problem lies in determining the release height. The best option to delineate the release height is comparing the elevation change of pre-event and post-event DEM. The initiation conditions, including the release volume, are the same as in DebrisFlow Predictor (Section 3.4.1).

#### 3.4.2.1 Erosion Module (RAMMS)

RAMMS under-predicts the runout if the simulation is performed only with the release volume at the upstream end (Frank et al. 2015). Therefore, the entrainment of sediment into the flow due to the erosion of the channel bed was implemented as an “erosion module” in RAMMS (Frank et al.

2015). The empirical model for entrainment was developed from field data (Frank et al. 2015; Frank et al. 2017). It is assumed that the depth of erosion ( $z$ ) is a linear function of basal shear stress,  $\tau$  ( $= \rho gh \cos\phi$ ) (i.e., the erosion proportionality factor,  $dz/d\tau$ , is constant), and the erosion occurs only if  $\tau$  is greater than critical shear stress ( $\tau_c$ ). The program also defines a maximum potential erosion depth ( $e_m$ ). In addition, the program uses an erosion rate ( $dz/dt$ , where  $t$  is the time) to ensure gradual entrainment of eroded materials and to prevent entering all the eroded sediment within one-time step.

In the present study, the simulations with the erosion module are performed only for Site 1. Note, however, that RAMMS without erosion was used to simulate all three cases. An erosion rate ( $dz/dt$ ) of 0.05–0.1 m/s was found in flume test results (Reid et al. 2011). However, higher values of the maximum erosion rate of 0.14 m/s and 0.25 m/s were found for a natural debris flow in Colorado, USA (McCoy et al. 2012) and Illgraben (Frank et al. 2015), respectively. The default  $dz/dt$  in the program is -0.013 m/s, which is used in this study. The values of the other erosion module parameters are shown in Table 3.4.

**Table 3.4.** Erosion parameters used in RAMMS for Site 1

<b>Erosion Parameters</b>	<b>Values</b>
Erosion rate, $dz/dt$ (m/s)	-0.013
Erosion proportionality factor, $dz/d\tau$ (m/kPa)	-0.05
Critical shear stress, $\tau_c$ (kPa)	1.50
Maximum erosion depth, $e_m$ (m)	0.20

### 3.4.3 Flow-R

Flow-R is a computer program developed in Matlab by researchers at the University of Lausanne, Switzerland, incorporating spatially distributed empirical models. After determining the initiation zone, the program calculates the runout/propagation extent over the DEM based on spreading algorithms and runout algorithms. The spreading algorithms provide the direction of flow, which are defined by two sub-algorithms, namely flow direction algorithm and inertial algorithm (also known as persistence function). Several direction algorithms were implemented in Flow-R, and the user can choose one of them for an analysis.

In the present study, modified Holmgren's algorithm was used (Holmgren 1994; Horton et al. 2013). In the modified Holmgren, the central cell height was increased by a factor  $dh$  (= 0.15 m for Site 2 and 0.2 m for Sites 1 and 3), which gives better simulation results that are less sensitive to DEM resolution (Horton et al. 2013). The Holmgren's Algorithm can be written as:

$$p_i^{fd} = \frac{(\tan\beta_i)^x}{\sum_{j=1}^8 (\tan\beta_j)^x} \quad \forall \begin{cases} \tan\beta > 0 \\ x \in [1; +\infty] \end{cases} \quad (3.3)$$

where  $i, j$  are flow directions;  $p_i^{fd}$  is the susceptibility proportion in direction  $i$ ;  $\beta_i$  and  $\beta_j$  are the slope angles at the central cell in the  $i, j$  directions, and  $x$  is an exponent of convergence that controls the spreading. A higher value of  $x$  represents a higher degree of convergence. Claessens et al. (2005) recommended  $x$  of 4–6 for debris flow. The present study uses  $x = 3.5$  for Site 1 and  $x = 4$  for Sites 2 and 3. Two options are available for the inertial algorithm: weight and direction memory. In this study, the weight option is selected, which calculates the flow with a change in direction relative to the prior direction as

$$p_i^p = w_{\alpha_i} \quad (3.4)$$

where  $p_i^p$  is the flow proportion in direction  $i$ , and  $\alpha_i$  is the angle between the previous direction and the direction from the central cell to cell  $i$ . The weight ( $w_{\alpha_i}$ ) was selected based on the work of Gamma (2000). Further details on inertial algorithms are available in Horton et al. (2013).

Debris flow runout can be determined by combining the flow direction algorithm and the persistence function (Eq. 3.5).

$$p_i = \frac{p_i^{fd} p_i^p}{\sum_{j=1}^8 p_j^{fd} p_j^p} p_0 \quad (3.5)$$

where  $p_i$  is the susceptibility value in direction  $i$ ,  $p_0$  is previously determined flow proportion of the central cell.

The runout distance algorithms were developed based on energy balance,

$$E_k^i = E_k^0 + \Delta E_p^i - E_f^i \quad (3.6)$$

where  $E_k^i$  is the kinetic energy of the cell in the direction  $i$ ;  $E_k^0$  is the kinetic energy of the central cell;  $\Delta E_p^i$  is the change in potential energy and  $E_f^i$  is the energy loss due to the friction for the flow in direction  $i$ . The friction loss can be calculated either by Perla et al. (1980) or the simplified friction limited model (Corominas 1996). Perlas' model utilizes nonlinear friction law using mass-to-drag ratio and friction coefficient. However, determining these values is challenging due to their variability along the path (Park et al. 2016). The friction loss was calculated in this study by using a simplified model (Corominas 1996) as:

$$E_f^i = g \Delta x \tan \varphi \quad (3.7)$$

where  $\Delta x$  is the increment displacement in the horizontal plane in direction  $i$  from the central cell to the cell where debris moves;  $\varphi$  is the angle that connects the source area to the most distant point reached by debris flow (travel angle);  $g$  is the gravitational acceleration. Previous studies reported

$\varphi = 7^\circ\text{--}11^\circ$  where the lower values are for fine-grained materials (Rickenmann and Zimmermann 1993; Bathurst et al. 1997; Zimmermann et al. 1997; Huggel et al. 2002; Horton et al. 2013).

The simulated runout extent could be misleading if the slope is very steep because of unrealistic amounts of energy generation (Jiang et al. 2021). To control that, Flow-R incorporated a limiting velocity ( $v_{\max}$ ), as suggested by Horton et al. (2013). That is,

$$v_i = \min \left\{ \sqrt{(v_0^2 + 2g\Delta h - 2gx\Delta x \tan\varphi)}, v_{\max} \right\} \quad (3.8)$$

where  $v_0$  and  $v_i$  are the velocity at the beginning and end of the segment, respectively, and  $\Delta h$  is the difference between the elevation of the central cell and the cell in the direction  $i$ . The maximum velocity of debris flows in Switzerland ranges from 13–14 m/s (Rickenmann and Zimmermann 1993). While the velocity of debris torrents in western Canada is 3–12 m/s (VanDine 1985). In this study,  $v_{\max} = 15\text{--}20$  m/s was considered (Table 3.5).

**Table 3.5.** Algorithms and parameters used in Flow-R

Parameters	Site 1	Site 2	Site 3
Direction Algorithm	Modified	Modified	Modified
	Holmgren	Holmgren	Holmgren
Inertial Algorithm	Gamma	Gamma	Gamma
Slope of energy line, $\varphi$ ( $^\circ$ )	7 $^\circ$	11 $^\circ$ for channelized	11 $^\circ$
		15 $^\circ$ for unchannelized	
Limiting velocity, $v_{\max}$ (m/s)	20	15	15

## 3.5 Results

As mentioned above, simulations are performed for the three sites using three programs. The simulations are performed by changing the values of the model parameters to obtain the best possible results compared with field observation. For brevity, the best-fit simulation results are discussed in the following sections. Some other simulation results, including the video of time-dependent displacement of the debris, are provided in Appendix-III and supplemental materials.

### *3.5.1 Site 1: Highway 7, Hope-Agassiz*

Both DebrisFlow Predictor and Flow-R were developed from probabilistic models; therefore, these programs give the probability of the likelihood of debris flow occurring at any location for the given landscape and model scenarios. Figures 3.4(a) and 3.4(b) show the susceptibility maps generated by DebrisFlow Predictor and Flow-R, respectively, where the darker colours represent the higher susceptibilities. The spreading and runout simulated by DebrisFlow Predictor are similar to that observed in the satellite image, as shown by the dashed lines in Fig. 3.4. The probability of debris flow inundation is very high ( $> 80\%$ ) in some upslope areas and immediately behind the highway. The debris also crossed the highway, although the probability of inundation is relatively low ( $< 20\%$ ). Note that, in the field, some amount of debris passed the highway (Fig. 3.1(a)). The debris flow susceptibility map obtained from Flow-R also gives similar results (Fig. 3.4(b)) as obtained from DebrisFlow Predictor (Fig. 3.4(a)) but with some notable differences. Firstly, after the initiation of failure from the apex, the DebrisFlow Predictor simulates a high prevalence of flow towards the left gully (point B in Figs. 3.1(a) and 3.4(a)); however, the susceptibility of flow in this area is relatively low in Flow-R simulation results. The Flow-R produced mainly three channels of almost vertical flow below the crown. Secondly, the debris did not cross the highway

in Flow-R. Thirdly, in the downslope area around point D in Fig. 3.4, DebrisFlow Predictor gave the probability of flow primarily through two channelized areas and then merged to one channelized area around point E. However, spreading was observed in satellite images between points D to E, as shown in Fig. 3.1(a). In this respect, more spreading in this area was simulated by RAMMS (Fig. 3.4(c)).

RAMMS is a deterministic approach that can simulate the time-dependent debris flow process. The flow height (i.e., the thickness of debris) changes with time as the debris moves. Figure 3.4(c) shows the flood height (maximum flow height during the whole period of simulation) over the whole area of debris flow. This simulation is performed without considering the erosion module. The effects of the erosion module are discussed further in the later sections. The flood height is an indicator of flow direction. Figure 3.4(c) shows that, similar to Flow-R (Fig. 4(b)), the main flow occurred through three narrow channelized areas. However, some lateral spreading of debris ( $\leq 1.0$  m height) occurs in the surrounding zone. Comparing satellite images (Fig. 3.1(a)), it seems that RAMMS over-predicts the lateral spreading in the upslope areas. Near the toe, a small amount of debris crosses the highway; however, the spreading in this area is less compared to the satellite imagery observation (Fig. 3.1(a)) and the simulation using DebrisFlow Predictor (Fig. 3.4(a)). Figure 3.4(d) shows the final deposition height of the debris predicted by RAMMS at the end of the event ( $t = 220$  s). As this simulation is performed without erosion of the base over which debris flow occurred, the debris volume originated only from the initiation zone displaced with time. As shown in Fig. 3.4(d), deposition primarily occurred behind the highway, while some amount of debris (0–0.5 m) was deposited on the way during downslope movement.

### 3.5.1.1 Effects of erosion

While the simulation results shown in Figs. 3.4(a) and 4(c) are comparable, the following differences need to be highlighted. Debris does not spread much or cross the highway in RAMMS simulation, as observed in the field (Fig. 3.1(a)) and DebrisFlow Predictor (Fig. 3.4(a)). One potential reason might be the use of higher strength parameters for debris. Therefore, a number of simulations are performed with lower values of  $\mu$  ( $= 0.05$  &  $0.07$ ) and higher values of  $\xi$  ( $= 1,000$   $\text{m/s}^2$ – $2,000$   $\text{m/s}^2$ ), which increases the accumulation of debris near the toe area but still is not sufficiently large or crosses the highway. On the other hand, debris spreads over the whole upslope area if such low-strength material parameters are used, while in the field, some treed areas were observed (e.g., at point C in Fig. 3.1(a)). Moreover, the maximum velocity of the debris was up to  $40$   $\text{m/s}$  with these weaker model parameters, which is considerably high for western Canada ( $3$ – $12$   $\text{m/s}$ , VanDine 1985) and in extremely rapid class ( $>5$   $\text{m/s}$ ) as per Hungr et al. 2013. As shown in later sections, the deposition volume calculated by RAMMS without erosion is considerably lower than that obtained from DebrisFlow Predictor. Therefore, another simulation is performed with RAMMS considering the erosion module, as discussed in Section 3.4.2.1.

In RAMMS, the erosion zone has to be specified by the user, which could be an intricate task. This could be obtained if high-resolution DEM is available for pre- and post-event. However, such information may not be available in many cases, and the interpretation might be difficult as some areas might be covered with vegetation. In the present study, the simulation results obtained from DebrisFlow Predictor are used to define the erosion zone. Figure 3.5 shows the scour and deposition depths along the runout path obtained from DebrisFlow Predictor. The orange-coloured zone (Scour and Transportation) shows the area where scouring occurred during the flow of materials. The other coloured zones in Fig. 3.5 show the areas where deposition occurred.

In the simulation with the erosion module in RAMMS, a polygon enclosing the pink-coloured zone in Fig. 3.1(a) is defined as the erosion zone, and the simulation is performed with the parameters listed in Tables 3 and 4. Figures 3.6(a) and 3.6(b) show the flood depth and final deposition depth, respectively, obtained from RAMMS simulations considering the erosion module. Comparing these figures with Figs. 3.4(c) and 3.4(d) with 3.6(a) and 3.6(b), respectively, it can be shown that the flood height and deposition depth near the toe increased when erosion is considered. To clarify it further, the flow height at three locations on the flow paths (points P1, P2, and P3 in Fig. 3.6(b)) are plotted in Fig. 3.6(c). At points P1 and P2, the flood height (shown by circles) is higher when the erosion module is considered; however, the final deposition height (shown by triangles) is almost the same for both simulations as the material moved to the toe. The final deposition height at point P3 near the toe increased by  $\sim 0.8$  m when the erosion module was considered.

Both programs (DebrisFlow Predictor and RAMMS, Figs. 3.5 and 3.6(b)) simulated deposition primarily near the toe and behind the highway. Therefore, deposition in this area is examined further. For that purpose, an area enclosed by the polygon X shown in Fig. 3.5 is considered. The calculated volume of the debris deposited in this zone X is  $27,700 \text{ m}^3$  and  $27,900 \text{ m}^3$  using DebrisFlow Predictor and RAMMS with erosion module, respectively. Note that the release volume is  $20,000 \text{ m}^3$ . The extra amount of debris was added due to the scouring of the base during the flow. When the erosion module is not considered in RAMMS (Fig. 3.4(d)), the final deposition volume in the same area is  $19,000 \text{ m}^3$ , which is significantly lower than above, although release volumes are the same for all these analyses. Therefore, it can be concluded that the DebrisFlow Predictor simulated scour and deposition zone could be used in RAMMS as the erosion zone when detailed information about the erosion zone is not available.

While the volume deposited near the toe is comparable in DebrisFlow Predictor and RAMMS, the height of the debris in each cell in the polygon X is also examined. Figure 3.7(a) shows the contour within polygon X before the event. The central part of the polygon (around point K in Fig. 3.7(a)) is approximately 1 m higher than L or M. Figure 3.7(b) shows the contour of debris thickness obtained from DebrisFlow Predictor. If the debris becomes horizontally leveled at the end of the event, the contours shown in Figs. 3.7(a) and 3.7(b) are comparable—the higher the ground elevation before the event (Fig. 3.7(a)), the smaller the debris thickness. The contour of the final deposition depth obtained from RAMMS (Fig. 3.7(c)) is slightly different from that of DebrisFlow Predictor (Fig. 3.7(b)). In RAMMS, the highest amount of debris is deposited where the material comes from the upper gully. Note that, in RAMMS, the displacement of debris continues until the kinetic energy becomes zero.

To understand the simulation results better, the percentage of the cells within the polygon X occupied by the debris of the same height is shown in Fig. 3.8 for both DebrisFlow Predictor and RAMMS. Note that the cell size is the same (5 m × 5 m) for both simulations. In RAMMS, the flood height in some cells within this zone was up to 4.0–4.5 m, while the final height was up to 2.5–3.0 m. The DebrisFlow Predictor gave the heights up to 4.5–5.0 m. While it is difficult to compare results directly for each cell as these simulation tools were developed from different approaches (time-dependent deterministic vs. empirical-statistical), overall debris height and deposition volume near the toe for these two programs are comparable.

Figure 3.9(a) shows the maximum velocity of the debris, which is up to 20 m/s, except for an area immediately below the initiation zone where it is more than 20 m/s. Note that significantly large velocities in some localized areas (e.g., below the crown) were also found in the numerical simulations using RAMMS and DAN3D (Gardezi et al. 2020). The maximum pressure is as high

as 800 kPa, except for a small zone near the top where the pressure is greater than 800 kPa (Fig. 3.9(b)). When the debris hits the highway, the maximum velocity ( $< 5$  m/s) and maximum pressure ( $< 100$  kPa) are relatively low. The velocity and impact pressure are needed for hazard assessment of debris flow.

### ***3.5.2 Site 2: Klanawa Watershed***

Figure 3.10 shows the simulation results of an unchannelized and a channelized debris flow at the Klanawa watershed. As shown in Fig. 3.2, the unchannelized debris flow initiated from point A and then traveled  $\sim 285$  m horizontal distance up to point A' near the road. The average slope along this path is 38%, and the maximum slope is 59%. The flow spread  $\sim 20$  m near the initiation point but narrowed down near the end. Note, however, that the exact spreading could not be identified from the current satellite image, especially in the treed areas. Figure 3.10(a) shows that the DebrisFlow Predictor gives a similar flow path as observed in the field (Fig. 3.2) and spreads over a larger area near the toe. Again, such spreading near the toe was not visible in the satellite image (Fig. 3.2) because of vegetation cover.

Figure 10(b) shows the simulation using Flow-R, which is similar to Fig. 3.10(a). However, there is susceptibility to spreading over a larger area, especially near the toe. Figure 3.10(c) shows the results for RAMMS, which also simulates a similar flow path as observed in the field. Larger spreading occurred near the initiation zone, and some amount of debris flowed toward the channel at the right. Moreover, a considerable amount of debris ( $< 0.5$  m thick) crossed the road in this case.

Figures 3.10(a–c) also show the simulations of a channelized flow that originated from point B. Flow occurred through a pre-existing gully, and the trace of a long debris flow path along this

gully was observed in the Google Earth image in 2021 after the event. The materials flowed more than 870 m along the curved path, where the maximum elevation difference was ~248 m. All three programs could simulate this debris flow. However, at the toe, the pattern of spreading is different. In DebrisFlow Predictor, the flow continued up to point B', and then spreading started to occur through different channels. A closer examination of the bare earth image around point B' shows the existence of some shallow channels through which debris diverted into separate paths in the simulation using DebrisFlow Predictor. On the other hand, in Flow-R and RAMMS, some debris started to divert as a fan prior to reaching the road (point B'). The spreading near the toe is more in RAMMS than in Flow-R. While DebrisFlow Predictor could simulate the channelized flow, the following points are to be noted in the parameter selection in Table 3.2. In the channelized case, the material flows primarily through the channel bounded by side slopes without much spreading and associated deposition. Therefore, a lower value of the maximum spawn ( $N_{\max}$ ), deposition multiplier, and mass loss per 45° turns should be used. Otherwise, a smaller runout distance will be obtained.

### ***3.5.3 Site 3: Solalex-Anzeindaz***

Unlike Sites 1 and 2, where the individual debris flow was the focus (Figs. 3.1 & 3.2), the accumulation of debris in Site 3 (Fig. 3.3) resulted from multiple events. In the present study, three debris flow paths (along P1, P2, and P3 in Fig. 3.3(a)) are considered. The debris flow along these paths hit the upper road and the highway below. Figure 3.3(b) shows a considerable amount of debris on the highway, which might have come from the multiple upslope failure. It is very difficult to model multiple events of failure because the release volume, initiation locations, and sequence of the events are not known. Therefore, the aim of the present study is to predict the flow path and

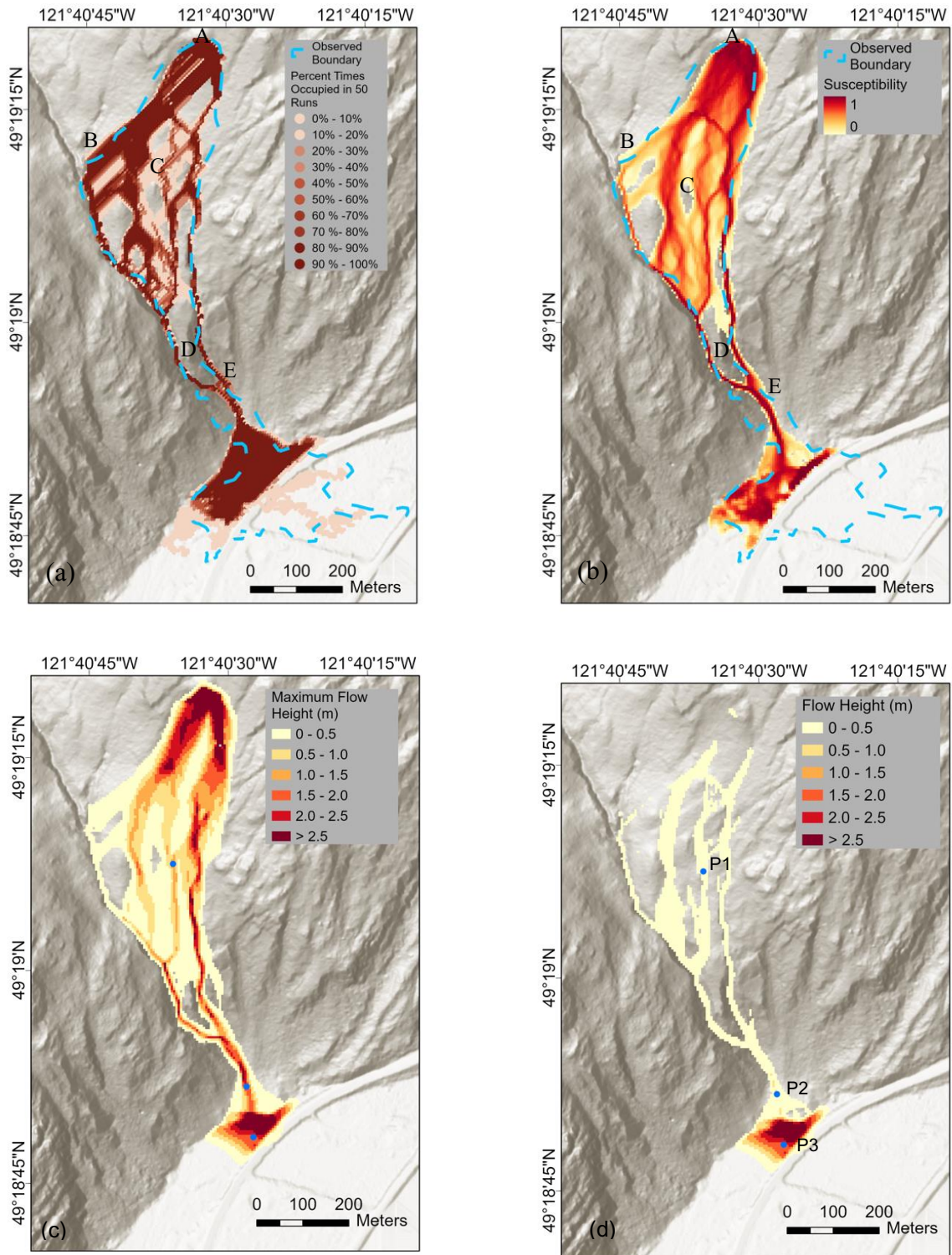


**Fig. 3.4.** Simulated runout at Site 1: (a) DebrisFlow Predictor; (b) Flow-R; and (c) RAMMS flood height without erosion; (d) RAMMS final deposition height without erosion

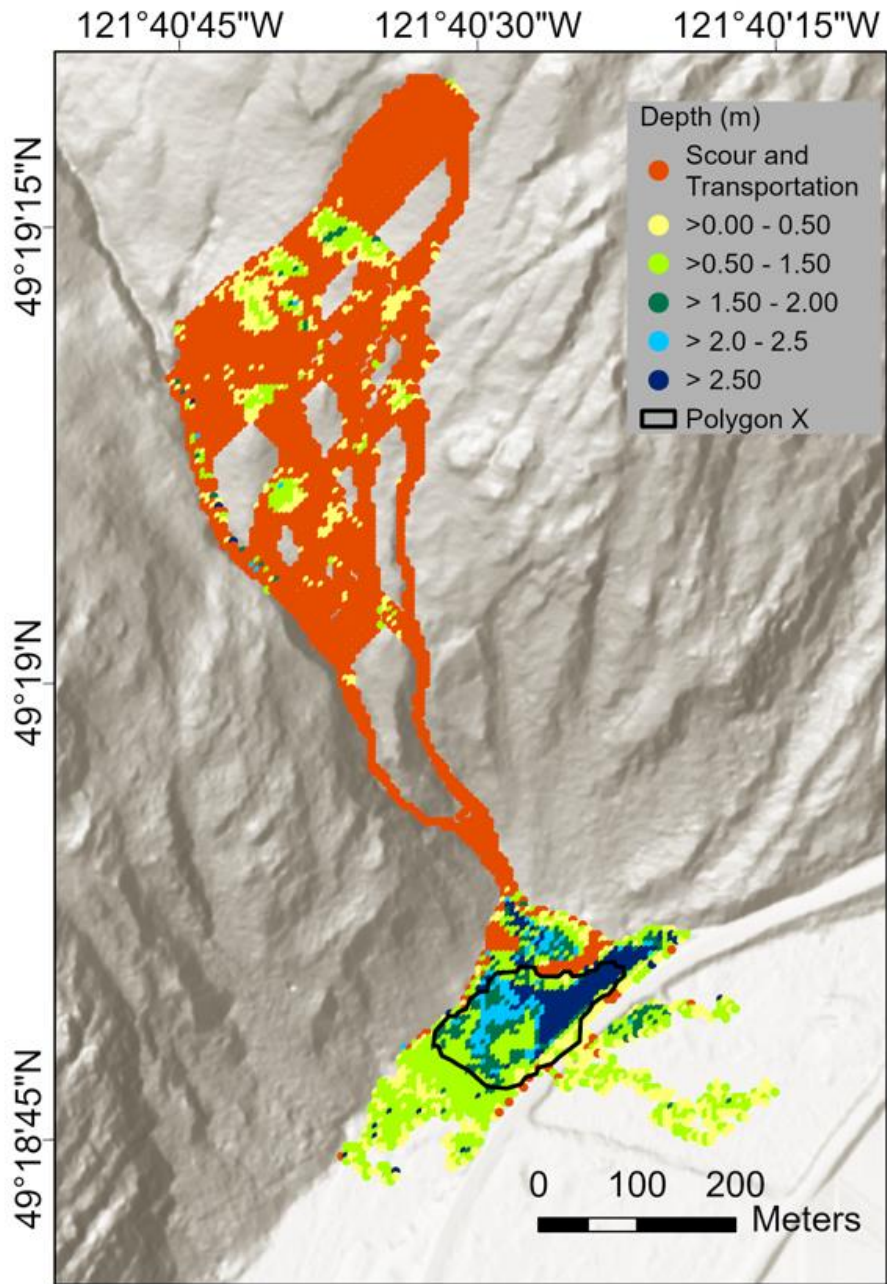


**Fig. 3.5.** Simulated scour and deposition depths at Site 1 using DebrisFlow Predictor

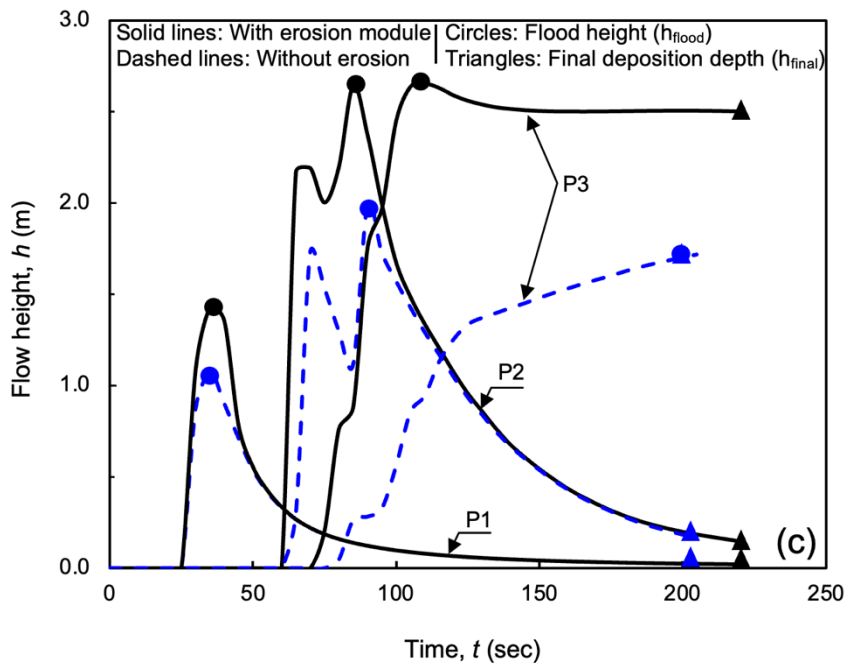
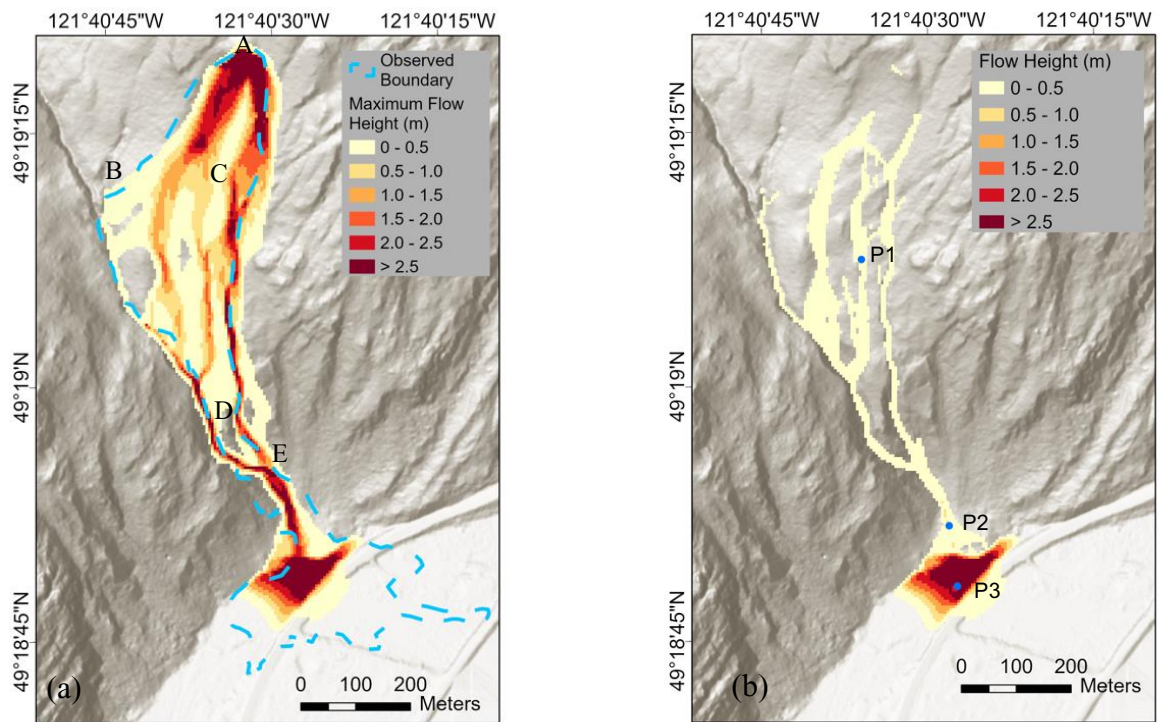


**Fig. 3.6.** Effects of erosion in RAMMS: (a) flood height; (b) final deposition depth; (c) variation of flow height with time at three locations shown in Figs. 3.4(d) and 3.6(b)

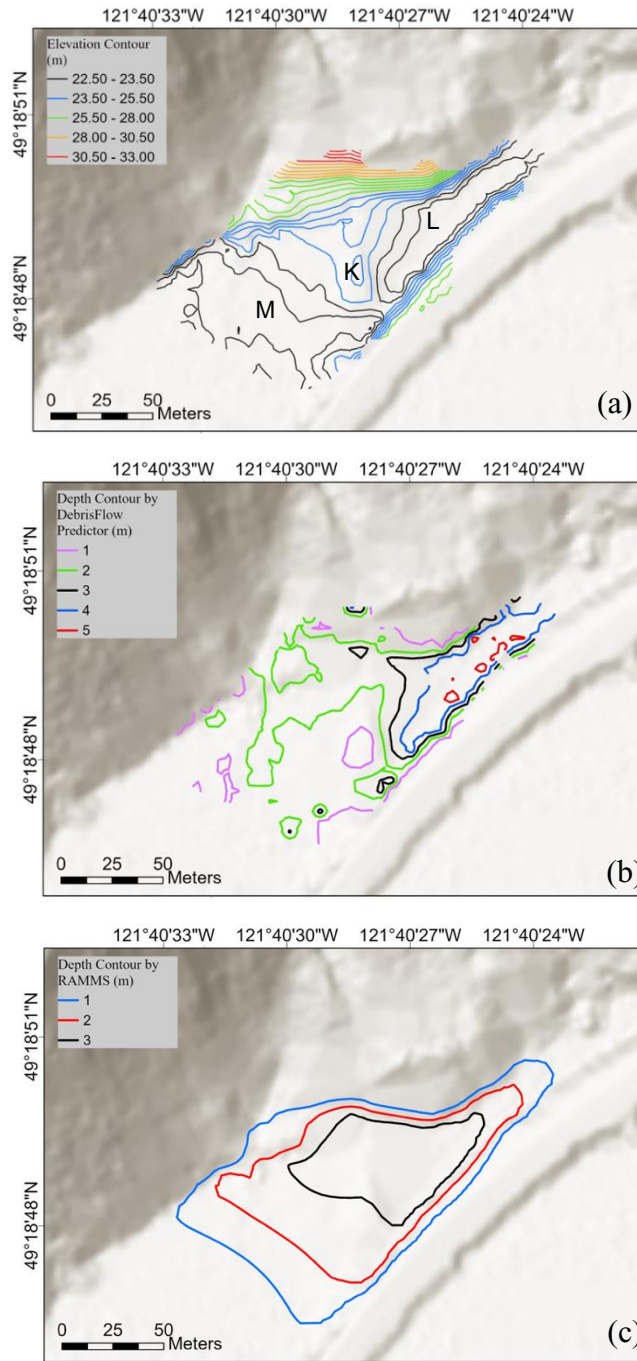


**Fig. 3.7.** Ground elevation and deposition height near the toe: (a) ground elevation before the event; (b) debris thickness obtained from DebrisFlow Predictor; (c) final deposition height from RAMMS with erosion module

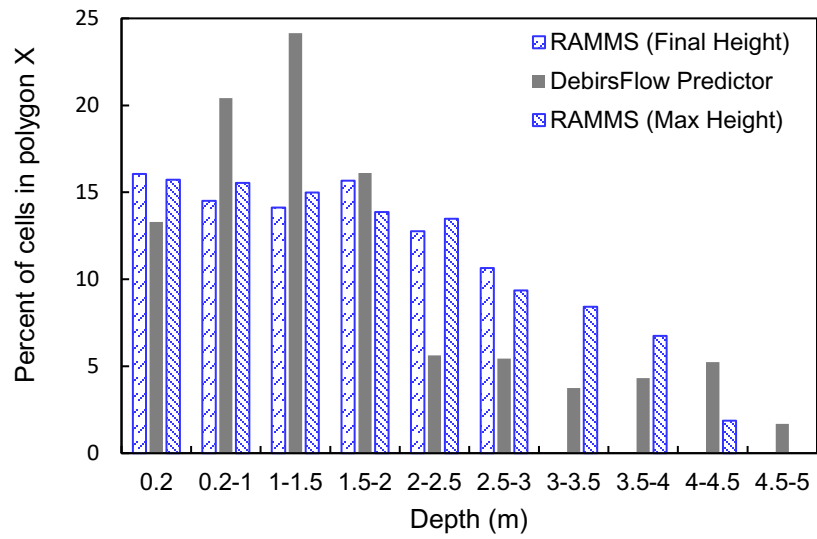


**Fig. 3.8.** Thickness of debris in polygon X

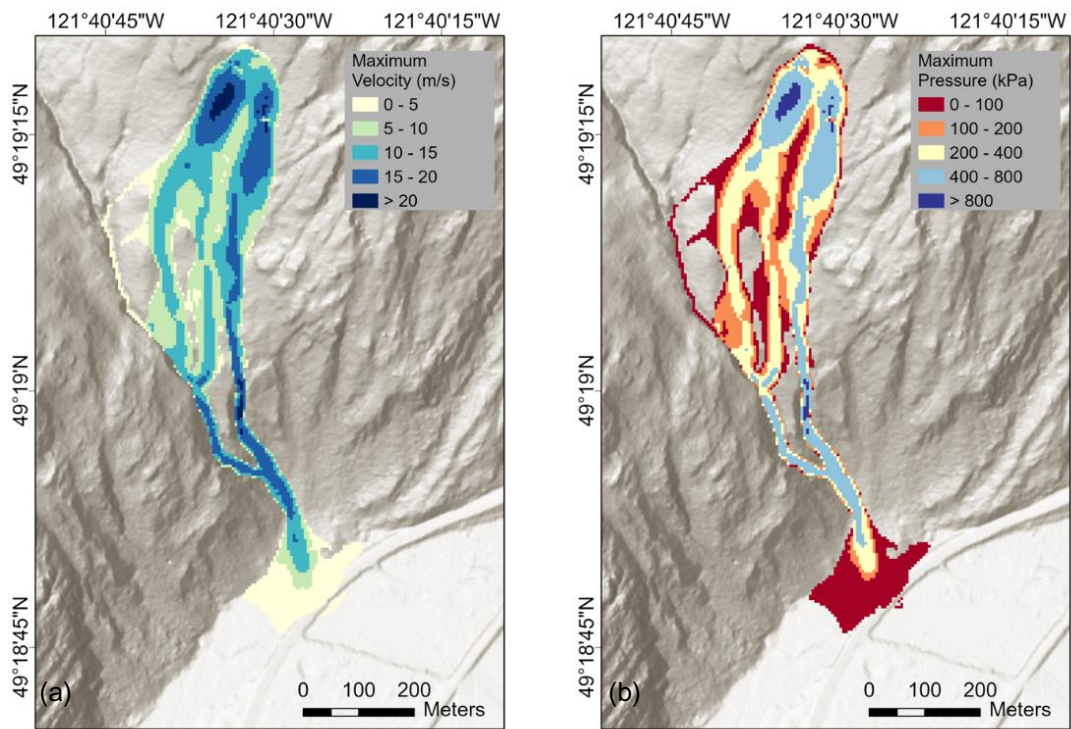


**Fig. 3.9.** Maximum velocity and maximum pressure map at Site 1 generated by RAMMS

spreading when several failures occur at the top at the same time. Note that debris originating from different locations might interact with each other during downslope movement.

Defining the initiation zone for multiple events is a challenging task. In Flow-R, there is an option for automatic identification of the initiation zone based on several factors (e.g., slope angle, curvature, flow accumulation), which gives a general idea of the potential initiation zone. For this site, there is no vegetation in the upslope areas from where failure was initiated, and 10-cm high-resolution maps are available. Interpreting the scars from the map at the top of the flow path and examining the results of the automatic identification of the initiation zone from Flow-R, ten possible initiation zones are defined (Fig. 3.3(a)).

Figure 3.11 shows the simulation results of 10 events in Site 3. Again, the simulations are performed using DebrisFlow Predictor, Flow-R, and RAMMS (without erosion). Figures 3.11(a–c) show that all three programs provide almost similar runout extent. Flow paths in the downslope areas are very similar to that observed in the field (Fig. 3.3). For example, around point P1, the flow diverted into multiple channels, while the flow primarily occurs through one channel around point P2 and two channels around point P3, which are very similar to that observed in the field (Figs. 3.3(a) & 3.3(b)). In the upslope areas, simulations show flow through some narrow paths starting from the initiation zone. However, the trace of widely spread debris flow path is observed in the field, which is because of the occurrence of multiple events over the period of time, which has not been simulated in this study. In summary, all three programs can simulate the debris flow paths for a given origin. Using Flow-R, a regional-scale susceptibility map for debris flow of an area could be developed as Horton et al. (2013). Flow-R could also be used for preliminary estimation of the initiation zones of a debris flow fan. However, if detailed information is needed

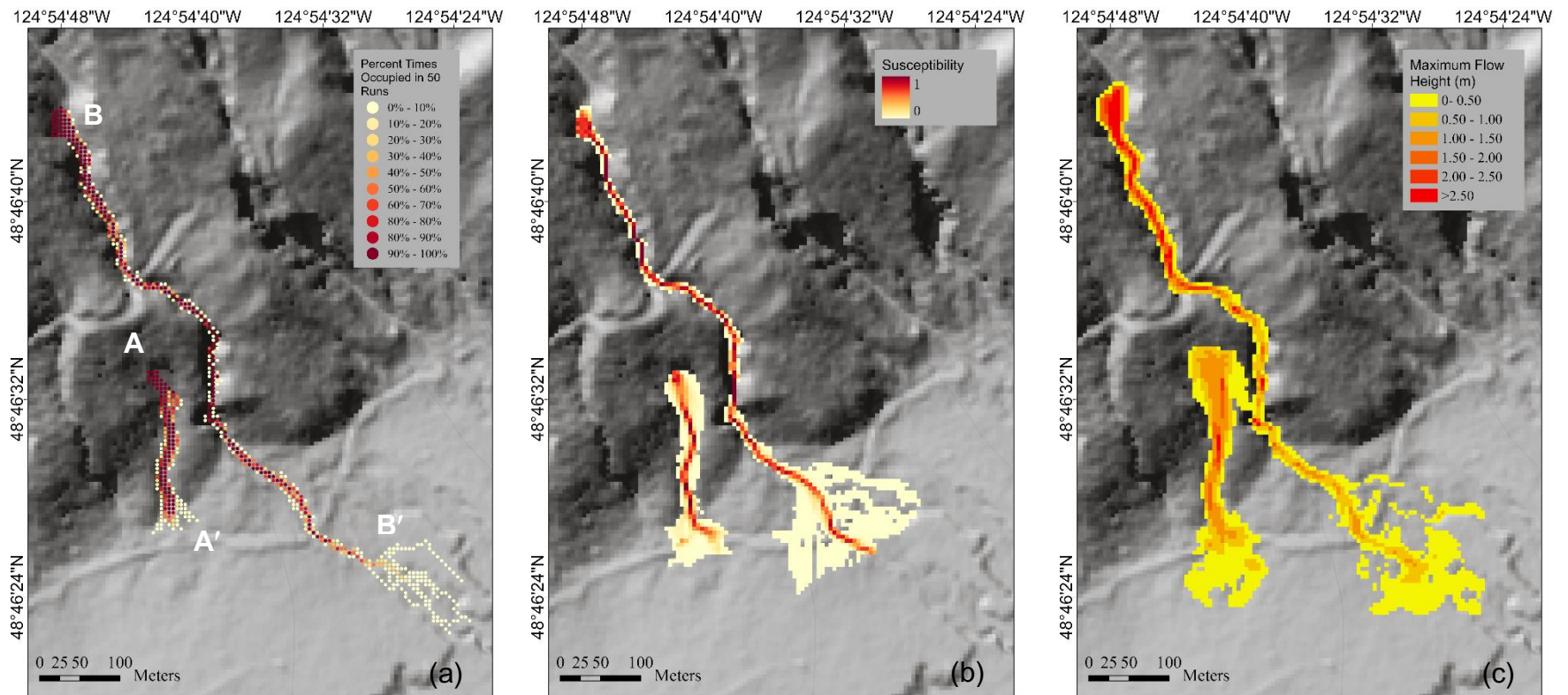


**Fig. 3.10.** Channelized and unchannelized debris flow at Site 2: (a) DebrisFlow Predictor; (b) Flow-R; (c) RAMMS without erosion

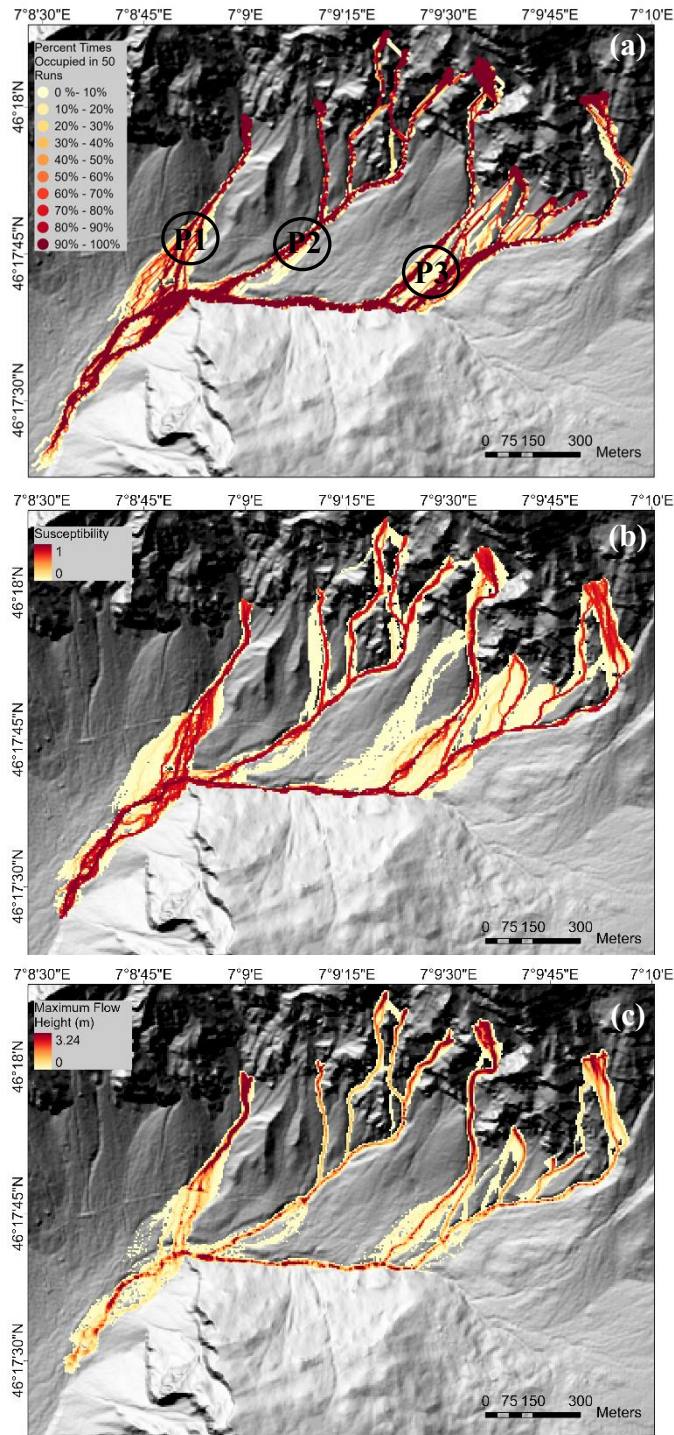


**Fig. 3.11.** Simulation results for Site 3: (a) DebrisFlow Predictor; (b) Flow-R; (c) RAMMS

without erosion

(e.g., flow height), DebrisFlow Predictor and RAMMS could be used in conjunction with Flow-R.

### **3.6 Conclusions**

In the present study, three debris flow programs named Flow-R, DebrisFlow Predictor, and RAMMS were used to model single and multiple debris flow events at three different sites where both channelized and unchannelized type debris flows occurred. The first two programs were developed from empirical/probabilistic approaches, while the last one is a mechanics-based numerical tool, where a simplified material model was implemented. Numerical analyses show that all three programs can simulate the debris flow at these sites, provided appropriate input parameters are used. The following conclusions can be drawn from this study.

- i) The back-calculated values that give the best simulation results compared to the field observation for the three cases considered in this study are within the ranges recommended in previous studies.
- ii) Reducing the number of the maximum spawns allowed in DebrisFlow Predictor, the lateral spreading could be reduced in channelized flow to simulate the runout as observed in the field.
- iii) Erosion at the base could play a major role, and this process can be modelled using RAMMS. When sufficient information is not available from the field, the erosion zone identified by DebrisFlow Predictor could be used as an input for RAMMS modelling.
- iv) For a debris flow fan of multiple events, Flow-R could be used for the preliminary development of debris flow susceptibility maps, identification of initiation zones, and critical

flow paths for hazard assessment. DebrisFlow Predictor and RAMMS can then be used to get more information (e.g., the thickness of debris and flow velocity) for decision-making.

Finally, it should be noted that a direct comparison of the performance of these programs is difficult because the modelling approach and the algorithms used are very different. Also, this study has some limitations. For Sites 1 and 2, limited field information is available, which includes post-event DEM and field measurement of debris thickness. Further studies are required for a better calibration of the model parameters when additional field data is available.

## **Chapter 4: Conclusions and Future Recommendations**

### **4.1 Conclusions**

Debris flow could be one of the most dangerous and unpredictable events that could cause loss of lives and damage properties, infrastructure, and the environment. Therefore, accurate prediction of the runout extent and hazard intensity parameters, including velocity, volume, depth of debris, and impact pressure, are necessary for any development in landslide-prone areas. Various tools and techniques have been developed to assess the occurrence of debris flow. For example, high-resolution Digital Elevation Models (DEM) have been developed using LiDAR data and satellite images. The development of such DEM helps to assess pre- and post-slide information on the area of landslide and debris flow extent.

Over the last several decades, a number of numerical modelling techniques have also been developed, which can incorporate many complex phenomena, including the proper use of advanced DEM and the evaluation of initiation zones. Still, most of the simulations are performed with simplified models. For example, the behaviour of the complex mixture of debris is modelled using simple models. In many cases, empirical-statistical approaches are used to simulate the flow. Therefore, selecting model input parameters for these numerical methods is the biggest challenge for practitioners as it might be site-dependent. In other words, model parameters should be obtained through calibration of the simulation results with case history data.

The present study simulates the runout of some reported debris flows from three different geological settings using three computer programs named DebrisFlow Predictor, Flow-R, and RAMMS. The first two programs are based on the empirical–statistical approach, while the last one is based on the numerical approach. All the simulations are performed using 5 m × 5 m DEM

and with critically evaluated parameters from field observation. While the specific conclusions are presented in Chapter 3, the following are the overall conclusions of this study.

The back-calculated model parameters that can simulate the observed runout extent fall within the ranges recommended in previous studies. In DebrisFlow Predictor, reducing the number of maximum spawns allowed, the lateral spreading could be reduced in channelized flow. RAMMS can model the erosion process of debris flow at the base while flowing. It is difficult to determine the erosion zone when sufficient information is unavailable from the field (i.e., LiDAR-derived post-event DEM). To overcome it, the erosion zone identified by DebrisFlow Predictor could be used as an input for RAMMS modelling. While dealing with a debris flow fan that experienced multiple events, Flow-R could be used for the initial development of debris flow susceptibility maps, identification of initiation zones, and critical flow paths for hazard assessment. DebrisFlow Predictor and RAMMS can then be used to get more information (e.g., the thickness of debris and flow velocity) to support the decision-making process.

## **4.2 Future Recommendations**

Although the three computer programs used in this study can simulate the observed debris flows at three different sites, this study has some limitations which could be addressed in future studies.

- i) In many cases, limited field information is available, which includes post-event DEM and field measurement of debris thickness. Further studies are required for a better calibration of the model parameters when these additional field data are available.
- ii) The erosion module of RAMMS is based on observed debris flows in Illgraben valley in Switzerland. Applying this module in other geological settings is challenging. Further studies are needed to evaluate the suitability of this module in other geological settings.

iii) RAMMS and Flow-R were originally designed using data from debris flow events in Switzerland, while DebrisFlow Predictor was specifically developed based on debris flow information in British Columbia. Therefore, further work with larger datasets is needed to get more standardized values of the parameters of these three programs for other regions.

## REFERENCES

- Abe, K., and Konagai, K. 2016. Numerical simulation for runout process of debris flow using depth-averaged material point method. *Soils and Foundations*, 56(5): 869–888.
- Abraham, M.T., Satyam, N., Pradhan, B., and Tian, H. 2022. Debris flow simulation 2D (DFS 2D): Numerical modelling of debris flows and calibration of friction parameters. *Journal of Rock Mechanics and Geotechnical Engineering*, 14(6): 1747–1760.
- Anaconda, P.I., Norton, K., Mackintosh, A., Escobar, F., Allen, S., Mazzorana, B., and Schaefer, M. 2018. Dynamics of an outburst flood originating from a small and high-altitude glacier in the Arid Andes of Chile. *Natural Hazards*, 94: 93–119.
- Anderson, S.A., and Sitar, N. 1995. Analysis of rainfall-induced debris flows. *Journal of Geotechnical Engineering*, 14(6): 544–552.
- Arghya, A.B., Hawlader, B., and Guthrie, R., 2022a. A comparison of two runout programs for debris flow assessment at the Solalex-Anzeindaz region of Switzerland. *In: 8<sup>th</sup> Canadian Conference on Geotechnique and Natural Hazards*, Quebec, Canada.
- Arghya, A.B., Hawlader, B., Guthrie, R., and Knibbs, G., 2022b. Simulation of some debris flows in Klanawa watershed in Vancouver, British Columbia. *In: 75<sup>th</sup> Canadian Geotechnical Conference*, Calgary, Canada.
- Badoux, H. and Gabus, J.H. 1990. Atlas géologique de la Suisse, feuille n° 1285, 1:25000, Les Diablerets avec notice explicative (In French).
- Bartelt, P., Buehler, Y., Christen, M., Deubelbeiss, Y., Graph, C., McArdell, B., Salz, M., and Schneider, M. 2022. RAMMS user manual v1.8 debris flow.

- Bathurst, J.C., Burton, A., and Ward, T.J. 1997. Debris flow runout and landslide sediment delivery model tests. *Journal of Hydraulic Engineering*, 123(5): 410–419.
- Barpi, F., Borri-Brunetto, M., and Veneri, L.D. 2007. Cellular-automata model for dense-snow avalanches. *Journal of Cold Regions Engineering*, 21(4): 121–140.
- Baumann, V., Wick, E., Horton, P., and Jaboyedoff, M. 2011. Debris flow susceptibility mapping at a regional scale along the national road N7, Argentina. *In: 14th Pan-American Conference on Soil Mechanics and Geotechnical Engineering*, Toronto, Ontario, Canada.
- Begueria, S., Van Asch, Th.W.J., Malet, J.P., and Gröndahl, S. 2009. A GIS-based numerical model for simulating the kinematics of mud and debris flows over complex terrain. *Natural Hazards and Earth System Sciences*, 9: 1897–1909.
- Benda, L.E., and Cundy, T.W. 1990. Predicting deposition of debris flows in mountain channels. *Canadian Geotechnical Journal*, 27(4): 409–417.
- Berger, C., McArdell, B.W., and Lauber, G., 2012. Debris flow modeling in illgraben, switzerland, using the numerical 2D model RAMMS. *In: 12<sup>th</sup> Congress INTERPRAEVENT*, 37.
- Bezák, N., Sodnik, J., and Mikoš, M. 2019. Impact of a random sequence of debris flows on torrential fan formation. *Geosciences*, 9(2): 64.
- Bezák, N., Jež, J., Sodnik, J., Auflič, J.M., and Mikoš, M. 2020. An extreme May 2018 debris flood case study in northern slovenia: analysis, modelling, and mitigation. *Landslides*, 17: 2373–2383.
- Bianco, G., and Franzi, L. 2000. Estimation of debris-flow volumes from storm events. *In: Debris-Flow Hazards Mitigation: Mechanics, Prediction and Assessment*, 441–448.
- Blahut, J., Horton, P., Sterlacchini, S., and Jaboyedoff, M. 2010. Debris flow hazard modelling on medium scale: Valtellina di Tirano, Italy. *Natural Hazards and Earth System Sciences*, 10(11): 2379–2390.

- Blais-Stevens, A., and Behnia, P. 2016. Debris flow susceptibility mapping using a qualitative heuristic method and Flow-R along the Yukon Alaska Highway Corridor, Canada. *Natural Hazards and Earth System Sciences*, 16(2): 449–462.
- Bovis, M.J., and Jakob, M. 1999. The role of debris supply conditions in predicting debris flow activity. *Earth Surface Processes and Landforms*, 24(11): 1039–1054.
- Bui, H.H., Fukagawa, R., Sako, K., and Wells, J.C. 2011. Slope stability analysis and discontinuous slope failure simulation by elasto-plastic smoothed particle hydrodynamics (SPH). *Géotechnique*, 61(7): 565–574.
- Calista, M., Menna, V., Mancinelli, V., Sciarra, N., and Miccadei, E. 2020. Rockfall and debris flow hazard assessment in the SW escarpment of montagna del morrone ridge (Abruzzo, Central Italy). *Water*, 12(4): 1206.
- Costa, J.E. 1984. Physical geomorphology of debris flows. In: *Developments and Applications of Geomorphology*, 268–317.
- Cesca, M., and D’Agostino, V. 2008. Comparison between FLO-2D and RAMMS in debris-flow modelling: A case study in the dolomites. *WIT Transactions on Engineering Science*, 60: 197–206.
- Christen, M., Kowalski J., and Bartelt, P. 2010 RAMMS: Numerical simulation of dense snow avalanches in three-dimensional terrain. *Cold Regions Science and Technology*, 63(1-2): 1–14.
- Chung, M.C., Chen, C.H., Lee, C.F., Huang, W.K., and Tan, C.H. 2018. Failure impact assessment for large-scale landslides located near human settlement: Case study in southern Taiwan. *Sustainable Times*, 10(5): 1–25.

- Chattoraj, S.L., Champati, R.P.K., and Kannaujiya, S. 2019. Simulation outputs of major debris flows in Garhwal Himalaya: A geotechnical modeling approach for hazard mitigation. *Remote Sensing of Northwest Himalayan Ecosystems*, 37–56.
- Chattoraj, S.L., Champati R.P.K., Pardeshi, S., Gupta, V., and Ketholia, Y. 2018. 3-dimensional modeling of 2014-Malin landslide, Maharashtra using satellite-derived data: A quantitative approach to numerical simulation technique. *Natural Hazards And Earth System Sciences Discussions*, 1–19.
- Chen, H., and Lee, C.F. 2004. Geohazards of slope mass movement and its prevention in Hong Kong. *Engineering Geology*, 76(1-2): 3–25.
- Chen, H.X., Zhang, L.M., and Zhang, S. 2014. Evolution of debris flow properties and physical interactions in debris-flow mixtures in the Wenchuan earthquake zone. *Engineering Geology*, 182: 136–147.
- Chiarle, M., Iannotti, S., Mortara, G., and Deline, P. 2007. Recent debris flow occurrences associated with glaciers in the Alps. *Global and Planetary Change*, 56(1–2): 123–136.
- Claessens, L., Heuvelink, G.B.M., Schoorl, J.M. and Veldkamp, A. 2005. DEM resolution effects on shallow landslide hazard and soil redistribution modelling. *Earth Surface Processes and Landforms*, 30(4): 461–477.
- Clark, B. 2018. Numerical modelling of debris flow hazards using computational fluid dynamics. Master's Thesis, Norwegian University of Science and Technology, Norway.
- Corominas, J. 1996. The angle of reach as a mobility index for small and large landslides. *Canadian Geotechnical Journal*, 33(2): 260–271.
- Dash, R.K., Kanungo, D.P., and Malet, J.P. 2021. Runout modelling and hazard assessment of tangni debris flow in Garhwal Himalayas, India. *Environmental Earth Sciences*, 80: 1–19.

- Davies, T.R.H. 1990. Debris-flow surges — Experimental simulation. *Journal of Hydrology (New Zealand)*, 29(1): 18–46.
- D’Ambrosio, D., Di Gregorio, S., Iovine, G., Lupiano, V., Rongo, R., V., and Spataro, W. 2003a. First simulations of the Sarno debris flows through cellular automata modelling. *Geomorphology*, 54(1–2): 91–117.
- D’Ambrosio, D., Di Gregorio, S., and Iovine, G. 2003b. Simulating debris flows through a hexagonal cellular automata. *Natural Hazard and Earth System Sciences*, 3: 545–559.
- Decaulne, A., Sæmundsson, T., and Petursson, O. 2005. Debris flow triggered by rapid snowmelt: A case study in the Gleiarhjalli area, Northwestern Iceland. *Geografiska Annaler: Series A, Physical Geography*, 87(4): 487–500.
- De Finis, E., Gattinoni, P., Marchi, L., and Scesi, L. 2017a. Modeling debris flows in anomalous basin-fan systems. *In: Advancing Culture of Living with Landslides*. Springer International Publishing.
- De Finis, E., Gattinoni, P., and Scesi, L. 2017b. Forecasting the hydrogeological hazard in the anomalous basin-fan system of Sernio (Northern Italy). *In: Advancing Culture of Living with Landslides*. Springer International Publishing.
- De Finis, E., Gattinoni, P., Marchi, L., and Scesi, L. 2018. Anomalous alpine fans: From the genesis to the present hazard. *Landslides*, 15: 683–694.
- Delmonaco, G., Leoni, G., Margottini, C., Puglisi, C., and Spizzichino, D. 2003. Large scale debris-flow hazard assessment: A geotechnical approach and GIS modeling. *Natural Hazards and Earth System Sciences*, 3: 443–455.
- Dey, R., Hawlader, B., Phillips, R., and Soga, K. 2015. Large deformation finite-element modeling of progressive failure leading to spread in sensitive clay slopes. *Géotechnique*, 65(8): 657–668.

- Dietrich, A., and Krautblatter, M. 2019. Deciphering controls for debris-flow erosion derived from a LiDAR-recorded extreme event and a calibrated numerical model (Roßbichelbach, Germany). *Earth Surface Process Landforms*, 44: 1346–1361.
- Do, H.M., Yin, K.L., and Guo, Z.Z. 2020. A comparative study on the integrative ability of the analytical hierarchy process, weights of evidence and logistic regression methods with the Flow-R model for landslide susceptibility assessment. *Geomatics, Natural Hazards and Risk*, 11(1): 2449–2485.
- dos Santos Corrêa, C.V., Vieira Reis, F.A.G., do Carmo Giordano, L., Cabral, V.C., Targa, D.A., and Brito, H.D. 2019. Possibilities and limitations for the back analysis of an event in mountain areas on the coast of São Paulo state, Brazil using RAMMS numerical simulation. *In: 7<sup>th</sup> International Conference on Debris-Flow Hazards Mitigation*.
- Fannin, R.J., and Wise, M.P. 2001. An empirical-statistical model for debris flow travel distance. *Canadian Geotechnical Journal*, 38: 982–994.
- Federico, F., and Cesali, C. 2015. An energy-based approach to predict debris flow mobility and analyze empirical relationships. *Canadian Geotechnical Journal*, 52(12): 2113–2133.
- Fischer, L., Rubensdotter, L., Sletten, K., Stalsberg, K., Melchiorre, C., Horton, P., and Jaboyedoff, M. 2012. Debris flow modeling for susceptibility mapping at regional to national scale in Norway. *11<sup>th</sup> International and 2nd North American symposium on landslides, Banff, Alberta, Canada*, 723–729.
- Fischer, F. Von., Keiler, M., and Zimmermann, M. 2016. Modelling of individual debris flows using Flow-R: A case study in four Swiss torrents. *In: 13<sup>th</sup> Congress Interpravent, Lucerne, Switzerland*, 257–264.

- FLO-2D Software Inc. 2007. FLO-2D user's manual. Version 2007.06. Froese, C.R., and Moreno, F. 2014. Structure and components for the emergency response and warning system on Turtle Mountain, Alberta, Canada. *Natural Hazards*, 70(3): 1689–1712.
- Franco-Ramos, O., Ballesteros-Cánovas, J.A., Figueroa-García, J.E., Vázquez-Selem, L., Stoffel, M., and Caballero, L. 2020. Modelling the 2012 lahar in a sector of Jamapa Gorge (Pico de Orizaba Volcano, Mexico) using RAMMS and Tree-Ring Evidence. *Water*, 12(2): 333.
- Frank, F., McArdell, B.W., Huggel, C., and Vieli, A. 2015. The importance of entrainment and bulking on debris flow runout modeling: Examples from The Swiss Alps. *Natural Hazards and Earth System Sciences*, 15(11): 2569–2583.
- Frank, F., McArdell, B.W., Oggier, N., Baer, P., Christen, M., and Vieli, A. 2017. Debris-flow modeling at Meretschibach and Bondasca catchments, Switzerland: Sensitivity testing of field-data-based entrainment model. *Natural hazards and Earth System Sciences*, 17(5): 801–815.
- Frey, H., Huggel, C., Bühler, Y., Buis, D., Burga, M.D., Choquevilca, W., Fernandez, F., García Hernández, J., Giráldez, C., Loarte, E., Masias, P., Portocarrero, C., Vicuña, L., and Walser, M. 2016. A robust debris-flow and GLOF risk management strategy for a data-scarce catchment in Santa Teresa, Peru. *Landslides*, 13(6): 1493–1507.
- Fiorillo, F., and Wilson, R.C. 2004. Rainfall induced debris flows in pyroclastic deposits, Campania (Southern Italy). *Engineering Geology*, 75(3–4): 263–289.
- Gamma, P. 2000. dfwalk—Ein Murgang-simulations programm zur Gefahrenzonierung (dfwalk—A debris flow simulation program for natural hazard zonation. *Geographica Bernensia* G66, Bern, Switzerland (in German).
- Gan, J., and Zhang, Y.S. 2019. Numerical simulation of debris flow runout using RAMMS: A case study of Luzhuang Gully in China. *Computer Modeling in Engineering and Sciences*, 981–1009.

- Gardezi, H., Bilal, M., Cheng, Q., Xing, A., Zhuang, Y., and Masood, T. 2021. A comparative analysis of Attabad Landslide on January 4, 2010, using two numerical models. *Natural Hazards*, 107(1): 519–538.
- Grasso, K., Wasklewicz, T., and Hur, M. 2022. Informing zoning ordinance decision-making with the aid of probabilistic debris flow modeling. *In: 8<sup>th</sup> Canadian Conference on Geotechnique and Natural Hazards*, Quebec, Canada.
- Guthrie, R.H. 2009. The occurrence and behavior of rainfall-triggered landslides in coastal British Columbia. Ph.D. Dissertation, The University of Waterloo, Ontario, Canada.
- Guthrie, R.H. 2021. Debris Flow Runout Model: North Shore Cowichan Lake, Stantec Consultancy Ltd, Canada.
- Guthrie, R.H., and Befus, A. 2021. DebrisFlow Predictor: An agent-based runout program for shallow landslides. *Natural Hazards and Earth System Sciences*, 21(3): 1029–1049.
- Guthrie, R.H., and Brown, K.J. 2008. Denudation and landslides in coastal mountain watersheds: 10,000 years of erosion. *Geographica Helvetica*, 63: 26–33.
- Guthrie, R.H., Deadman, P., Cabrera, R., and Evans, S.G. 2008. Exploring the magnitude-frequency distribution: A cellular automata model for landslides. *Landslides*, 5: 151–159.
- Guthrie, R.H., Hockin, A., Colquhoun, L., Nagy, T., Evans, S.G., and Ayles, C. 2010. An examination of controls on debris flow mobility: Evidence from coastal British Columbia. *Geomorphology*, 114(4): 601–613.
- Guzzetti, F., Peruccacci, S., Rossi, M., and Stark, C.P. 2008. The rainfall intensity–duration control of shallow landslides and debris flows: An update. *Landslides*, 5(1): 3–17.

- Han, Z., Li, Y., Huang, J., Chen, G., Xu, Li., Tang, C., Zhang, H., Shang, Y. 2017. Numerical simulations for runout extent of debris flows using an improved cellular automation model. *Bulletin of Engineering Geology and the Environment*,76: 961–974.
- Hansen, K. 2021. Severe flooding in the Pacific Northwest. Retrieved from <https://earthobservatory.nasa.gov/images/149100/severe-flooding-in-the-pacific-northwest>.
- Holmgren, P. 1994. Multiple flow direction algorithms for runoff modelling in grid based elevation models: An empirical evaluation. *Hydrological Processes*, 8(4): 327–334.
- Harianto, T., Muhiddin, A.B., Nur, S.H., and Wibowo, C.E. 2021. Properties of debris flow deposits in Masamba, South Sulawesi, Indonesia. *In: IOP Conference Series: Earth and Environmental Science*, 921(1): 012062.
- Hatchett, B., Bacon, S., Brandt, W.T., Heggli, A., and Lancaster, J. 2023. Snowmelt-triggered debris flows in seasonal snowpacks. *E3S Web of Conferences*, 415: 04006.
- Hauser, D. 2011. Interaction between debris flow and forest: Reconstruction of events using RAMMS. Master's Thesis, ETH, Zürich, Switzerland.
- Highland, L., and Bobrowsky, P. 2013. *The landslide handbook-A guide to understanding landslides: a landmark publication for landslide education and preparedness*, Springer, Berlin.
- Horton, P., Jaboyedoff, M., Rudaz, B., and Zimmermann, M. 2013. Flow-R, a model for susceptibility mapping of debris flows and other gravitational hazards at a regional scale. *Natural Hazards and Earth System Sciences*, 13(4): 869–885.
- Huang, D., Jiang, Y. J., Qiao, J.P., and Wang, M. 2017. Hazard assessment comparison of Tazhiping landslide before and after treatment using the finite-volume method. *Natural Hazards and Earth System Sciences*, 17(9): 1611–1621.

- Huggel, C., Kääb, A., Haeberli, W., Teysseire, P., and Paul, F. 2002. Remote sensing based assessment of hazards from glacier lake outbursts: A case study in the Swiss Alps. *Canadian Geotechnical Journal*, 39(2): 316–330.
- Hungr, O. 1995. A model for the runout analysis of rapid flow slides, debris flows and avalanches. *Canadian Geotechnical Journal*, 32, 610–623.
- Hungr, O. 2001. A review of the classification of landslides of the flow type. *Environmental and Engineering Geoscience*, 8(3): 221–238.
- Hungr, O. 2005. A model for the runout analysis of rapid flow slides, debris flows, and avalanches. *Canadian Geotechnical Journal*, 32: 610–623.
- Hungr, O., Corominas, J., and Eberhardt, E., 2005. Estimating landslide motion mechanism, travel distance and velocity, landslide risk management. CRC Press, 99–128.
- Hungr, O., Leroueil, S., and Picarelli, L. 2013. The Varnes classification of landslide types, an update. *Landslides*, 11(2).
- Hungr, O., McDougall, S., Bovis, M. 2005. Entrainment of material by debris flows. *In: Debris-flow hazards and related phenomena*, 135–158.
- Hungr, O., McDougall, S., Wise, M., Cullen, M. 2008. Magnitude-frequency relationships of debris flows and debris avalanches in relation to slope relief. *Geomorphology*, 96: 355–365.
- Hungr, O., and McDougall, S. 2009. Two numerical models for landslide dynamic analysis. *Computers and Geosciences*, 35(5): 978–992.
- Hunter, G., and Fell, R. 2003. Travel distance angle for “rapid” landslides in constructed and natural soil slopes. *Canadian Geotechnical Journal*, 40(6): 1123–1141.

- Hürlimann, M., Rickenmann, D., Medina, V., and Bateman, A. 2008. Evaluation of approaches to calculate debris-flow parameters for hazard assessment. *Engineering Geology*, 102 (3-4): 152–163.
- Hussin, H.Y. 2011. Probabilistic Runout modeling of a debris flow in Barcelonnette, France. Master's Thesis, University of Twente, France.
- Hussin, H.Y., Quan Luna, B., VanWesten, C. J., Christen, M., Malet, J.-P., and Van Asch, T. W. J. 2012. Parameterization of a numerical 2-D debris flow model with entrainment: A case study of the Faucon catchment, Southern French Alps. *Natural Hazards Earth System Science*, 12: 3075–3090.
- Hutchinson, J.N. 1986. A sliding-consolidation model for flow slides. *Canadian Geotechnical Journal*, 23: 115–126.
- Ikeya, H. 1981. A method of designation for area in danger of debris flow, erosion and sediment transport in Pacific Rim steeplands. *IAHS Special Publication*. 132: 576–588.
- Iovine, G., Di Gregorio, S., Lupiano, V. 2003. Debris-flow susceptibility assessment through cellular automata modeling: An example from 15–16 December 1999 Disaster at Cervinara and San Martino Valle Caudina (Campania, Southern Italy). *Natural Hazards Earth System Science*, 3: 457–468.
- Iverson, R.M. 1997. The physics of debris flows. *Reviews of Geophysics*, 35(3): 245–296.
- Iverson, R.M., and Denlinger, R. P. 1987. The physics of debris flows—A conceptual assessment. *In: International symposium on erosion and sedimentation in the Pacific Rim*, 155–165.
- Iverson, R.M., and George, D.L. 2016. Modelling landslide liquefaction, mobility bifurcation and the dynamics of the 2014 Oso disaster. *Géotechnique*, 66(3): 175–187.
- Jakob, M., and Hungr, O. 2005. *Debris-flow hazards and related phenomena*, 739, Springer, Berlin.

- Jiang, N., Su, F., Li, Y., Guo, X., Zhang, J., Liu, X. 2021. Corrigendum: Debris flow assessment in the Gaizi-Bulunkou section of Karakoram Highway. *Frontiers in Earth Science*, 9: 660579.
- Jaboyedoff, M., Rudaz, B., and Horton, P. 2011. Concepts and parameterization of Perla and FLM model using Flow-R for debris flow. *In: 5<sup>th</sup> Canadian Conference on Geotechnique and Natural Hazards*, Kelowna, BC, Canada, 15–17.
- Kaltak, S. 2018. Mathematical modeling of debris flows and formation of torrential fans. Master's Thesis, University of Ljubljana, Slovenia.
- Kang, D., Nam, D., Lee, S., Yang, W., You, K. and Kim, B., 2017. Comparison of impact forces generated by debris flows using numerical analysis models. *WIT Transaction on Ecology and the Environment*, 220: 195–203.
- Kang, S., and Lee, S.R. 2018. Debris flow susceptibility assessment based on an empirical approach in the central region of South Korea. *Geomorphology*, 308: 1–12.
- Kappes, M.S., Malet, J.P., Remaître, A., Horton, P., Jaboyedoff, M. and Bell, R. 2011. Assessment of debris-flow susceptibility at medium-scale in the Barcelonnette Basin, France. *Natural Hazards and Earth System Sciences*, 11(2): 627–641.
- Kelfoun, K., and Druitt, T.H. 2005. Numerical modeling of the emplacement of socompa rock avalanche, Chile. *Journal of Geophysical Research: Solid Earth*, 110(B12): 2156–2202.
- Klaus, S., Barbara, T., Brian, M., Christoph, G., Oldrich, H., and Roland, K. 2015. Modeling Debris-flow runout pattern on a forested Alpine fan with different dynamic simulation models. *In: Engineering Geology for Society and Territory-Volume 2: Landslide Processes*, 1673-1676.
- Knibbs, G., Guthrie, R., and Wasklewicz, T. 2023. Debris flow hazard mapping along linear infrastructure: an agent based model and GIS approach. *In: 8<sup>th</sup> International Conference on Debris Flow Hazard Mitigation*, Torino, Italy.

- Krušić J., Abolmasov B., Marjanović and M., Djurić D. 2018. Numerical modelling in RAMMS–Selanac debris flow. *In: Second JTC1 Work Triggering Propagation of Rapid Flow-like Landslides*, Hong Kong, China.
- Krušić, J., Abolmasov, B., and Samardžić-Petrović, M. 2019. Influence of DEM resolution on numerical modelling of debris flows in RAMMS-Selanac case study. *In: Proceedings of the 4<sup>th</sup> Regional Symposium on in the Adriatic—Balkan Region*, 23–25.
- Lucia, P. 1981. Review of experiences with flow failures of tailing dams and waste impoundments. Ph.D. Dissertation, University of California, Berkeley.
- Mangeney-Castelnau, A., Vilotte, J.P., Bristeau, M.O., Perthame, B., Bouchut, F., Simeoni, C., and Yerneni, S. 2003. Numerical modelling of avalanches based on Saint Venant equations using a kinetic scheme. *Journal of Geophysical Research*, 108(B11): 2527.
- McCoy, S.W., Kean, J.W., Coe, J.A., Tucker, G.E., Staley, D.M., and Wasklewicz, T.A. 2012. Sediment entrainment by debris flows: In situ measurements from the headwaters of a steep catchment. *Journal of Geophysical Research: Earth Surface*, 117(F3).
- McDougall, S. 2006. A New Continuum dynamic model for the analysis of extremely rapid landslide motion across complex 3d terrain. Ph.D. Dissertation, The University of British Columbia, Vancouver, British Columbia, Canada.
- McDougall, S. 2017. 2014 Canadian geotechnical colloquium: Landslide runout analysis — current practice and challenges. *Canadian Geotechnical Journal*, 54(5): 605–620.
- McDougall, S., Hungr, O. 2004. A model for the analysis of rapid landslide motion across three-dimensional terrain. *Canadian Geotechnical Journal*, 41: 1084–1097.
- McGuire, L.A., Rengers, F.K., Kean, J.W., Staley, D.M., and Mirus, B.B. 2018. Incorporating spatially heterogeneous infiltration capacity into hydrologic models with applications for

- simulating post-wildfire debris flow initiation: Post-wildfire runoff and debris flow initiation. *Hydrological Processes*, 32(9): 1173–1187.
- Medina, V., Hürlimann, M., and Bateman, A. 2008. Application of FLATMODEL, a 2D finite volume code, to debris flows in the northeastern part of the Iberian Peninsula. *Landslides*, 5: 127–142.
- Mergili, M., Fischer, J.T., Krenn, J., and Pudasaini, S.P. 2017. r.avaflow v1, an advanced open-source computational framework for the propagation and interaction of two-phase mass flows. *Geoscientific Model Development*, 10(2): 553–569.
- Mergili, M., Schratz, K., Ostermann, A., and Fellin, W. 2012. Physically-based modelling of granular flows with open source GIS. *Natural Hazards and Earth System Sciences*, 12: 187–200.
- Mikoš, M., and Bezak, N. 2021. Debris Flow modelling using RAMMS model in the Alpine environment with focus on the model parameters and main characteristics. *Frontiers in Earth Science*, 8, 605061.
- Morgan, D. 2001. Fish habitat overview assessment for the Klanawa river watershed. Ministry of Forests, Victoria, British Columbia.
- Nam, D.H., Kim, M.I., Kang, D.H., and Kim, B.S. 2019. Debris flow damage assessment by considering debris flow direction and direction angle of structure in South Korea. *Water*, 11: 328.
- Naqvi, M.W. 2020. Numerical simulation of debris flows using a multi-phase model and case studies of two well-documented events. Master's Thesis, The University of Toledo, United States.
- Nettleton, I.M., Martin, S., Hencher, S., and Moore, R. 2005. Debris flow types and mechanisms.
- Nyman, P., Sheridan, G.J., Smith, H.G., and Lane, P.N.J. 2011. Evidence of debris flow occurrence after wildfire in upland catchments of Southeast Australia. *Geomorphology*, 125(3): 383–401.

- O'Brien, J.S., Julien, P.Y., and Fullerton, W.T. 1993. Two-dimensional water flood and mudflow simulation. *Journal of Hydraulic Engineering*, 119(2): 244–261.
- Paudel, B.P. 2019. GIS-based Assessment of debris flow susceptibility and hazard in mountainous regions of Nepal. University of Ottawa, Ph.D. Dissertation, Ottawa, Canada.
- Pastor, M., Haddad, B., Sorbino, G., Cuomo, S., and Drempetic, V. 2009b. A depth-integrated, coupled SPH model for flow-like landslides and related phenomena. *International Journal for Numerical and Analytical Methods in Geomechanics*, 33: 143–172.
- Parise, M., and Cannon, S.H. 2012. Wildfire impacts on the processes that generate debris flows in burned watersheds. *Natural Hazards*, 61(1): 217–227.
- Park, D.W., Lee, S.R., Vasu, N.N., Kang, S.H., and Park, J.Y. 2016. Coupled model for simulation of landslides and debris flows at local scale. *Natural Hazards*, 81(3): 1653–1682.
- Perla, R., Cheng, T.T., and McClung, D.M. 1980. A Two-parameter model of snow-avalanche motion. *Journal of Glaciology*, 26: 197–207.
- Pitman, E.B., and Le, L. 2005. A Two-fluid model for avalanche and debris flows. *Philosophical Transactions of the Royal Society A: Mathematical, Physical and Engineering Sciences*, 363(1832): 1573–1601.
- Pirulli, M. 2005. Numerical modelling of landslide runout: A continuum mechanics approach. Ph.D. Dissertation, Politecnico di Torino, Torino.
- Poisel, R., and Preh, A. 2008. 3D landslide runout modelling using the particle flow code PFC3D. *In: Proceedings of the 10th International Symposium on Landslides and Engineered Slopes*, Taylor and Francis, London, 873–879.

- Quinn, P., Beven, K., Chevallier, P., and Planchon, O. 1991. The prediction of hillslope flow paths for distributed hydrological modelling using digital terrain models. *Hydrological Process*, 5: 59–79.
- RAMMS, 2017. RAMMS::DEBRISFLOW user manual, Available at: [https://ramms.slf.ch/ramms/downloads/RAMMS\\_DBF\\_Manual.pdf](https://ramms.slf.ch/ramms/downloads/RAMMS_DBF_Manual.pdf).
- Randin, C.F., Vuissoz, G., Liston, G.E., Vittoz, P., and Guisan, A. 2009. Introduction of snow and geomorphic disturbance variables into predictive models of alpine plant distribution in the Western Swiss Alps. *Arctic, Antarctic, and Alpine Research*, 41(3): 347–361.
- Reid, M.E., Iverson, R.M., Logan, M., Lahusen, R.G., Godt, J.W., and Griswold, J.G. 2011. Entrainment of bed sediment by debris flows: results from large-scale experiments. *In: International Conference on Debris-flow Hazards Mitigation, Mechanics, Prediction and Assessment*, 367–374.
- Rengers, F.K., McGuire, L.A., Kean, J.W., Staley, D.M., and Hobley, D.E.J. 2016. Model simulations of flood and debris flow timing in steep catchments after wildfire. *Water Resources Research*, 52(8): 6041–6061.
- Rickenmann, D. 1999. Empirical relationships for debris flows. *Natural Hazards*, 19: 47–77.
- Rickenmann, D. 2005. Runout prediction methods. *Debris-flow Hazards and Related Phenomena*, 305–324.
- Rickenmann, D., and Zimmermann, M. 1993. The 1987 debris flows in Switzerland: Documentation and analysis. *Geomorphology*, 8(2-3): 175–189.
- Roddeman, D.G. 2002. TOCHNOG user’s manual – a free explicit/implicit FE program. FEAT. Available from [www.feat.nl/manuals/user/user.html](http://www.feat.nl/manuals/user/user.html).

- Rodríguez-Morata, C., Villacorta, S., Stoffel, M., and Ballesteros-Cánovas, J.A. 2019. Assessing strategies to mitigate debris-flow risk in Abancay province, south-central Peruvian Andes. *Geomorphology*, 342: 127–139.
- Rollerson, T., Maynard, D., Higman, S., and Ortmayr, E. 2004. Klanawa landslide hazard mapping pilot project. *In: A Joint Conference IUFRO S*, 3: 13–16.
- Rollerson, T., Millard, T., Thomson, B. 2002. Using terrain attributes to predict post-logging landslide likelihood on southwestern Vancouver Island, Forest Service, British Columbia.
- Law, R.P.H., Choi, C.E., and Ng, C.W.W. 2016. Discrete-element investigation of influence of granular debris flow baffles on rigid barrier impact. *Canadian Geotechnical Journal*, 53(1): 179–185.
- Scheidl, C., Rickenmann, D., and McArdell, B.W. 2013. Runout prediction of debris flows and similar mass movements. *In: Landslide science and practice*, 221–229.
- Scheuner, T., Schwab, S., and McArdell, B.W. 2011. Application of a two dimensional numerical model in risk and hazard assessment in Switzerland. *Italian Journal of Engineering Geology and Environment*, 993–1001.
- Schneider, D., Huggel, C., Cochachin, A., Guillén, S., and García, J. 2014. Mapping hazards from glacier lake outburst floods based on modelling of process cascades at Lake 513, Carhuaz, Peru. *Advanced Geoscience*, 35: 145–155.
- Schraml, K., Thomschitz, B., McArdell, B.W., Graf, C., and Kaitna, R. 2015. Modeling debris-flow runout patterns on two alpine fans with different dynamic simulation models. *Natural Hazards and Earth System Sciences*, 15(7), 1483–1492.

- Shen, W., Zhao, T., Dai, F., and Jing, L. 2018. Investigation of dry debris flow impact against a rigid barrier via a discrete element approach. *In: GeoShanghai 2018 International Conference: Geoenvironment and Geohazard*, 20–27.
- Simoni A., Mammoliti M., and Graf C. 2012. Performance of 2D debris flow simulation model RAMMS. *In: Annual International Conference on Geological and Earth Sciences, GEOS*, Singapore.
- Soga, K., Alonso, E., Yerro, A., Kumar, K., and Bandara, S. 2016. Trends in large-deformation analysis of landslide mass movements with particular emphasis on the material point method. *Géotechnique*, 66(3). 248–273.
- Spataro, W., D'Ambrosio, D., Rongo, R., and Trunfio, A.G. 2004. An evolutionary approach for modelling lava flows through cellular automata. *In: Cellular Automata: 6<sup>th</sup> International Conference on Cellular Automata for Research and Industry, ACRI 2004, Amsterdam*, 725–743.
- Staley, D.M., Tillery, A.C., Kean, J.W., McGuire, L.A., Pauling, H.E., Rengers, F.K., and Smith, J. B. 2018. Estimating post-fire debris-flow hazards prior to wildfire using a statistical analysis of historical distributions of fire severity from remote sensing data. *International Journal of Wildland Fire*, 27(9): 595.
- Sturzenegger, M., Holm, K., Lau, C.A., and Jakob, M. 2021. Debris-flow and debris-flood susceptibility mapping for geohazard risk prioritization. *Environmental and Engineering Geoscience*, 27(2): 179–194.
- Takahashi, T. 2007. *Debris flow: Mechanics, prediction and countermeasures*. Taylor and Francis.
- Takahashi, T. 1981. Debris flow. *Annual Review of Fluid Mechanics* 13(1): 57–77.

- Thomas, B.W., Hunt, D., Bittman, S., Hannam, K.D., Messiga, A.J., Haak, D., Sharifi, M., and Hao, X. 2019, Soil health indicators after 21 yr of no-tillage in south coastal British Columbia. *Canadian Journal of Soil Science*, 99(2): 222–225.
- Tsao, T.C., Hsu, C.H., Yin, H.Y., and Cheng, K.P. 2019. Debris-flow building damage level and vulnerability curve—a case study of a 2015 typhoon event in northern Taiwan. *In: Proceedings of the 7<sup>th</sup> International Conference on Debris-Flow Hazards Mitigation*.
- Tsao, T.C., Huang, C.Y., Chien, J.H., Yin, H.Y., and Chen, C.Y. 2018. Comparison of debris flow hazard mapping between empirical function and numerical simulation—A case study in Taiwan. *In: Proceedings of the INTERPRAENENT Symposium 2018 in the Pacific Rim, Taiwan, China*.
- Vandre, B.C. 1985. Rudd creek debris flow. *In: Delineation of landslide, flash flood, and debris flow hazards in Utah*, Utah Water Research Laboratory, Utah State University, Logan, Utah.
- VanDine, D.F. 1985. Debris flows and debris torrents in the southern Canadian Cordillera. *Canadian Geotechnical Journal*, 22(1): 44–68.
- Varnes, D.J. 1978. Slope movement types and processes. Special report, 176:11–33.
- Vergara Dal Pont, I., Moreiras, S. M., Santibañez Ossa, F., Araneo, D., and Ferrando, F. 2020. Debris flows triggered from melt of seasonal snow and ice within the active layer in the semi-arid Andes. *Permafrost and Periglacial Processes*, 31(1): 57–68.
- Von Neumann, J. 1966. *Theory of self-reproducing automata*. University of Illinois Press, Urbana and London.
- Wang, X. 2008. Geotechnical analysis of flow slides, debris flows, and related phenomena. Ph.D. Dissertation, University of Alberta, Edmonton.
- Wang, F.W., and Sassa, K. 2002. A modified geotechnical simulation model for the areal prediction of landslide motion. *In: Proceedings of the 1st European Conference on Landslides*, 735–740.

- Wasklewicz, T., Guthrie, R., and Knibbs, G. 2023. Advancing debris flow hazard and risk assessments using debris flow modeling and radar derived rainfall intensity data. *In*: 8<sup>th</sup> International Conference on Debris Flow Hazard Mitigation, Torino, Italy.
- Wasklewicz, T., Guthrie, R.H., Eickenberg, P., and Kramka, B. 2022. Lessons learned from the local calibration of a debris flow model and importance to a geohazard assessment. *In*: 8<sup>th</sup> Canadian Conference on Geotechnique and Natural Hazards Geohazard , Quebec, Canada.
- Wieczorek, G.F., Mandrone, G. and DeCola, L. 1997. The influence of hillslope shape on debris-flow initiation. *In*: International Conference Water Resources Engineering Division, ASCE, San Francisco, California, 21–31.
- Wichmann, V., and Becht, M. 2003. Modeling of geomorphological processes in an Alpine catchment. 7<sup>th</sup> International Conference on GeoComputation, Southampton.
- Wise, M.P. 1997. Probabilistic modelling of debris flow travel distance using empirical volumetric relationships. MSc Thesis, University of British Columbia, Vancouver, BC.
- Wolfram, S. 1984. Cellular automata as models of complexity. *Nature*, 311: 419–424.
- Zhuang, Y., Xing, A., Leng, Y., Bilal, M., Zhang, Y., Jin, K., and He, J. 2021. Investigation of characteristics of long runout landslides based on the multi-source data collaboration: A case study of the Shuicheng Basalt landslide in Guizhou, China. *Rock Mechanics and Rock Engineering*, 54(8): 3783–3798.
- Zhou, G.G.D., Du, J., Song, D., Choi, C.E., Hu, H.S., and Jiang, C. 2020. Numerical study of granular debris flow run-up against slit dams by discrete element method. *Landslides*, 17(3): 585–595.
- Zimmermann, M., Mani, P., and Gamma, P 1997. Murganggefahr und Klimaänderung - ein GIS-basierter Ansatz. Schlussbericht, NFP 31 (in German).

Zimmermann, F., McArdell, B.W., Rickli, C., and Scheidl, C. 2020. 2D runout modelling of hillslope debris flows, based on well-documented events in Switzerland. *Geosciences*, 10(2): 70.

**Appendix I: A comparison of two runout programs for debris flow  
assessment at the Solalex-Anzeindaz region of Switzerland**

This paper has been published in the 8<sup>th</sup> Canadian Conference on Geotechnique and Natural Hazards (Geohazards 8, 2022), Quebec, Canada. Most of the research work presented in this paper was conducted by the first author. The other authors supervised this research.

# A comparison of two runout programs for debris flow assessment at the Solalex-Anzeindaz region of Switzerland

Arijit Biswas Arghya, Bipul Hawlader  
*Memorial University of Newfoundland, St. John's, NL, Canada*  
Richard H. Guthrie  
*Stantec, Calgary, Alberta, Canada*



## ABSTRACT

Debris flows are a major consideration in land-use planning and assessing the integrity of infrastructure in mountainous regions. In the present study, two computer programs, "Flow-R" and "DebrisFlow Predictor," are used to simulate debris flows in the Solalex-Anzeindaz region of the Swiss Alps, where many historic debris flow hazards are known. Both tools use the same Digital Elevation Model. Flow-R simulates the process based on spreading and runout distance algorithms. DebrisFlow Predictor uses a set of probabilistic rules for scour, deposition, path selection, and spreading. In the present simulations, both programs give comparable results in terms of spread. However, the additional information on the area, volume, and depth of debris along the landslide path provided by the DebrisFlow Predictor might make it a better hazard assessment tool.

## RÉSUMÉ

Les coulées de débris sont à prendre en considération dans la planification de l'utilisation des terres et l'évaluation de l'intégrité des infrastructures dans les régions montagneuses. Dans la présente étude, deux programmes informatiques, « Flow-R » et « DebrisFlow Predictor », sont utilisés pour simuler des coulées de débris dans la région de Solalex-Anzeindaz dans les Alpes suisses, où de nombreux cas historiques de coulée de débris sont connus. Les deux outils utilisent le même modèle numérique d'élévation. Flow-R simule le processus en se basant sur des algorithmes de distance d'étalement et d'étalement. DebrisFlow Predictor utilise un ensemble de règles probabilistes pour l'érosion, la déposition, la sélection de chemin et le comportement des débris. Sur la base des résultats de simulation, les deux programmes donnent des résultats comparables en termes de propagation. Cependant, les informations supplémentaires sur l'aire, le volume et la profondeur des débris le long de la trajectoire du glissement de terrain fournies par le DebrisFlow Predictor pourraient en faire un meilleur outil d'évaluation des risques.

## 1 INTRODUCTION

Debris flow is a gravity-driven moving mass of soil, mud, rock, and water. It is an extremely rapid flow-type landslide, which tends to travel long distances from its source (Hung et al. 2014). Debris flows pose considerable threats to communities, infrastructure, people, and resources.

Debris flow runout analysis can simulate the displacement of the failed materials originating from past landslides and can also predict the motion of debris in future landslides (McDougall 2017). This type of analysis should be a key component of hazard and risk assessment (Loew et al. 2016). Runout analysis can further help to estimate the runup height and impact loads on structures, a necessary step when assessing mitigation strategies (Kwan 2012). Estimating landslide extents, runout distances, and depths of debris is one of the most challenging tasks. Complete models of debris flow incorporating appropriate constitutive relationships of the flowing materials may not be practical because of significant uncertainties involved in material behaviour and the computational cost of the simulation, especially when it occurs over a large area. McDougall (2017) classified the available runout analysis methods into two broad categories: (i) empirical–statistical methods and (ii) analytical methods. Analytical modelling can provide in-depth information; however, it is highly reliant on correct

parameterization and may be difficult to implement at the regional scale. Iverson (1997) suggested using simplified spatially distributed models based on empirical or semi-empirical approaches for regional-scale modelling. These simplified approaches can incorporate the information derived from statistical analysis of data.

Flow-R is a computer program developed in Matlab by the researchers at the University of Lausanne, Switzerland, incorporating spatially distributed empirical models, which can be used to identify the debris flow initiation zones based on the combination of user-defined criteria. The program can also calculate the extent (inundation) and directions (path) of debris flows. This open-source software has been used for runout assessments of debris flows in different countries, including Switzerland (Horton et al. 2008; Horton et al. 2013), France (Kappes et al. 2011), Italy (Blahut et al. 2010), Norway (Fischer et al. 2012), and Argentina (Baumann et al. 2011).

DebrisFlow Predictor is a separate stand-alone computer program that was developed by Stantec (Guthrie and Befus 2021) based on the cellular automata methods (Wolfram 1984). It follows a set of simple rules for scour, deposition, path selection, and spread. The simulation of runout with this program provides, in addition to inundation and path selection, the area, volume, and depth of debris along the flow path. Guthrie and Befus (2021) used this program to estimate sediment input to a stream network in

a mountainous area in Papua province in Indonesia and also assessed the risk of debris flow in a community in Vancouver, Canada.

### 1.1 Study Area

The Solalex-Anzeindaz region in the Swiss Alps is considered herein to test the performance of both above-mentioned programs. Debris flows are very frequent on the south side of the Diablerets Range and regularly block the road that traverses the Solalex-Anzeindaz region (Horton et al. 2013). The accumulations of sediment on fans in the area of interest are ongoing and constructed of sediment from folded limestone and marl layers from the upslope Diablerets nappes (Badoux and Gabus 1990). We selected a subset of the region (~4 km<sup>2</sup>) for computational efficiency.

The objective of the study was to compare the simulation results of debris flow runout in the Solalex-Anzeindaz region using Flow-R and DebrisFlow Predictor.

## 2 MODEL CONCEPTS

### 2.1 Flow-R

In Flow-R, the users primarily define two sets of parameters/criteria. First, in source areas, the debris flow initiation zones are identified. There are several options available within the program. For example, the initiation zone could be identified based on the combination of user-defined criteria for geological, morphological and hydrological conditions. The users can also select predefined sources (e.g., if the landslide initiation zones are known). Second, for propagation, debris flow criteria are defined.

#### 2.1.1 Source Area Identification

Debris flow source areas can be identified by applying conditions to selected parameters, including slope gradient, aspect, curvature, flow accumulation, geology, land-use and lithology. According to Rickenmann and Zimmermann (1993), the combination of three criteria, namely sediment availability, water input, and slope gradient, primarily controls the initiation zone for the Swiss Alps. Sediment availability basically refers to the lithological unit. The majority of debris flows in the Swiss Alps originate from the terrain with slope gradients greater than 15° (Rickenmann and Zimmermann 1993). Water inputs can be represented by flow accumulations. Horton et al. (2013) determined that 0.01 km<sup>2</sup> was an appropriate threshold for the upslope contributing area for identifying the debris flow initiation zones in the Central Alps; however, these values can fluctuate depending upon the location. Analyzing the past events in Switzerland, a limit relationship was developed between slope gradient and upslope contributing area for the Central Alps. Every point above that limit should be considered critical (Rickenmann and Zimmermann 1993; Horton et al. 2013).

Curvature is another morphological characteristic considered for identifying debris flow initiation zones. It is the second derivative of the slope, and debris flows tend to be concentrated in slope concavities (i.e., gullies rather than ridges) (Delmonaco et al. 2003; Wieczorek et al. 1997). Plan curvature, which is perpendicular to the direction of the steepest slope, was considered to identify the gullies. By analyzing the orthophotographs, Horton et al. (2013) suggested the plan curvature value of 2/100 m<sup>-1</sup> for a 10-m DEM of the Solalex-Anzeindaz region.

Fischer et al. (2012) applied Flow-R to develop a national debris flow susceptibility map for Norway. They chose five different sites (Troms county, Balsfjord, Junkerdal, Nesna, and alpine fjord landscape) of varying topography and geomorphology to test and calibrate the model. They determined different threshold values of the criteria for identifying the initiation zones, including plan curvature of -1.5/100 m<sup>-1</sup> to -0.5/100 m<sup>-1</sup>, upslope contributing area of 0.3–1.0 ha, and slope thresholds 25°–45°.

Despite the ability to model debris flow sources found in Flow-R, susceptibility maps (for source zones) are common in literature and practice. This step has been excluded from the present study. Instead, the debris flow trajectories provided by SilvaProtect-CH were used, where the extent of debris flow (bounded by two solid black lines in Figure 1) was developed based on historical debris flow and simulations. We considered the starting point of the individual trajectory as the initiation point (red circles in Figure 1).

A total of 190 initiation points were considered in this study. A 0.5 m DEM was downloaded from the Federal Office of Topography database (swissALTI3D) and resampled into a 5 m DEM for simulation using Flow-R and DebrisFlow Predictor.

#### 2.1.2 Assessment of Propagation

From initiation points, the program calculates the debris flow over the DEM according to the following: (i) a spreading algorithm and (ii) a runout distance algorithm. The spreading algorithms provide the direction of flow, which are defined by two sub-algorithms, namely flow direction algorithm and inertial algorithm (also known as persistence function). Several direction algorithms were implemented in Flow-R, and the user can choose one of them for an analysis. In the present study, the algorithm proposed by Holmgren (1994) was selected (Eq. 1).

$$p_i^{fd} = \frac{(\tan\beta_i)^x}{\sum_{j=1}^8 (\tan\beta_j)^x} \forall \begin{cases} \tan\beta > 0 \\ x \in [1; +\infty] \end{cases} \quad [1]$$

where  $i, j$  are flow directions;  $p_i^{fd}$  is the susceptibility proportion in direction  $i$ ;  $\tan\beta_i$  is the slope gradient between the central cell and the cell in direction  $i$ , and  $x$  is an exponent. In this study,  $x = 4$  is considered based on the work of Claessens et al. (2005).

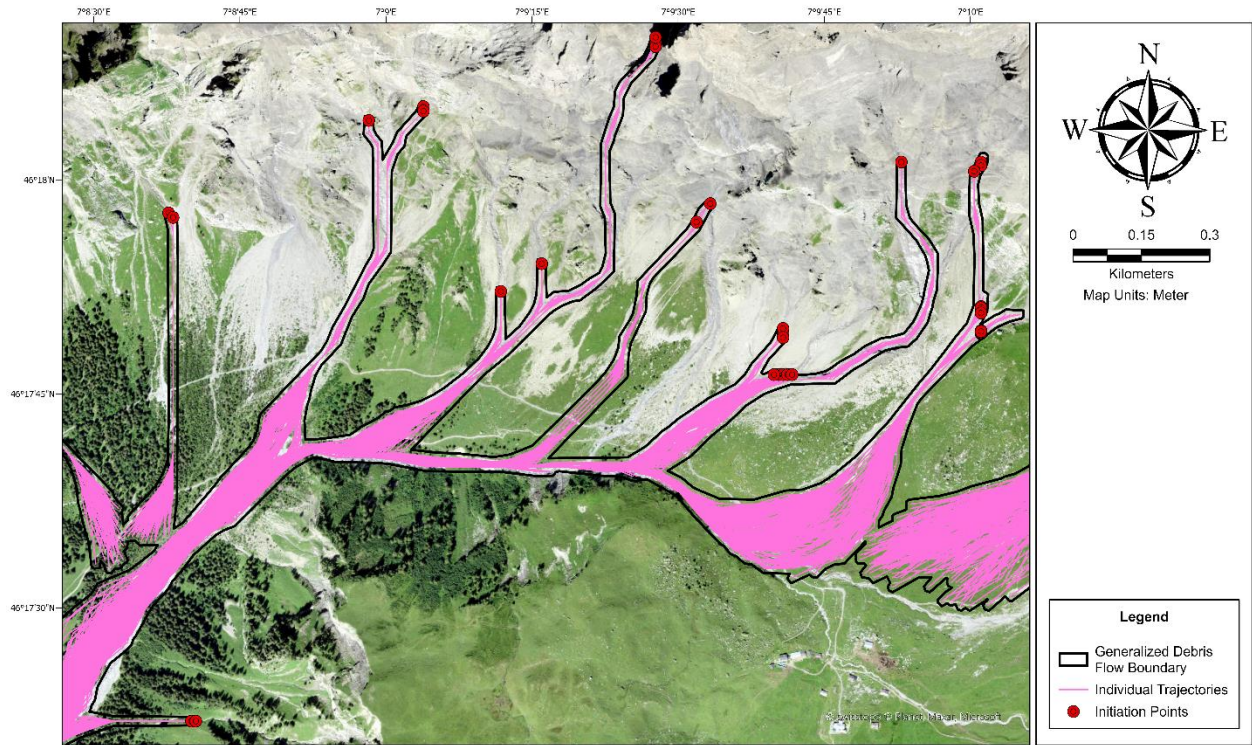


Figure 1: Debris flow trajectories developed by SilvaProtect-CH for Solalex-Anzeindaz region, Source: SilvaProtect-CH © BAFU

Two options are available for the inertial algorithm (weight and direction memory). In this study, the weight option is selected, which calculates the flow with a change in direction relative to the prior direction as

$$p_i^p = w_{\alpha_i} \quad [2]$$

where  $p_i^p$  is the flow proportion in direction  $i$ , and  $\alpha_i$  is the angle between the previous direction and the direction from the central cell to cell  $i$ . The weight ( $w_{\alpha_i}$ ) was selected based on the work of Gamma (2000). Further details on inertial algorithms are available in Horton et al. (2013).

Debris flow runout can be determined by combining the flow direction algorithm and the persistence function (Eq. 3).

$$p_i = \frac{p_i^{fd} p_i^p}{\sum_{j=1}^8 p_j^{fd} p_j^p} p_0 \quad [3]$$

where  $p_i$  is the susceptibility value in direction  $i$ ,  $p_0$  is previously determined flow proportion of the central cell.

The runout distance algorithms were developed based on energy balance, which can be written as

$$E_k^i = E_k^0 + \Delta E_p^i - E_f^i \quad [4]$$

where  $E_k^i$  is the kinetic energy of the cell in the direction  $i$ ;  $E_k^0$  is the kinetic energy of the central cell;  $\Delta E_p^i$  is the change in potential energy, and  $E_f^i$  is the energy loss due to friction for the flow in direction  $i$ . The friction loss was calculated in this study by using a simplified-friction limited model (Corominas 1996), as discussed below. Note, however, that the user can also choose the two-parameter friction model proposed by Perla et al. (1980).

Corominas (1996) proposed a simplified approach to calculate the energy loss due to friction as:

$$E_f^i = g \Delta x \tan \varphi \quad [5]$$

where  $\Delta x$  is the increment of horizontal displacement in direction  $i$ ;  $\tan \varphi$  is the gradient of energy line in the direction  $i$ ;  $\varphi$  is the travel angle, and  $g$  is the gravitational acceleration. An average slope angle (that connects the starting and ending points of the debris flow track) of roughly  $11^\circ$  characterizes the most probable maximum runout in the Central Alps (Rickenmann and Zimmermann 1993; Huggel et al. 2002; Horton et al. 2013). Therefore,  $\varphi = 11^\circ$  is considered in this study.

Finally, simulation results might be misleading if the slope is very steep. To control that, Flow-R incorporated a limiting velocity ( $V_{max}$ ), as suggested by Horton et al. (2013). That is,

$$V_i = \min \left\{ \sqrt{V_0^2 + 2g\Delta h - 2gx\Delta x \tan \varphi}, V_{max} \right\} \quad [6]$$

where  $\Delta h$  is the difference between the elevation of the central cell and the cell in the direction  $i$ . The maximum velocity measured in debris flow incidents in Switzerland was 13 to 14 m/s (Rickenmann and Zimmermann 1993). Therefore,  $V_{max} = 15$  m/s is used in the present study.

## 2.2 DebrisFlow Predictor

The DebrisFlow Predictor is also a landslide runout simulation tool, which is similar to Flow-R, as both are empirically based. However, the underlying mechanics differ somewhat; DebrisFlow Predictor is an agent-based program where the landslide is represented by agents that occupy cells on a raster grid at a specific time step on which a set of rules could be applied. Also, the identification of source areas and debris flow propagation criteria are different from those used in Flow-R (Sections 2.1.1 & 2.1.2).

For source areas, using the tools in the program itself, users of DebrisFlow Predictor can manually select a single cell (5 m x 5 m), a small group of a 15 m x 15 m slide initiation zone, or multiple cells (a larger

source zone) simply by painting over a larger area. Manual selection is done directly on the DEM in the program itself. Landslide initiation areas can also be imported from a point shapefile (.shp) and automatically populated with 15 m x 15 m landslide initiation zones.

In the simulations using DebrisFlow Predictor, the same initiation points used in the Flow-R simulation were used.

In DebrisFlow Predictor, the direction of movement is identified by a Moore Neighbourhood algorithm, where the elevations of the surrounding eight cells around the central cell are obtained. In each time step, the agent faces and will flow toward the lowest unoccupied cells. In the case where cells are not unoccupied or where three cells have the same elevation, the direction is a combination of random chance and the preservation of momentum. A detailed description of this approach is available in Guthrie et al. (2008)

Also different in DebrisFlow Predictor is that agents scour and deposit in each timestep and account for their mass. Occasionally mass is shed to new cells on the matrix (DEM), spawning additional agents. The redistribution of mass is described by a probability density function defining the standard deviation ( $\sigma$ ) as

$$\sigma = \left( \frac{m_{max} - m}{m_{max}} \right)^n (\sigma_L - \sigma_S) + \sigma_S \quad [7]$$

where  $m_{max}$  is the fan maximum slope to limit spreading above the selected slope value,  $m$  represents DEM slope,  $n$  is a skew coefficient,  $\sigma_L$  is low slope coefficient and  $\sigma_S$  is steep slope coefficient. Further details of these parameters could be found in Guthrie and Befus (2021).

The parameters used in this application of DebrisFlow Predictor are listed in Table 1. Parameters can be calibrated in an iterative fashion within the model by adjusting the sliders and comparing results to known events or landforms. The parameter  $m_{max}$  limits spreading to slopes flatter than 27°, as recommended by Guthrie and Befus (2021), where additional information is not available. The parameters  $n$ ,  $\sigma_L$ , and  $\sigma_S$  control the amount of mass (and therefore the creation of new agents) redistributed to surrounding cells. With an increase in the value of  $\sigma_L$  and  $\sigma_S$  the spreading increases in the low and steep slope areas, respectively.

In DebrisFlow Predictor, the spread is controlled by the redistribution of mass (Eq. 7), spawning new agents, which, themselves, are subject to the same rules as existing agents. These parameters are adjusted efficiently by moving sliders within the program. The reader can compare this to the spreading algorithm in Flow-R (Eqs. 1–3).

Agent mass is a critical part of DebrisFlow Predictor, and each agent continues to move downslope so long as its mass > 0. Mass follows probabilistic rules for scour and deposition based on the underlying slope. The probability curves come from approximately 1700 field observations (Wise 1997; Guthrie et al. 2008, 2010). Nonetheless, variations in local geomorphology may necessitate adjustments to scour or deposition depth. These are achieved using the deposition and erosion multipliers (Table 1) that are independently applied to the agent mass after calculation in each timestep. DebrisFlow Predictor also considers mass loss during the turn. As the neighbouring cells are at 45° angle with respect to the central cell, the mass loss parameter is defined per 45° turn. Once again, each of these parameters is efficiently adjusted using sliders in the program itself. Overall, the role of these parameters could be compared to the runout distance algorithms in Flow-R (Eqs. 4–6).

DebrisFlow Predictor has the ability to set a minimum scour depth in the initiation zone to account for the observed experience of (for example) a half-

meter headscarp. The minimum scour depth is subtracted to the calculated depth for that slope.

Because the results are probabilistic, no two runs are identical; therefore, multiple runs are recommended to determine the potential cumulative footprint of a debris flow path and to calculate the probability that any location within the cumulative footprint will be occupied by an event. Five hundred landslide runs were modeled from each landslide initiation zone in this simulation.

Table 1. Parameters used DebrisFlow Predictor

Fan maximum slope ( $m_{max}$ )	27°
Low slope coefficient ( $\sigma_L$ )	0.36
Steep slope coefficient ( $\sigma_S$ )	1.36
Skew coefficient ( $n$ )	1.1
Maximum spawns allowed	100
Deposition multiplier	0.5x
Erosion multiplier	1x
Mass loss per 45° turn	20%
Minimum initiation depth	0
Number of model runs	500

### 3 RESULTS

Figure 2 represents the spreading of debris flow hazard potential for the Solalex-Anzeindaz region modeled in Flow-R. The darker color shows higher susceptibility, while the lighter color represents comparatively lower susceptibility. By using Flow-R, the user can determine runout distance and generally estimate the probability of occupying a place in the landscape. However, at least in this simulation, the susceptibility appears to be either high (dark lines) or low (lighter background), with limited intermediate values between the two.

DebrisFlow Predictor is functionally limited to a 5 m DEM (the same DEM was used in both models) but produces considerable additional information at that scale. It predicts the area, volume, and depth along the landslide path, as well as the probability of inundation over multiple runs. Figure 3 (DebrisFlow Predictor) is similar to Figure 2 (Flow-R), with a perhaps better discretization of intermediate probabilities. The darker areas represent higher inundation probabilities, and lighter areas represent lower inundation probabilities. If the reader considers only the high probability paths from both models, DebrisFlow Predictor, as modeled in this case, appears to produce more realistic fanning and path behaviour.

In our test, results of the DebrisFlow Predictor model runs were improved from those using Flow-R; for example, in Figures 2 and 3. Figure 4(a) shows an enlarged view of the landslide footprint where the debris comes from the upslope areas along the path PQ and then diverges into two flow paths (QRT and QST), converging later at point T. The Flow-R simulations in Figure 4(b) show only one flow path QST. While we acknowledge that this could be a parameterization problem, we note that the simulations conducted for SilvaProtect-CH found a similar path (see Figure 1). On the other hand, DebrisFlow Predictor simulates some flow of debris along QRT, as shown in Figure 4(c), which is consistent with the observed landslide footprint (Figure 4(a)).

Methods to estimate damage from debris flows include analytical (Corominas et al. 2014), empirical (Jakob et al. 2012), and engineering judgment approaches (Winter et al. 2014). Perhaps the simplest approach is to consider only landslide depth (Ciurean et al. 2017). In this case, the landslide depth is provided as an output from DebrisFlow Predictor (Figure 5). However, with those depths and assumptions about the velocity (estimated at 15 m/s over this site), detailed calculations could be performed, such as design parameters for mitigation structures. Similarly, with respect to mitigation, individual scenario runs from DebrisFlow Predictor will produce volumes. In other words, the operator can get a range of expected

volumes as well as the expected depths. Representativeness of volumes will depend on input parameters and the calibration stage, however, the calibration is efficient for a user with experience in debris flows, and was shown to match real world examples in several cases (Waskiewicz et al. 2022; Guthrie et al. 2022).

Both programs are highly dependent on DEM quality and resolution, with DebrisFlow Predictor being limited to a 5-m pixel size. Changing the ground surface from that surface represented in the DEM might result in some errors in the runout model.

Horton et al. (2013) showed that outcomes could vary substantially according to different resolutions of DEM. He proposed that a 10 m pixel resolution is appropriate for regional debris flow susceptible mapping. In recent years, the computational power has been increased rapidly; therefore, simulations could be performed even for smaller pixels. Guthrie and Befus (2021) suggested that a 5 m DEM strikes a balance of processing power and provides reasonable results

#### 4 CONCLUSIONS

Flow-R and Debrisflow Predictor were deployed at the Solalex-Anzeindaz region to simulate debris flow runouts. Both programs were developed based on empirical approaches, and neither of the models emphasizes local triggering factors or underlying conditions to determine the path. They rely instead on the overall behaviour of debris flows derived from

empirical studies. A number of successful case studies demonstrated the suitability and applicability of Flow-R for debris-flow susceptibility mapping, while DebrisFlow Predictor is, in comparison, relatively new.

For DebrisFlow Predictor, the source area is identified manually or computationally outside the program and imported. Flow-R, on the other hand, comes with a landslide susceptibility module (for landslide initiation). While landslide initiation zones are readily determined through a variety of methods, if the user wishes to automate this process in a single program, Flow-R is perhaps a better choice (though expert judgement is still required to parameterize the program correctly).

Once source zones are identified, DebrisFlow Predictor appears to provide more information and better path results (individual runs or high probability inundation zones from multiple runs to show morphological features that one would expect to see in a real debris flow) and additional depth information obtained along the runout path. That depth data (scour and deposition) can help engineers prepare mitigation strategies and design parameters. Calibration occurs within the program using a relatively intuitive GUI, and the model accounts, therefore, for second-order differences in local conditions (e.g. geology, viscosity, surficial geology) experimentally.

DebrisFlow Predictor, at this time of writing, is free for non-commercial use, while Flow-R is open-source software.

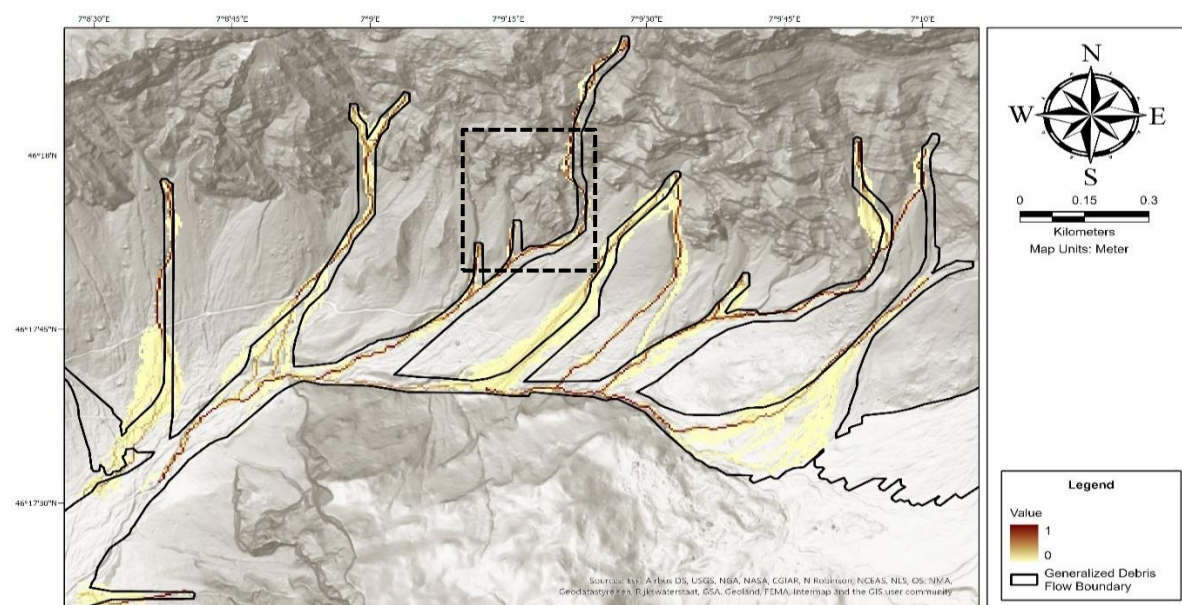


Figure 2: Debris flow runout modeled in Flow-R. The cumulative footprints and probability of occupying a cell are provided; however, the probability distribution appears to be bimodal, with only high and low probabilities well represented.

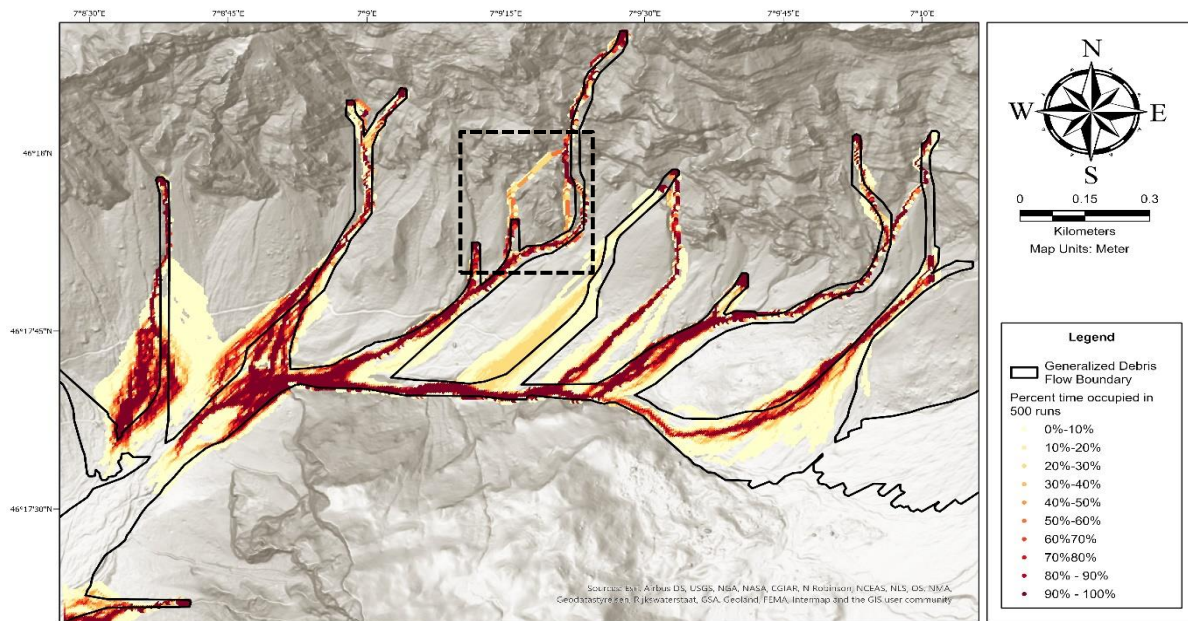


Figure 3: Debris flow runout from DebrisFlow Predictor. The result shows both the cumulative footprint of multiple runs and the likelihood that any location on the map would be occupied in a single run.

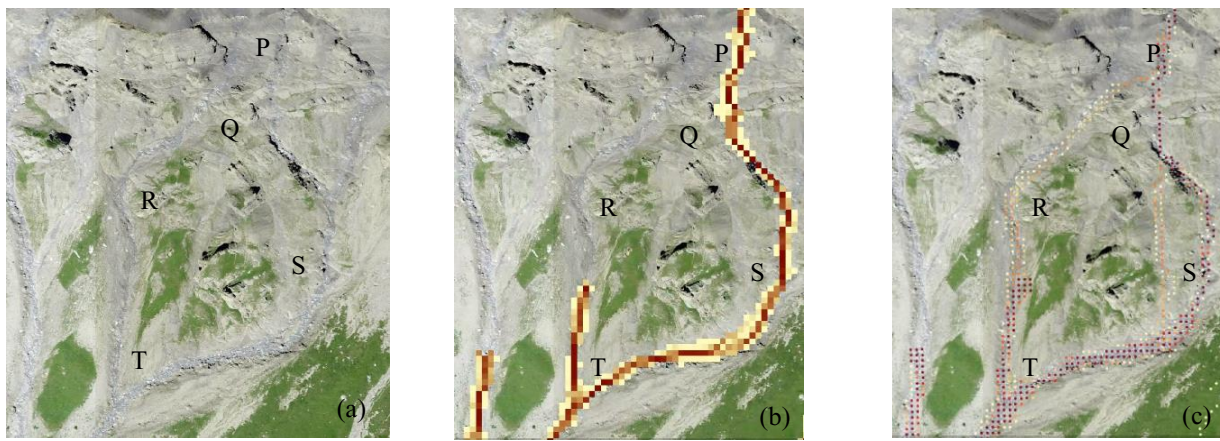


Figure 4: Comparison of simulation results with landslides footprints for a selected location: (a) landslide footprint; (b) Flow-R simulation; (c) DebrisFlow Predictor simulation (Background image source: [www.swisstopo.admin.ch/en/geodata/images.html](http://www.swisstopo.admin.ch/en/geodata/images.html))

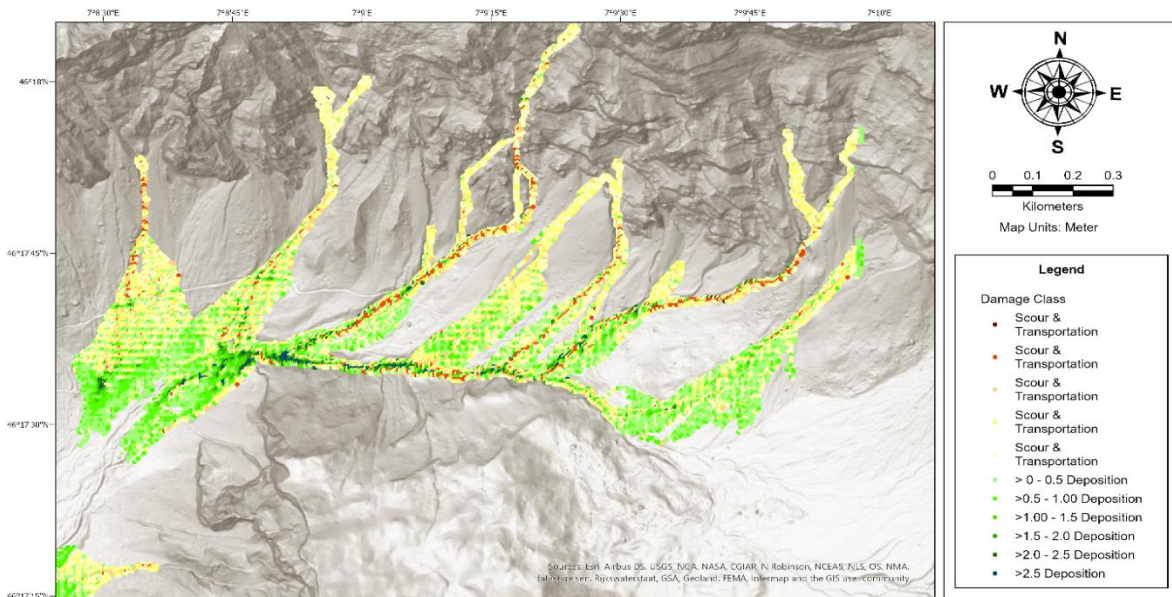


Figure 5: Debris flow runout showing depths (scour from red to yellow, deposition from green to dark green) along the path. Volume is retained for each individual landslide in the program and can be exported to Excel spreadsheets for scenario analysis.

## 5 ACKNOWLEDGEMENTS

The works presented in this paper were supported by the Natural Sciences and Engineering Research Council (NSERC) and Equinor Research Chair grants. Authors acknowledge Stantec and University of Lausanne for the computer programs.

## 6 REFERENCES

- Badoux, H. and Gabus, J.-H. 1990. Atlas géologique de la Suisse, feuille n° 1285, 1:25000, Les Diablerets avec notice explicative (In French).
- Baumann, V., Wick, E., Horton, P., and Jaboyedoff, M. 2011. Debris Flow Susceptibility Mapping at a Regional Scale along the National Road N7, Argentina, *14th Pan-American Conference on Soil Mechanics and Geotechnical Engineering*, Toronto, Ontario, Canada.
- Blahut, J., Horton, P., Sterlacchini, S., and Jaboyedoff, M. 2010. Debris Flow Hazard Modelling on Medium Scale: Valtellina di Tirano, Italy, *Natural Hazards and Earth System Sciences*, 10(11): 2379–2390.
- Ciurean, R. L., Hussin, H., vanWesten, C. J., Jaboyedoff, M., Nicolet, P., Chen, L., Frigerio, S. and Glade, T. 2017. Multi-scale Debris Flow Vulnerability Assessment and Direct Loss Estimation of Buildings in the Eastern Italian ALPS, *Natural Hazards*, 85: 929–957.
- Claessens, L., Heuvelink, G.B.M., School, J.M. and Veldkamp, A. 2005. DEM Resolution Effects on Shallow Landslide Hazard and Soil Redistribution Modelling, *Earth Surface Processes and Landforms*, 30(4): 461–477.
- Corominas, J. 1996. The Angle of Reach as a Mobility Index for Small and Large Landslides, *Canadian Geotechnical Journal*, 33(2): 260–271.
- Corominas, J., vanWesten, C., Frattini, P., Cascini, L., Mallet, J. P., Fotopoulou, S. and Catani, F. 2014. Recommendations for the Quantitative Analysis of Landslides Risk, *Bulletin of Engineering Geology and Environment*, 73: 209–263.
- Delmonaco, G., Leoni, G., Margottini, C., Puglisi, C. and Spizzichino, D. 2003. Large Scale Debris-flow Hazard Assessment: a Geotechnical Approach and GIS modeling, *Natural Hazards and Earth System Sciences*, 3: 443–455.
- Fischer, L., Rubensdotter, L., Sletten, K., Stalsberg, K., Melchiorre, C., Horton, P. and Jaboyedoff, M. 2012. Debris Flow Modeling for Susceptibility Mapping at Regional to National Scale in Norway, *11th International and 2nd North American Symposium on Landslides*, Banff, Alberta, Canada, 723–729.
- Gamma, P. 2000. *dfwalk*—Ein Murgang-Simulationsprogramm zur Gefahrenzonierung (*dfwalk*—A debris flow simulation program for natural hazard zonation. Geographica Bernensia G66, Bern, Switzerland (in German).
- Guthrie, R. H. and Befus, A. 2021. DebrisFlow Predictor: an Agent-based Runout Program for Shallow Landslides, *Natural Hazards and Earth System Sciences*, 21(3): 1029–1049.
- Guthrie, R.H., Deadman, P., Cabrera, R., and Evans, S. 2008. Exploring the Magnitude-frequency Distribution: a Cellular Automata Model for Landslides, *Landslides*, 5: 151–159.
- Guthrie, R. H., Grasso, K., Befus, A. 2022. A new landslide runout model and implications for understanding post wildfire and earthquake threats to communities in California. *ASCE Lifelines Conference, 2021 2022*, University of California, Los Angeles, 13.
- Guthrie, R. H., Hockin, A., Colquhoun, L., Nagy, T., Evans, S. G. and Ayles, C. 2010. An examination of Controls on Debris Flow Mobility: Evidence from Coastal British Columbia, *Geomorphology*, 114: 601–613.
- Holmgren, P. 1994. Multiple Flow Direction Algorithms for Runoff Modelling in Grid Based Elevation Models: an Empirical Evaluation, *Hydrological Processes*, 8(4): 327–334.
- Horton, P., Jaboyedoff, M. and Bardou, E. 2008. Debris Flow Susceptibility Mapping at a Regional Scale, *4th Canadian Conference on Geohazards*, Quebec, Canada, 339–406.
- Horton, P., Jaboyedoff, M., Rudaz, B. and Zimmermann, M. 2013. Flow-R, a Model for Susceptibility Mapping of Debris Flows and Other Gravitational Hazards at a Regional Scale, *Natural Hazards and Earth System Sciences*, 13(4): 869–885.
- Huggel, C., Kaab, A., Haeberli, W., Teysseire, P. and Paul, F. 2002. Remote Sensing Based Assessment of Hazards from Glacier Lake Outbursts: a Case Study in the Swiss Alps, *Canadian Geotechnical Journal*, 39: 316–330.
- Hungr, O., Leroueil, S. and Picarelli, L. 2014. The Varnes Classification of Landslide Types, an update, *Landslides*, 11: 167–194.
- Iverson, R.M. 1997. The Physics of Debris Flows, *Reviews of Geophysics*, 35(3): 245–296.
- Jakob, M., Stein, D. and Ulmi, M. 2012. Vulnerability of Buildings to Debris Flow Impact, *Natural Hazards*, 60: 241–261.
- Loew, S., Gschwind, S., Gischig, Keller-Signer, A. and Valenti, G. 2016. Monitoring and Early Warning of the 2012 Preonzo Catastrophic Rockslope Failure, *Landslides*, 14: 141–154.
- Kappes, M. S., Malet, J.-P., Remaître, A., Horton, P., Jaboyedoff, M. and Bell, R. 2011. Assessment of Debris-flow Susceptibility at Medium-scale in the Barcelonnette Basin, France, *Natural Hazards and Earth System Sciences*, 11(2): 627–641.
- Kwan, J.S.H. 2012. *Supplementary Technical Guidance on Design of Rigid Debris-resisting Barriers*, Hong Kong Geotechnical Engineering Office, Report No. 270.

- McDougall, S. 2017. 2014 Canadian Geotechnical Colloquium: Landslide Runout Analysis — Current Practice and Challenges, *Canadian Geotechnical Journal*, 54(5): 605–620.
- Perla, R., Cheng, T.T. and McClung, D.M. 1980. A Two-parameter Model of Snow-avalanche Motion, *Journal of Glaciology*, 26: 197–207.
- Rickenmann, D. and Zimmermann, M. 1993. The 1987 Debris Flows in Switzerland: Documentation and Analysis, *Geomorphology*, 8(2-3): 175–189.
- Wasklewicz, T., Guthrie, R. H., Eickenberg, P., Kramka, B., 2022. Modeling post-wildfire debris flow erosion for hazard assessment, *Environmental Connection*, 22–24.
- Wieczorek, G.F., Mandrone, G. and DeCola, L. 1997. The Influence of Hillslope Shape on Debris-flow Initiation. In: *International Conference Water Resources Engineering Division*, ASCE, San Francisco, CA, 21–31.
- Winter, M., Smith, J. T., Fotopoulou, S., Pitilakis, K., Mavrouli, O., Corominas, J. and Argyroudis, S. 2014. An Expert Judgement Approach to Determining the Physical Vulnerability of Roads to Debris Flow, *Bulletin of Engineering Geology and Environment*, 73: 291–305.
- Wise, M. P. 1997. *Probabilistic Modelling of Debris Flow Travel Distance Using Empirical Volumetric Relationships*, MSc Thesis, University of British Columbia, Vancouver, BC.
- Wolfram, S. 1984. Cellular Automata as Models of Complexity, *Nature*, 311: 419–424

## **Appendix II: Simulation of some debris flows in Klanawa watershed in Vancouver, British Columbia**

This paper has been published in the 75<sup>th</sup> Canadian Geotechnical Conference (GeoCalgary 2022), Calgary, Canada. Most of the research work presented in this paper was conducted by the first author. The other authors supervised this research.

# Simulation of some debris flows in Klanawa watershed in Vancouver, British Columbia

Arijit Biswas Arghya, Bipul Hawlader  
Memorial University of Newfoundland, St. John's, NL, Canada  
Richard Guthrie, Graham Knibbs  
Stantec, Canada



## ABSTRACT

Debris flows are steep mountain hazards that may impact infrastructure, human life and environment considerable distance from their source. Runout simulation tools often require site-specific parameters that may be difficult to estimate or impractical to deploy at a regional scale. In contrast, models that do work regionally tend to provide limited data to the user. In this study, a relatively new agent-based simulation program called DebrisFlow Predictor was used to estimate the scour, deposition and volume of debris flows which occurred in a selected area of the Klanawa Watershed in Vancouver Island, British Columbia. This program employs a group of autonomous subroutines, or agents, that act on a digital elevation model (DEM) using a set of probabilistic rules for scour, deposition, path selection, and spreading behaviour. The advantages of this program are that it requires limited input, including DEM and user-defined initiation zones, and only modest computational power.

## RÉSUMÉ

Les coulées de débris sont des risques liés aux montagnes escarpées qui peuvent avoir un impact sur les infrastructures, la vie humaine et l'environnement à une distance considérable de leur source. Les outils de simulation du ruissellement nécessitent souvent des paramètres spécifiques au site qui peuvent être difficiles à estimer ou peu pratiques à déployer à l'échelle régionale. En revanche, les modèles qui fonctionnent au niveau régional ont tendance à fournir des données limitées à l'utilisateur. Dans cette étude, un programme de simulation basé sur des agents relativement nouveau appelé DebrisFlow Predictor a été utilisé pour estimer l'affouillement, le dépôt et le volume des coulées de débris qui se sont produits dans une zone sélectionnée du bassin versant de Klanawa sur l'île de Vancouver, en Colombie-Britannique. Ce programme emploie un groupe de sous-programmes autonomes, ou agents, qui agissent sur un modèle numérique d'élévation (DEM) en utilisant un ensemble de règles probabilistes pour l'affouillement, le dépôt, la sélection de chemin et le comportement d'étalement. Les avantages de ce programme sont qu'il ne nécessite qu'un nombre limité d'entrées, y compris le MNE et les zones d'initiation définies par l'utilisateur, et une puissance de calcul modeste.

## 1 INTRODUCTION

Debris flow is the term given to a moving mass of loose mud, soil, rock and debris that travels extremely rapidly (velocities  $> 3$  m/s and typically between 5 and 10 m/s) down steep slopes in mountainous regions. Often triggered by heavy rainfall, debris flows tend to impact infrastructure, communities, lives, and the environment considerable distance from the source. Though debris flow mechanics are well understood, modelling the complex dynamic behaviour is complicated and can depend on several interacting static and dynamic parameters. Estimating the runout and extent of debris flows is, therefore, a challenging task.

Despite the challenge, the need to credibly estimate runout remains. Empirical, analytical, and numerical methods have been developed to assess debris flow impacts. By simulating the runout extent, volume, and velocity of debris, the impact loads and the effects of runup height on the infrastructure can be estimated (Kwan 2012). Properly simulated debris flow results could be used to identify the hazard and risk zones of a specific area, which can help engineers make decisions and develop mitigation strategies.

Landslides runout analysis includes the simulation of past landslides and prediction of future potential events. Debris flow runout analysis can be performed numerically by using three-dimension models such as smoothed particle hydrodynamics (SPH) (McDougall and Hungr 2004) and two-dimension models (i.e., shallow water equations) (Hungr et al. 2005). Over the last two decades, more than 20 different numerical tools have been developed based on the hydrodynamic modelling approaches (e.g., DAN3D, Flow-2D, RAMMS). An overview of these models can be found in McDougall (2017). One of the major challenges of this type of modelling technique is the selection of model parameters. Han et al. (2017) summarized the challenges in estimating model parameters for numerical simulations. For example, while SPH is based on advanced theories and can handle complex geometries, it requires estimates of yield strength and dynamic viscosity, which may themselves be unknown or difficult to obtain. In addition, the simulations tend to be computationally very expensive, especially for large areas and smaller mesh sizes. Therefore, comprehensive numerical simulations to identify the effects of key parameters are difficult.

To overcome some of the limitations of existing numerical modelling, a different methodology using cellular

automata (CA) has been deployed in several studies to model complex natural phenomena, including debris flows (Iovine 2003; Guthrie et al., 2008), snow avalanches (Barpi et al. 2007), and lava flows (Spataro et al. 2004). Cellular automata evolves in a discrete space-time context. It involves a collection of cells arranged in a grid shape, where the state of each cell depends on a function of time according to a defined set of rules driven by the states of neighbouring cells. The main advantages of cellular automata models are that they require fewer model parameters and less computational time than those of numerical simulation (e.g. SPH) yet provide satisfactory results. Several studies showed successful applications of the cellular automata model for debris flow runout simulations (Han et al. 2021; Guthrie and Befus 2021; Guthrie et al., 2008; D'Ambrosio et al. 2003(a); D'Ambrosio et al. 2003(b)). Further details on CA and its application in debris flow modelling are available in previous studies (Han et al. 2017).

Between 1880 and 2019, 123 landslides caused fatalities in British Columbia (BC), and among all landslides from 1950 to 2019 in BC, 53% were debris flows (Strouth and McDougall 2021). The frequency of debris flows is higher on the windward side of mountains exposed to higher rainfall. For example, the west coast of Vancouver Island has approximately three times as many debris flows as the eastern zone over similar time periods (Guthrie 2009).

Forestry, the primary resource-based industry over the last century in BC, has directly and indirectly increased the rate of landslides. Guthrie and Brown (2008), for example, reported that human activities that induced landslides (e.g. forest harvesting) had doubled the landscape erosion compared to the next highest millennia over the Holocene. Consequently, understanding potential debris flow impacts also represents an important management objective for the forest industry.

The objective of the present study was to simulate debris flows in a selected area of the Klanawa watershed on the west coast of Vancouver Island, BC, using the computer program DebrisFlow Predictor and then compare

the results with available historical debris flows. We intend to provide a calibrated model that could be used as a predictive tool for subsequent hazard assessment in this area.

## 2 STUDY AREA

The Klanawa watershed on Vancouver Island, British Columbia, is approximately 240 km<sup>2</sup> in size and located on the southwest coast side of the island. The floodplain is made up of glaciofluvial and alluvial sediments. Mid and upper slopes consist of glacially over-steepened morainal till or gravelly colluvium veneers (Morgan 2001) that frequently show signs of instability in the form of open slope and channelized debris flows. The watershed is also critical for the aquatic habitats, which are sensitive to peak flow disturbances and are affected by erosion and bedload sediment.

Guthrie et al. (2008) reported 331 debris flows over 500 m<sup>2</sup> in the Klanawa watershed from the available 1994–2001 air photograph record. Guthrie et al. (2010) examined the role of slope angle on erosion, deposition of debris, and the effects of topographic settings (i.e., presence of forest and roads) on spreading (e.g. width of the flow).

For the present study, approximately an 8 km<sup>2</sup> area was selected where debris flow footprint information was publicly available (Fig. 1). Ten debris flows within the study area were reported by Guthrie et al. (2008) (blue coloured landslides in Fig. 1). Of those, seven debris flows are simulated in this study and named P1–P7 (Fig. 1). Six more recent debris flows were identified using Google Earth Pro for the period of 2015–2021 (C1–C6 on Fig. 1). C1 occurred sometime between July 2019 and April 2021, while C2–C6 occurred between April 2021 and October 2021. We note that debris flow might have occurred during other periods (e.g., 2008–2015); however, because of vegetation and the unavailability of time series maps in Google Earth Pro, those debris flows were not recorded here.

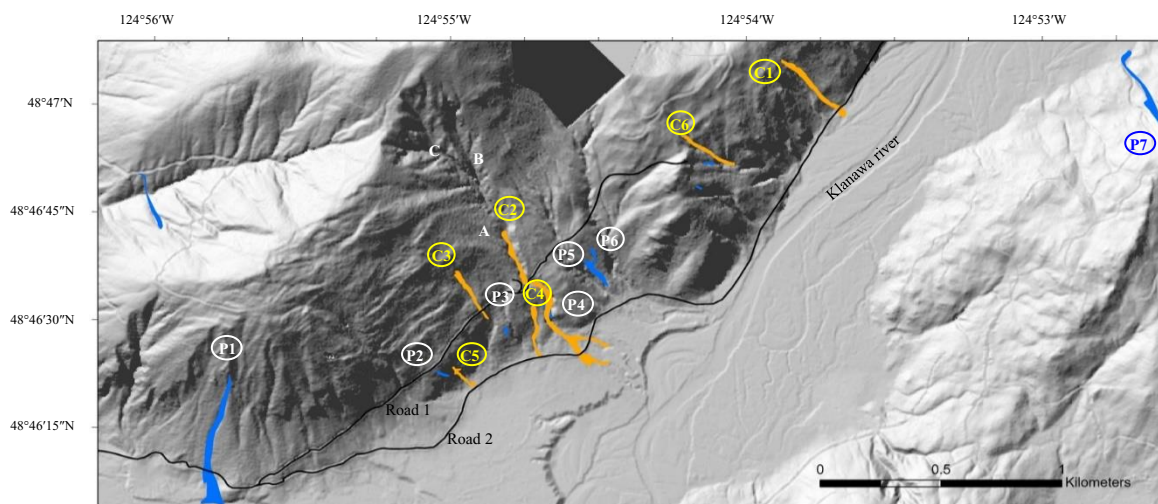


Figure 1. Debris flow footprints in the study area.

The above-mentioned debris flows (P1–P7 & C1–C6) occurred in varying settings (e.g., topography) and the spatial extent varied widely between them. The present study attempts to simulate these debris flows to show the performance of the program and to identify the influence of some input parameters which could be site-specific.

### 3 MODELLING CONCEPTS

DebrisFlow Predictor is a computer program developed by Guthrie and Befus (2021) and based on a cellular automata model. The simulation of runout with this program provides landslide pathways and sediment volume (scour and deposition) along the flow path. One of several advantages of the program is that these simulation results can be imported into any GIS software to compare with the mapped (actual) landslides and land use managers with subsequent decisions.

DebrisFlow Predictor follows a set of simple rules for scour, deposition, path selection, and spread. These rules were developed empirically based on the observations of debris flows in coastal areas of BC. These rules follow probability distributions for 12 slope classes (See Table.1 Guthrie and Befus 2021). These probabilities are based on the fieldwork conducted by Wise (1997), Guthrie et al. (2008) and on work by Guthrie and Befus (2021).

The program requires limited input parameters for runout assessment. Firstly, it requires the digital elevation model (DEM) of the area with a resolution of 5 m × 5 m. Secondly, the user has to identify the initiation zones of the debris, which can be done in multiple ways. Users can select a single cell (5 m × 5 m), a small group of cells (15 m × 15 m), or multiple cells (a larger source zone) simply by painting over a larger area. The user could also import the initiation zones as a shapefile in the program, which can automatically be turned into 15 m × 15 m initiation zones. In the present study, debris flow initiation points were imported (identified from google earth images) as a shapefile within the program.

When the DEM is imported into the program, each cell in the working grid collects the basic information from the DEM, including elevation, position, slope, and aspect. Each activated cell (i.e. each cell selected manually or by the computer model to generate an agent) contains an agent—an autonomous subroutine that interacts with the surface model and other agents. At a given time step, erosion and deposition are calculated, and the difference between these two gives the net mass. The mass is shed to the new cells by spawning additional agents. Each agent continues to move downslope until its mass balance is zero.

The direction of debris flow is determined by a Moore Neighbourhood algorithm. The Moore Neighbourhood method determines the direction of debris flow by obtaining the elevations of the eight cells surrounding the core cell. In each time step, the debris from the core cell flows toward the surrounding lowest vacant cells. When there are no vacant cells, or three cells have the same elevation, the flow direction is determined by a combination of random chance and momentum preservation.

The redistribution of mass or spreading behaviour is described by a probability density function defining the standard deviation ( $\sigma$ ) as

$$\sigma = \left( \frac{m_{max} - m}{m_{max}} \right)^n (\sigma_L - \sigma_S) + \sigma_S \quad [1]$$

where  $m_{max}$  is the fan maximum slope to limit spreading above the selected slope value,  $m$  represents DEM slope,  $n$  is a skew coefficient,  $\sigma_L$  is low slope coefficient, and  $\sigma_S$  is steep slope coefficient.

These parameters can be calibrated iteratively within the model, and the results compared to known (observable) events or landforms. The parameter  $m_{max}$  limits spreading to slopes flatter than the selected value. Guthrie and Befus (2021) recommended using 27° where additional information is not available. The parameters  $n$ ,  $\sigma_L$ , and  $\sigma_S$  control the amount of spread and, therefore, the creation of new agents redistributed to surrounding cells. With an increase in the value of  $\sigma_L$  and  $\sigma_S$  the spreading increases in the low and steep slope areas, respectively. The parameters used in this application of DebrisFlow Predictor are listed in Table 1. Further details of these parameters could be found in Guthrie and Befus (2021).

The user can make modifications to account for variations in local geomorphology (e.g. surficial material depth) by changing the program's deposition and erosion multiplier sliders button. The program also considers mass loss in turns, if crudely, specified every 45° of departure from a straight line. Finally, it has the ability to set a minimum scour depth in the initiation zone to account for the observed experience.

Table 1. Parameters used DebrisFlow Predictor

Fan maximum slope ( $m_{max}$ )	34°
Low slope coefficient ( $\sigma_L$ )	0.35
Steep slope coefficient ( $\sigma_S$ )	1.35
Skew coefficient ( $n$ )	1.1
Maximum spawns allowed	4
Deposition multiplier	1x
Erosion multiplier	0.7x
Mass loss per 45° turn	20%
Minimum initiation depth	0
Number of model runs	50

### 4 RESULTS AND DISCUSSION

Figures 2(a) and 2(b) show the debris flow over an area of a relatively steep slope (C1). The simulated debris flow trajectory shown in Fig. 2(b) is very similar to the mapped debris flow shown in Fig. 2(a). In the simulation, yellow and red colours represent scour, while green and blue represent the areas of deposition. Deeper deposition (blue) is found near the toe of the debris flow.

A close examination of the LiDAR slope profile shows that the slope angle along the path of this debris flow varies primarily between 40° and 50° with some local flatter

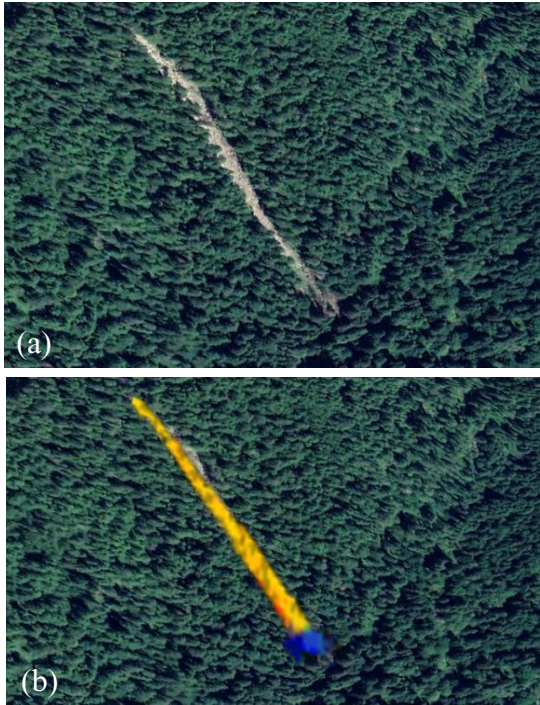


Figure 2: Debris flow in a steep area: (a) mapped footprint (background image from Google Earth); (b) DebrisFlow Predictor simulation.

slopes near the toe and steeper slopes near the initiation zone and at the middle of the travel path. In this case, flow occurred almost along a line without significant lateral spreading or formation of multiple paths or diversion because the slope is relatively steep and uniform.

The debris flow C2 was a channelized debris flow that occurred in a pre-existing gully (Fig. 3(a), 2019 map). Figure 3(b) shows the trace of a long debris flow(s) along this gully which occurred in 2021. Vegetation covered the upper part of the gully (above point A in Fig. 1) and the location and size of the debris flow initiation zone were difficult to find. Several attempts were made to simulate the observed debris flow footprint by varying the location (points A–C in Fig. 1) and the size of the initiation zones. The following were the key observations: (a) for a smaller initiation zone (15 m x 15 m) at point A, the debris flow stopped after travelling a small distance (~ 90 m); (b) when the size of the initiation zone was enlarged (e.g., ~ 50 m x ~ 50 m), the debris travel distance increased but still less than the observed extent; (c) when the location of the initiation zone was moved to a higher elevation (e.g., B or C), travel distance increased, presumably because of increased higher kinetic energy that facilitated the flow over gentler slopes (even opposite near the road) downstream; and (d) an increase in the size of the initiation zone for locations B and C increased the extent of debris flow. Better simulation results could be obtained by adjusting the parameters in Table 1. However, none of the simulations of case C2 for the above-mentioned conditions closely matched the observed debris flow pattern. Though this may be an error of parameterization, it may also represent a

complication modelling regional debris flows, particularly if parameters are different within a single area. Despite the ease of the use, the program does seem to require expert judgement to calibrate and provide representative scenarios.

Figure 4 highlights another program feature, the ability to determine the probability of inundation based on multiple runs (assuming calibration has been successful). In this case, the darker areas represent higher inundation probabilities. As the program results are probabilistic, any two runs are not identical, and multiple runs are recommended to reach a conclusion on the likely path of debris flow. In this study, the simulation was run for 50 times.



Figure 3: Satellite image along the flow path of C2: (a) image in 2019; (b) image in 2021.

The simulated debris flow paths for most cases are similar to the footprint observed in the field (compare Figs. 1 & 4). However, there are some differences. For example, three potential flow paths were identified in the simulation of P1, while there was only one path observed by Guthrie et al. (2008). This may simply be the stochastic distribution of individual runs in a similar landscape, but it could also be an effect of the DEM resolution or the actual 2019 topography that was altered by the earlier (mapped) landslide. Again, expert judgement as to the applicability of the results is recommended.

Debris travelled only a limited distance in C2 simulation and considerably less than the channelized flow observed in the field. Potential reasons for this have been described above. The simulated travel distance for case C6 was larger than that observed in the field. Again, this may be the result of local effects, parameterization, or simply the stochastic nature of a single event versus multiple modeled

events. Despite the foregoing, DebrisFlow Predictor gives, by and large, comparable flow paths to those observed in the field.

Several studies reported the role of roads and logging on the mobility of debris. For example, Guthrie (2009)

reported that while road building and logging could increase the occurrence of landslides, the existence of roads could also reduce debris flow volumes by creating a topographic resting place for sediment. For several cases (e.g., P1, C1 & C3), debris flows were reduced or were stopped by the two existing roads in this area.

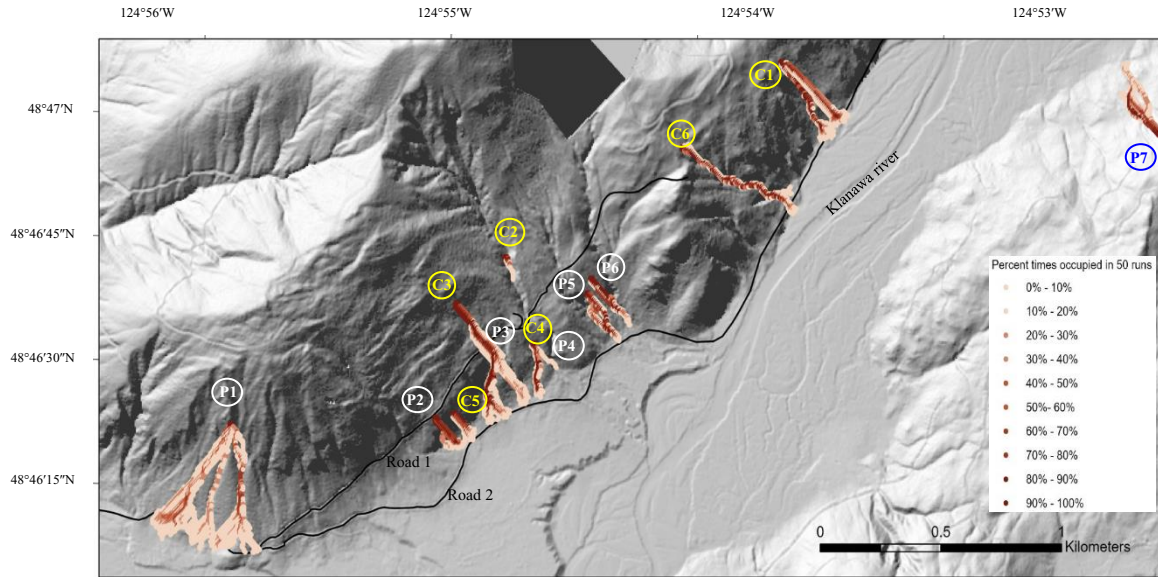


Figure 4: Debris flow simulation results. The results show both the cumulative footprint of multiple runs and the likelihood that any location on the map would be occupied in a single run.

The depth of the debris could be calculated using the simulated results. The depth information can be used to facilitate vulnerability calculations and ultimately develop mitigation strategies for the impact of debris flow. For example, Ciurean et al. (2017) used the depth of debris to

define damage class. As shown in Figure 5, a higher accumulation of debris occurred near the toe, and the maximum depth is 3.85 meters, which occurred in case C3.

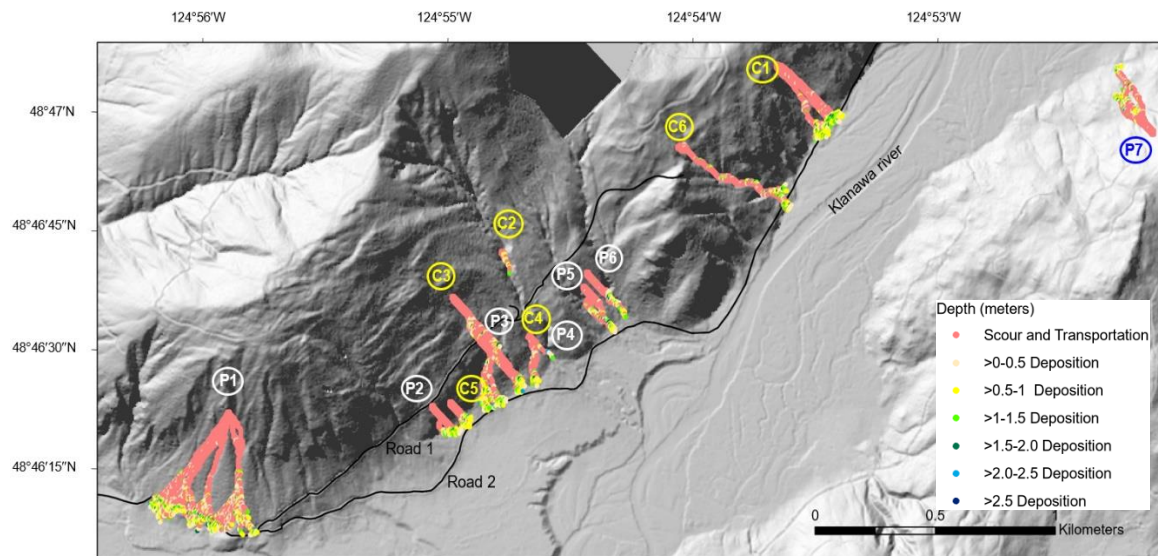


Figure 5: Depth of debris obtained from DebrisFlow Predictor.

## 5 CONCLUSIONS

DebrisFlow Predictor was used to simulate debris flow in a selected area of the Klanawa watershed, Vancouver Island. Simulations were performed for a total of 13 cases using the 2019 DEM. Most of the simulations showed debris flow patterns similar to the footprints observed in the field. For some, DebrisFlow Predictor provided multiple potential flow paths, of which the observed landslide used just one. Finally, with the parameters selected herein, the model underestimated the flow through a pre-existing channel.

Further studies are recommended to model channelized debris flows and provide a better estimation of model parameters.

## 6 ACKNOWLEDGEMENTS

The works presented in this paper were supported by the Natural Sciences and Engineering Research Council (NSERC) and Equinor Research Chair grants.

## 7 REFERENCES

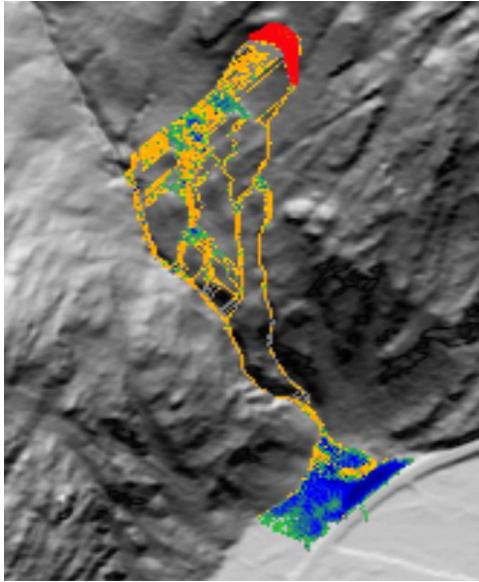
- Barpi, F., Borri-Brunetto, M., Veneri, L., D. 2007. Cellular-automata Model for Dense-snow Avalanches. *Journal of Cold Regions Engineering*, 21(4): 121–140.
- Ciurean, R. L., Hussin, H., vanWesten, C. J., Jaboyedoff, M., Nicolet, P., Chen, L., Frigerio, S., and Glade, T. 2017. Multi-scale Debris Flow Vulnerability Assessment and Direct Loss Estimation of Buildings in the Eastern Italian ALPS, *Natural Hazards*, 85: 929–957.
- D'Ambrosio, D., Di Gregorio, S., Iovine, G., Lupiano, V., Rocco, V., Spataro, W. 2003(a). First Simulations of the Sarno Debris Flows through Cellular Automata Modelling, *Geomorphology*, 54(1–2): 91–117.
- D'Ambrosio, D., Di Gregorio, S., Iovine. 2003(b). Simulating Debris Flows through a Hexagonal Cellular Automata, *Natural Hazard and Earth System Sciences*, 3: 545–559.
- Guthrie, R. H. 2009. *The Occurrence of Behaviour of Rainfall-triggered Landslides in Coastal British Columbia*, Doctoral dissertation, University of Waterloo, Ontario, Canada.
- Guthrie, R. H. and Befus, A. 2021. DebrisFlow Predictor: An Agent-based Runout Program for Shallow Landslides, *Natural Hazards and Earth System Sciences*, 21(3): 1029–1049.
- Guthrie, R. H. and Brown, K.J. 2008. Denudation and Landslides in Coastal Mountain Watersheds: 10,000 years of erosion, *Geographica Helvetica*, 63: 26–33.
- Guthrie, R.H., Deadman, P., Cabrera, R., and Evans, S. 2008. Exploring the Magnitude-Frequency Distribution: a Cellular Automata Model for Landslides, *Landslides*, 5: 151–159.
- Guthrie, R. H., Hockin, A., Colquhoun, L., Nagy, T., Evans, S. G. and Ayles, C. 2010. An Examination of Controls on Debris Flow Mobility: Evidence from Coastal British Columbia, *Geomorphology*, 114: 601–613.
- Han, Z., Li, Y., Huang, J., Chen, G., Xu, Li., Tang, C., Zhang, H., Shang, Y. 2017. Numerical Simulations for Run-out Extent of Debris Flows Using an Improved Cellular Automata Model, *Bulletin of Engineering Geology and the Environment*, 76: 961–974.
- Hungr, O., McDougall, S., Bovis. M. 2005. Entrainment of Material by Debris Flows, Debris-flow Hazards and Related Phenomena, Springer, Berlin, Heidelberg, 135–158.
- Iovine, G., Di Gregorio, S., Lupiano, V. 2003. Debris-flow Susceptibility Assessment through Cellular Automata Modeling: an Example from 15–16 December 1999 Disaster at Cervinara and San Martino Valle Caudina (Campania, Southern Italy), *Natural Hazards Earth System Science*, 3: 457–468.
- Kwan, J.S.H. 2012. *Supplementary Technical Guidance on Design of Rigid Debris-resisting Barriers*, Hong Kong Geotechnical Engineering Office, Report No. 270.
- Morgan, D. 2001. *Fish Habitat Overview Assessment for the Klanawa River Watershed*. Ministry of Forests, Victoria, British Columbia.
- McDougall, S. 2017. 2014 Canadian Geotechnical Colloquium: Landslide Runout Analysis — Current Practice and Challenges, *Canadian Geotechnical Journal*, 54(5): 605–620.
- McDougall, S., Hungr, O. 2004. A Model for the Analysis of Rapid Landslide Motion across Three-dimensional Terrain, *Canadian Geotechnical Journal*, 41: 1084–1097.
- Spataro, W., D'Ambrosio, D., Rongo, R., Trunfio, A., G. 2004. An Evolutionary Approach for Modelling Lava Flows Through Cellular Automata. *International Conference on Cellular Automata*. In: ACRI 2004, proceedings, LNCS, Springer, Berlin, 3305: 725–743.
- Strouth, A. and McDougall, S. 2021. Historical Landslides Fatalities in British Columbia, Canada: Trends and Implications for Risk Management, *Frontiers in Earth Science*.
- Wise, M. P. 1997. *Probabilistic Modelling of Debris Flow Travel Distance Using Empirical Volumetric Relationships*, MSc Thesis, University of British Columbia, Vancouver, BC

## **Appendix III**

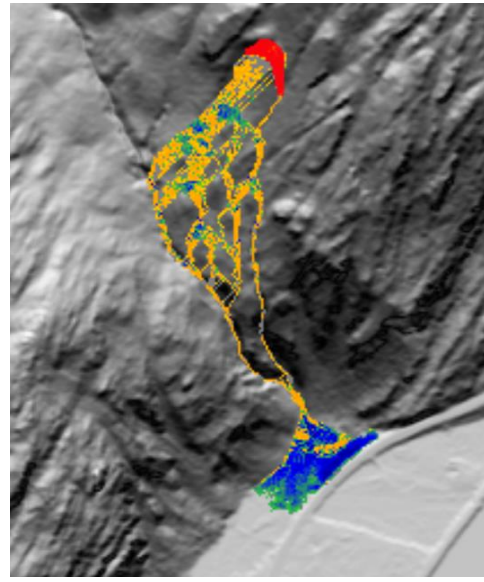
This appendix shows some additional simulation results of Site 1 by changing only one parameter while keeping the remaining parameters the same as the best-case scenarios, as mentioned in Chapter 3. These results can help to understand the sensitivity of each parameter.

## DebrisFlow Predictor Simulations

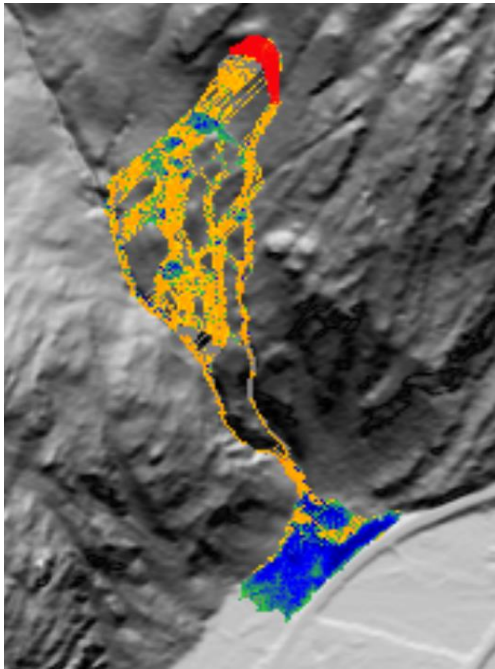
*Varying Fan Maximum Slope ( $m_{max}$ )*



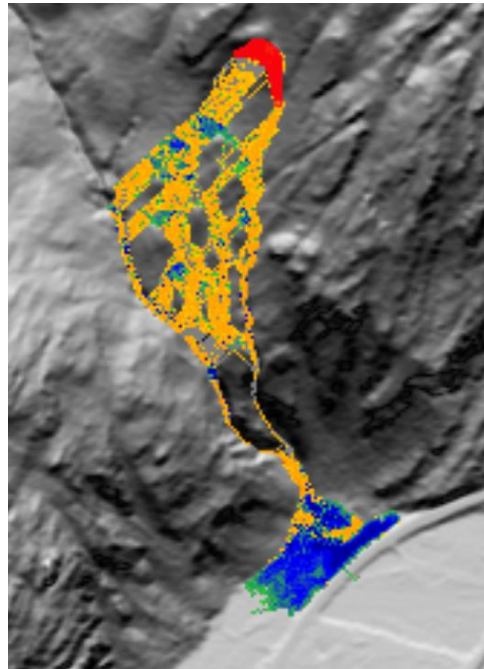
$m_{max} = 25^\circ$



$m_{max} = 29^\circ$

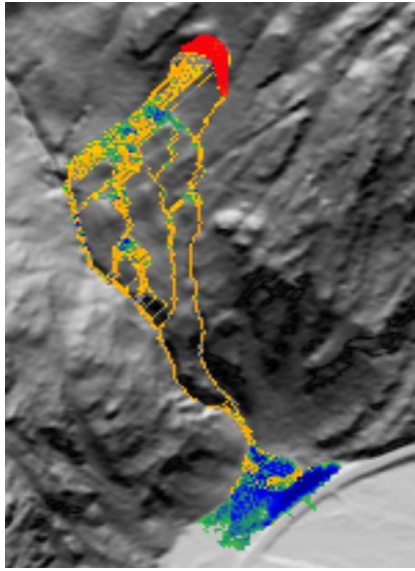


$m_{max} = 34^\circ$

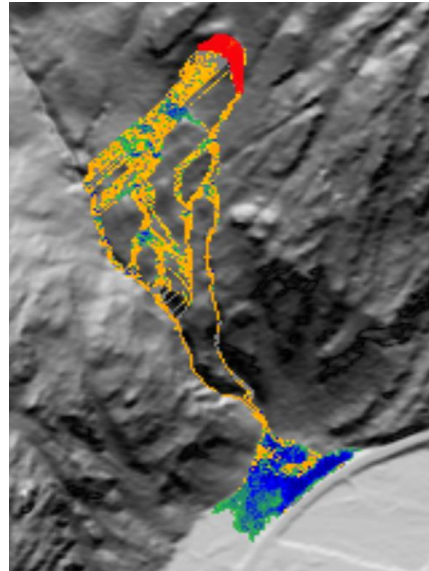


$m_{max} = 37^\circ$

*Varying Steep Slope Coefficient ( $\sigma_s$ )*

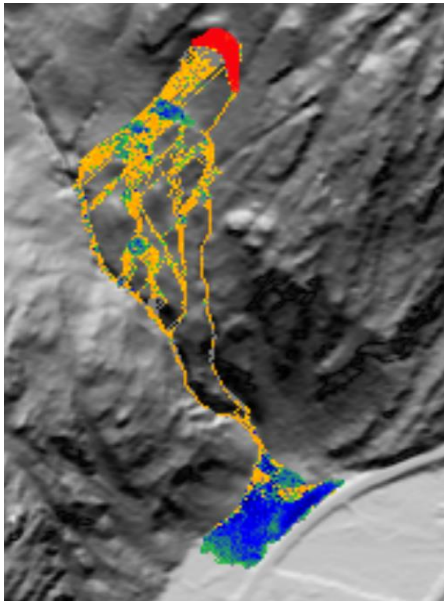


$\sigma_s = 0.3$

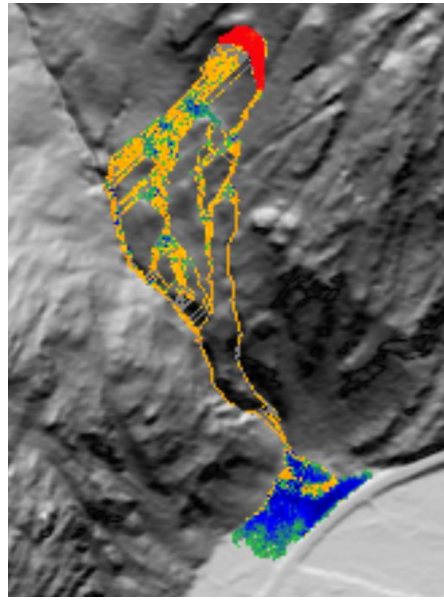


$\sigma_s = 0.4$

*Varying Mass loss per 45° Turn (%)*

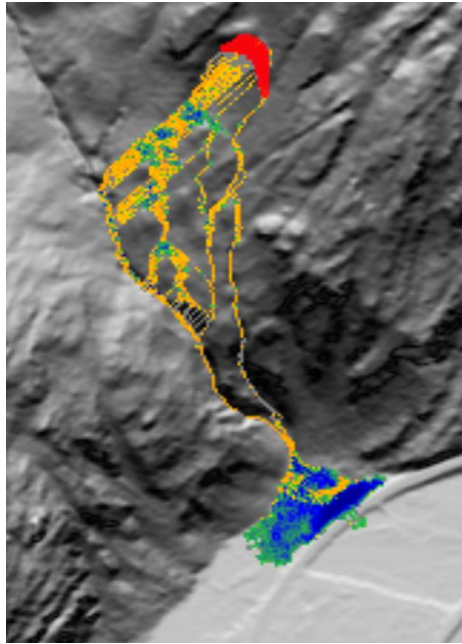


Mass Loss = 0%

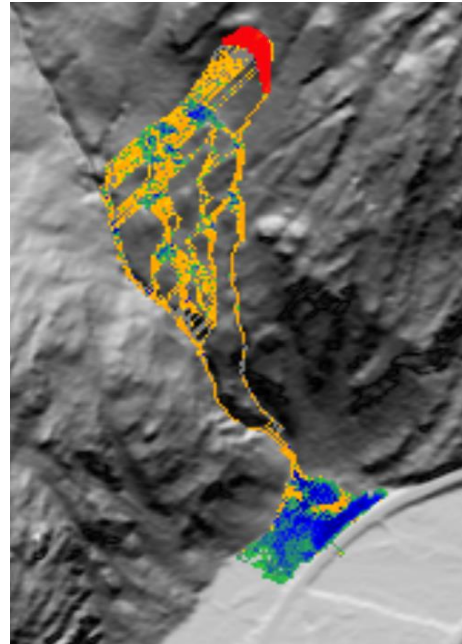


Mass Loss = 20%

*Varying Low Slope Coefficient ( $\sigma_L$ )*

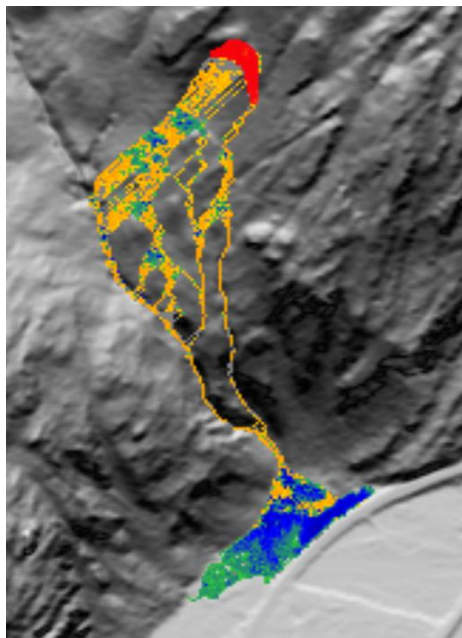


$\sigma_L = 1.15$

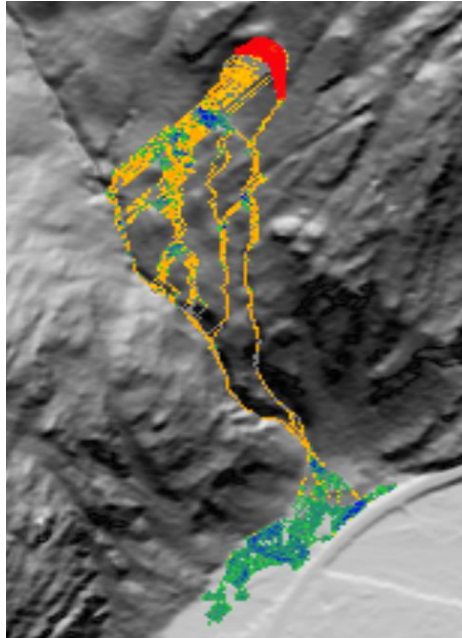


$\sigma_L = 1.55$

*Varying Maximum Spawns Allowed ( $N_{max}$ )*

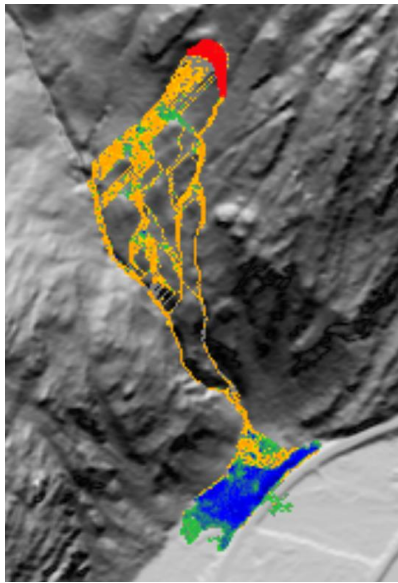


$N_{max} = 15$

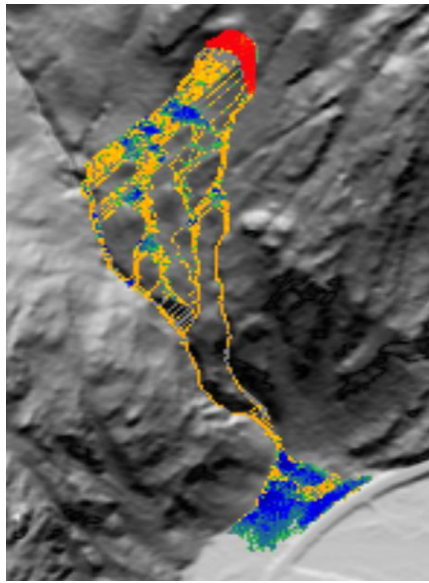


$N_{max} = 4$

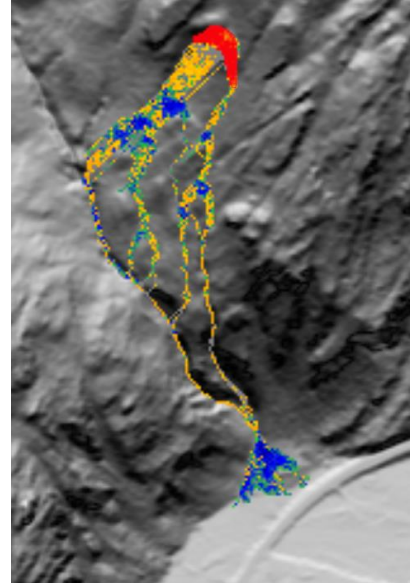
*Varying Deposition Multiplier*



Deposition Multiplier = 0.2

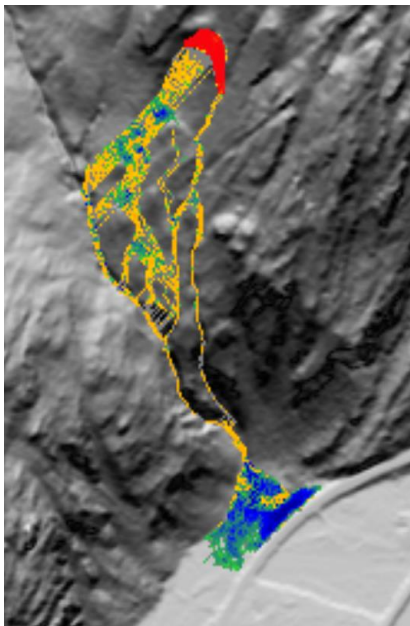


Deposition Multiplier = 0.6

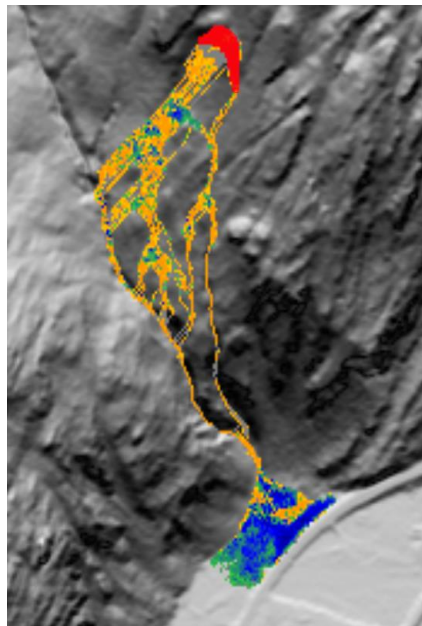


Deposition Multiplier = 1

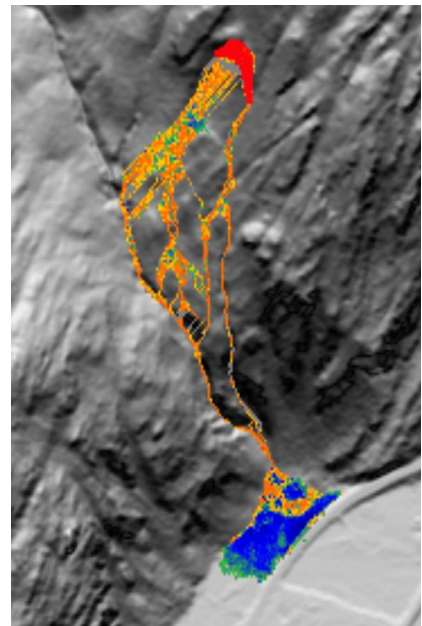
*Varying Erosion Multiplier*



Erosion Multiplier = 0.5

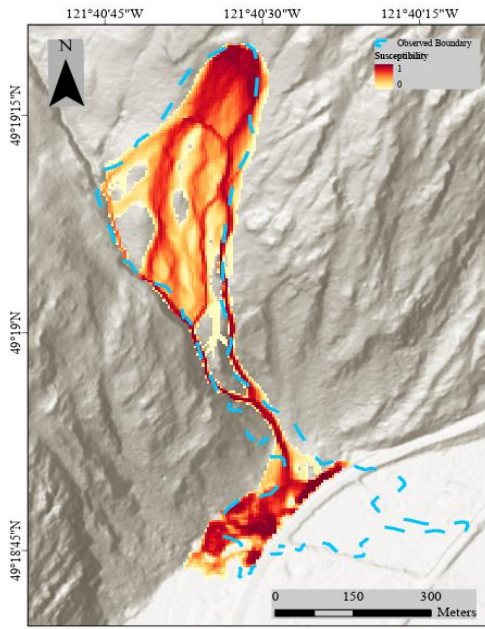


Erosion Multiplier = 1

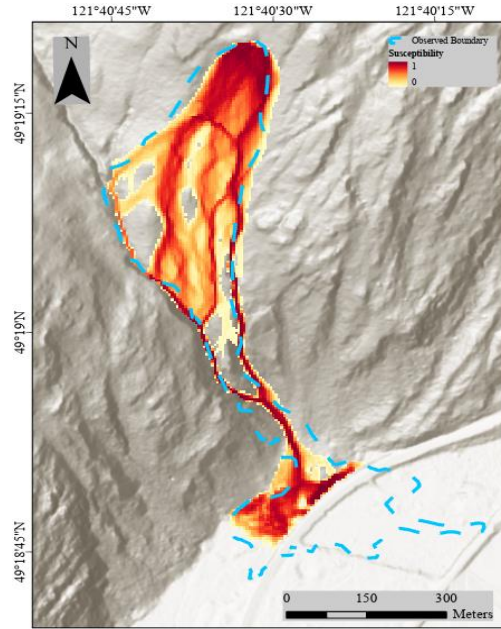


Erosion Multiplier = 1.5

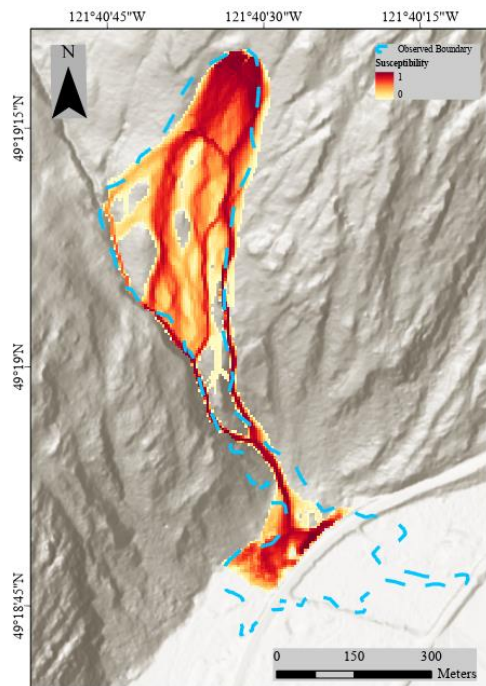
**Flow-R Simulations**  
*Varying Travel Angle ( $\varphi$ )*



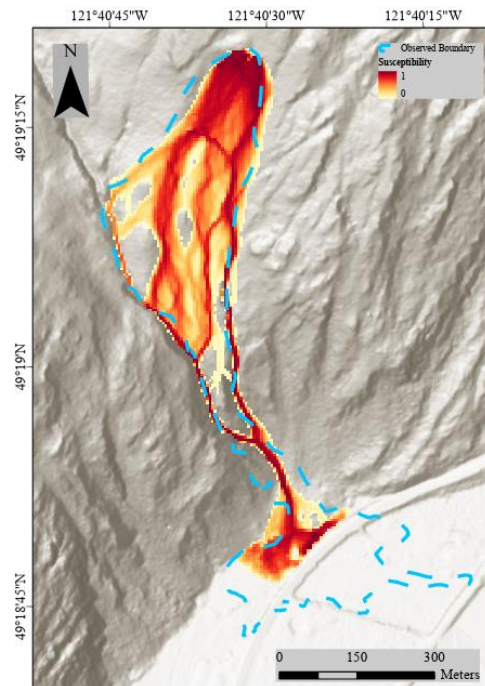
Travel angle = 5°



Travel angle = 9°

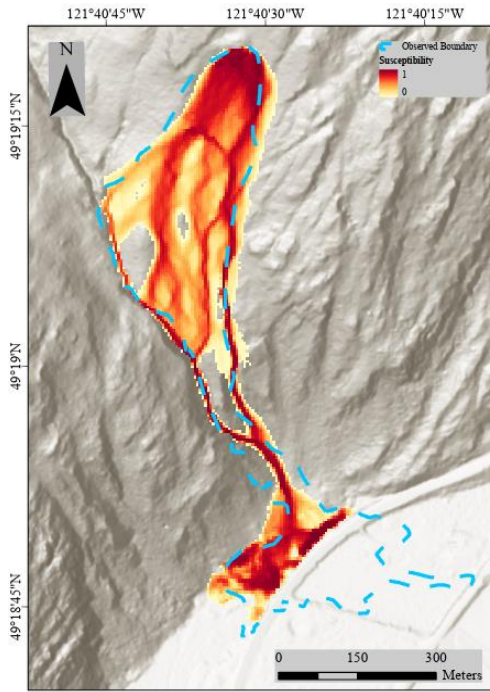


Travel angle = 11°

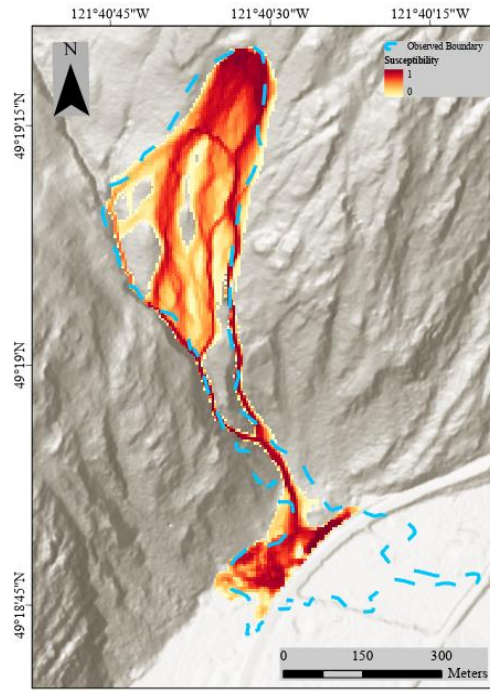


Travel angle = 13°

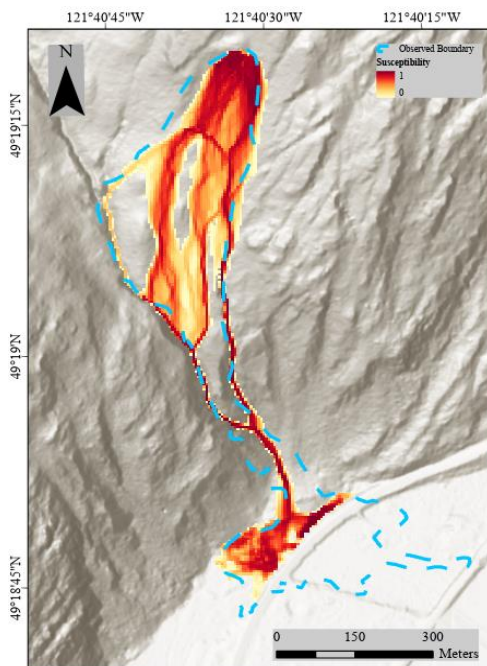
Varying exponent ( $x$ )



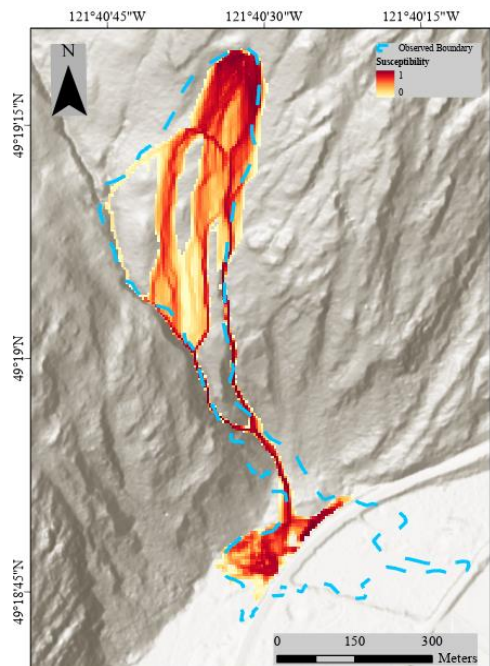
$x = 2$



$x = 4$

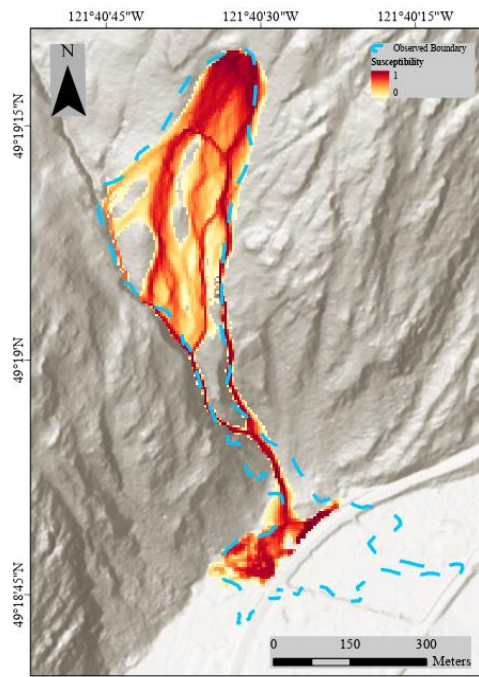


$x = 6$

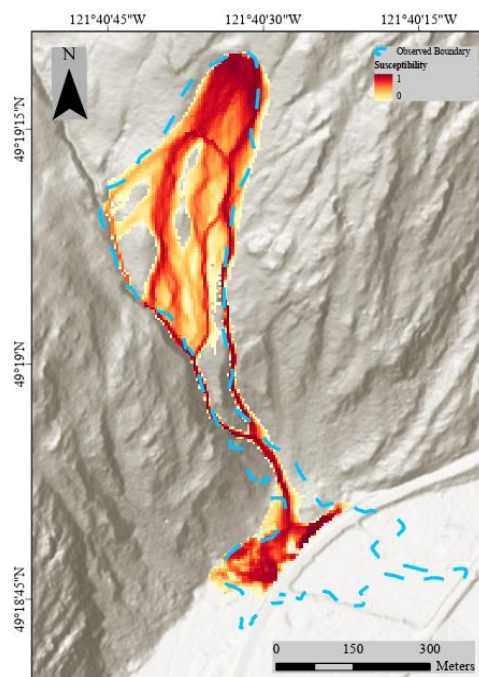


$x = 8$

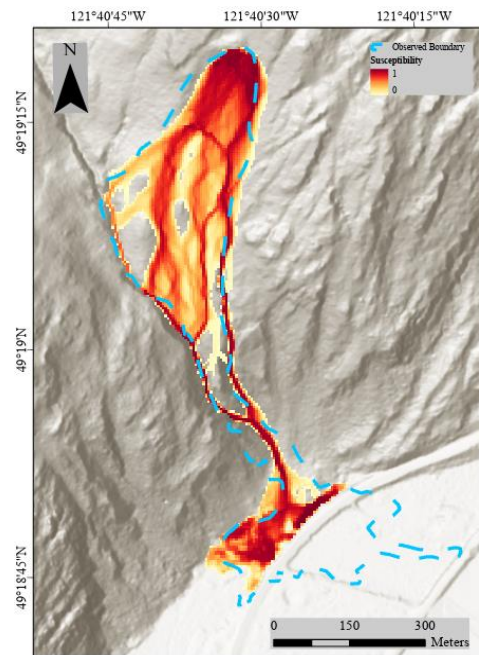
Varying Degree of Convergence ( $dh$ )



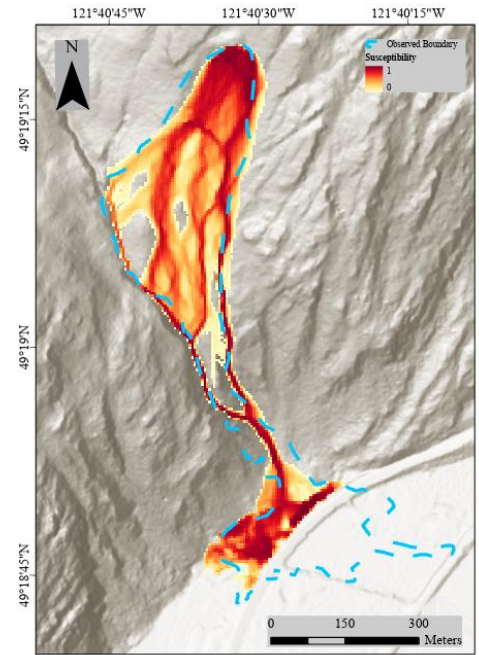
$dh=1$



$dh=1.5$

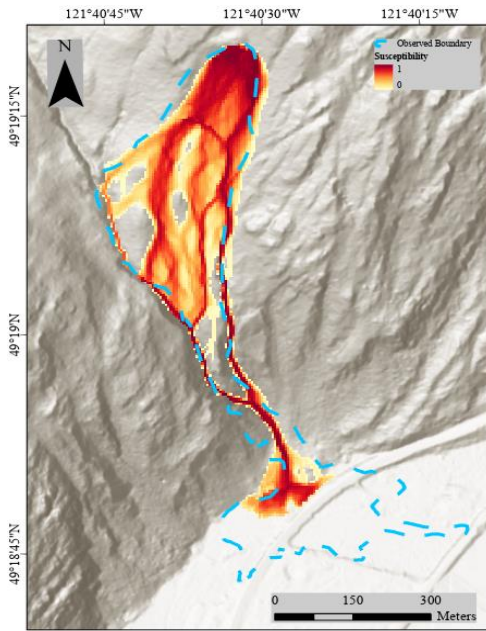


$dh=2$

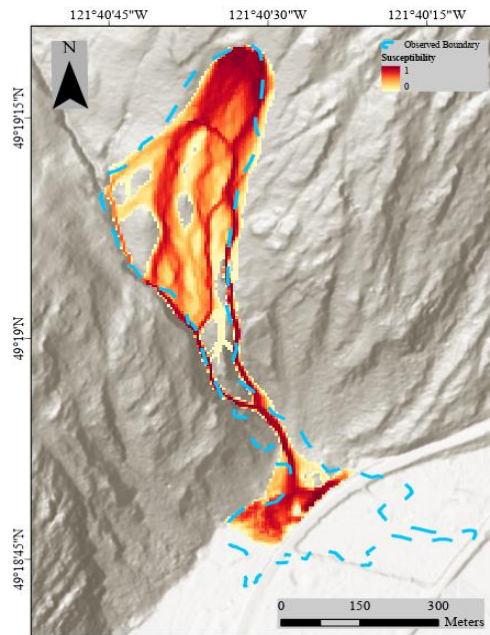


$dh=3$

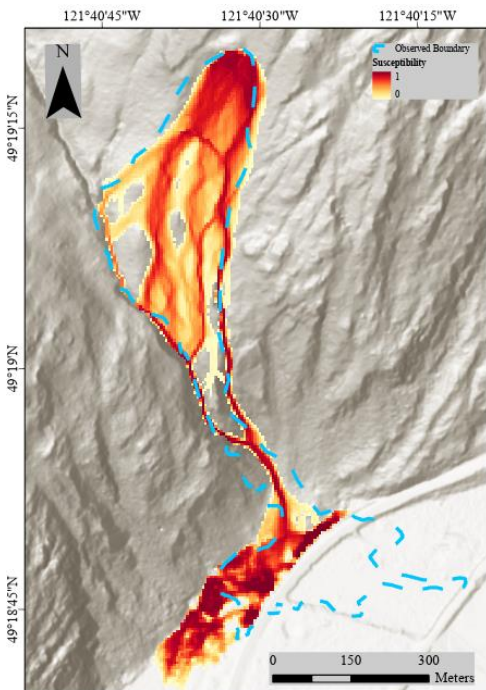
*Varying Velocity Threshold ( $v_{\max}$ )*



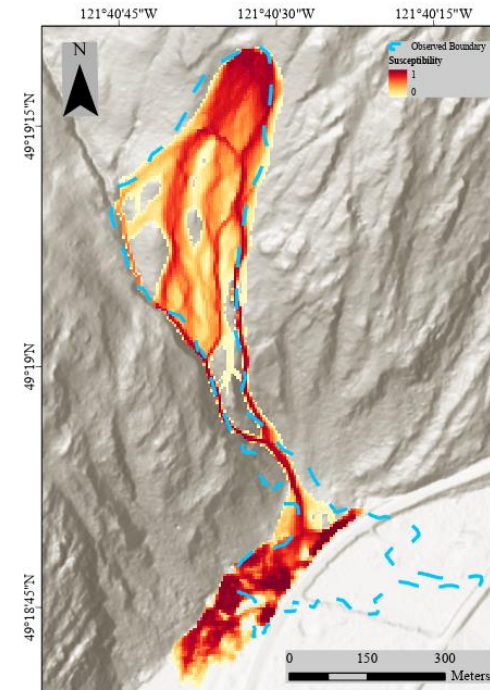
$v_{\max}=10$



$v_{\max}=15$

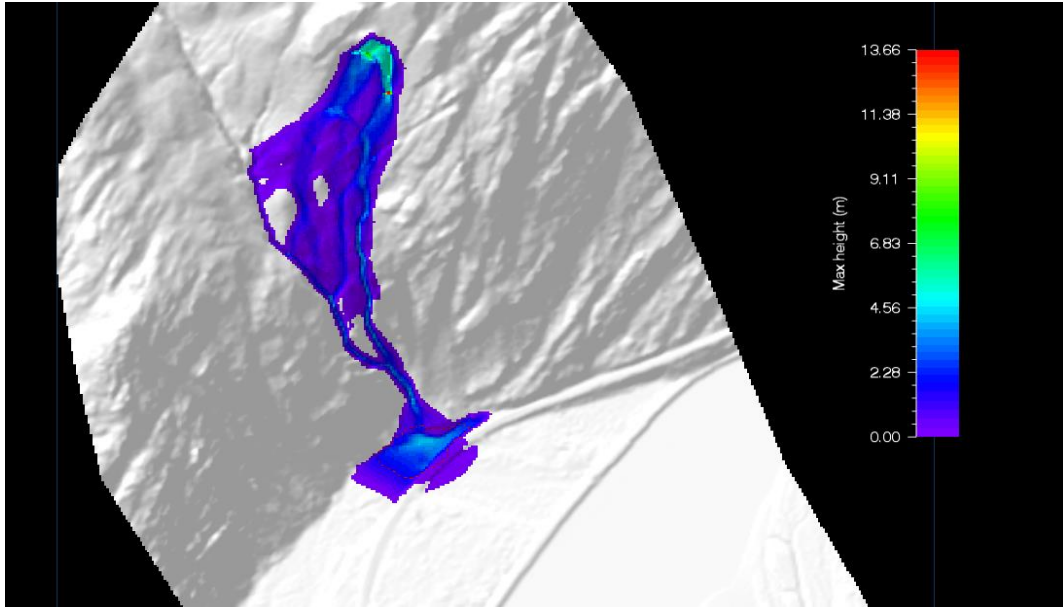


$v_{\max}=25$

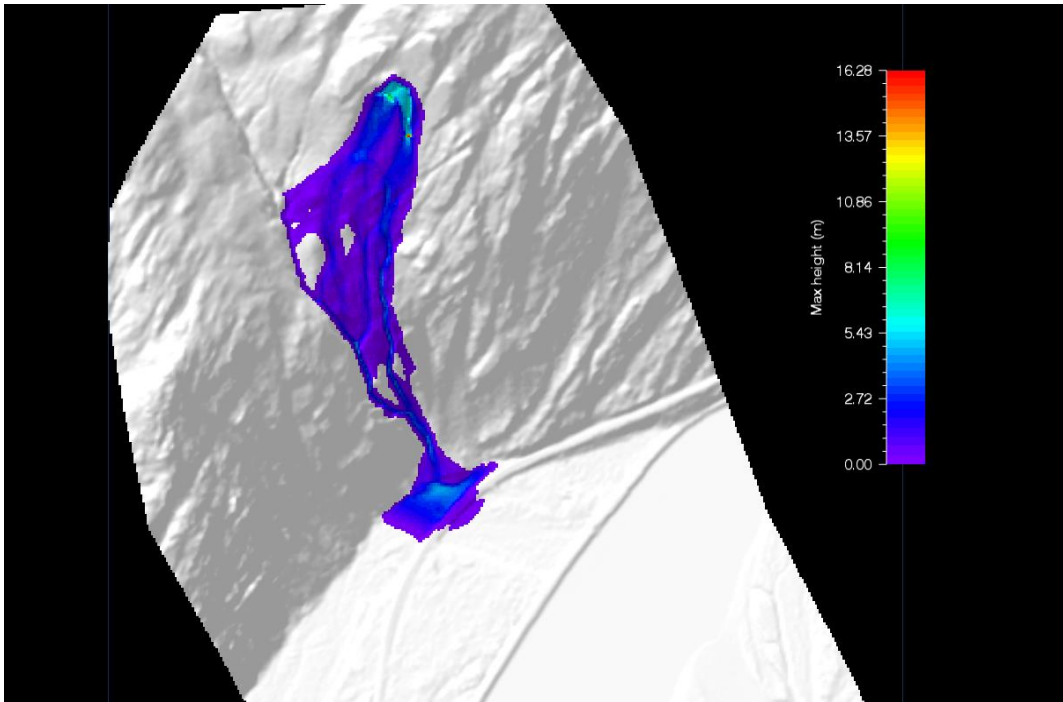


$v_{\max}=30$

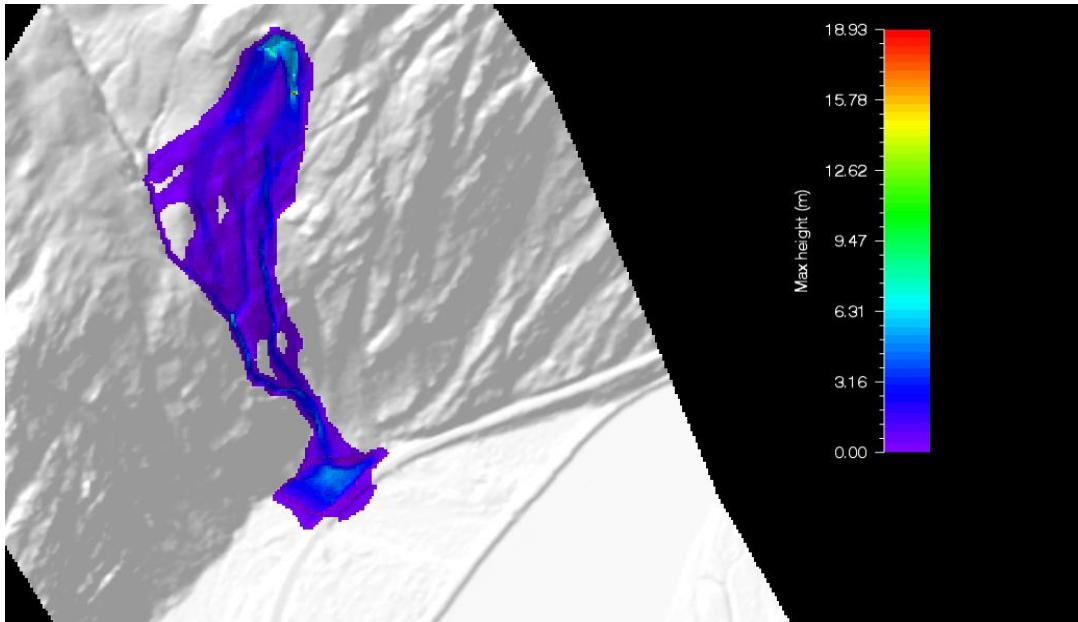
**RAMMS Simulations**  
*Varying viscous-turbulent Friction Coefficient*



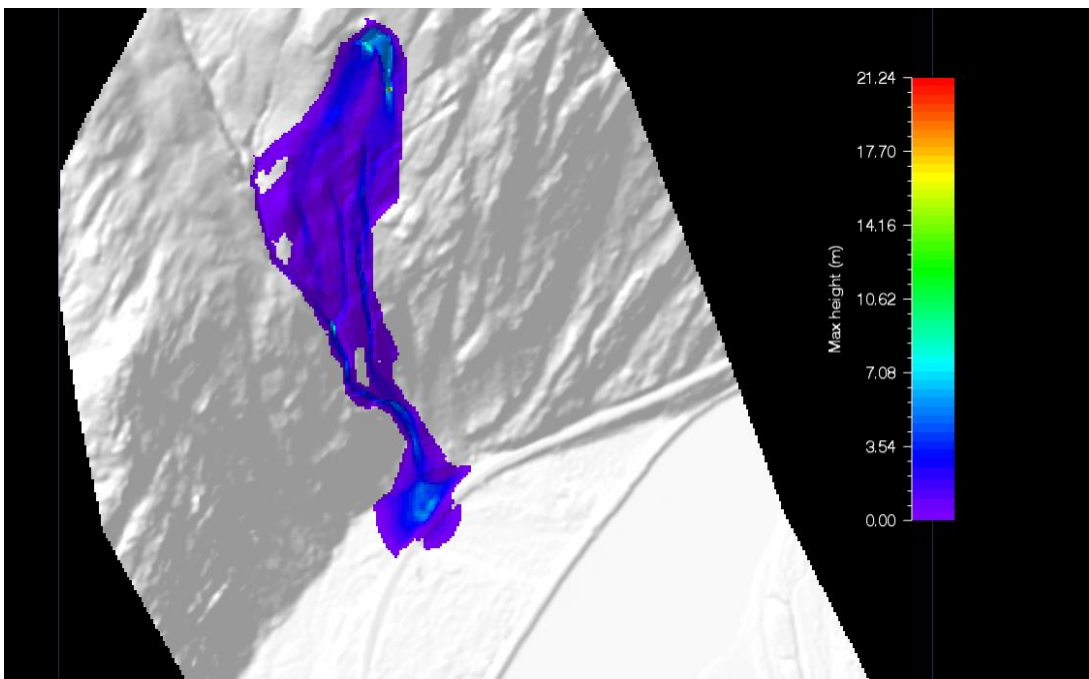
$\xi = 100$



$\xi = 200$

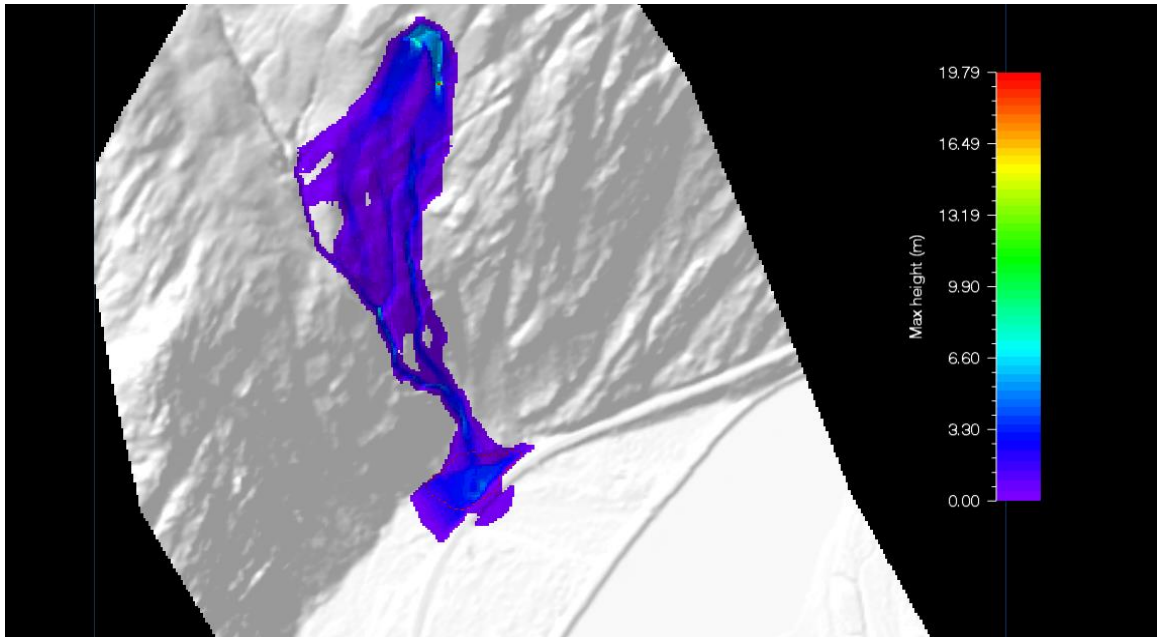


$\xi = 400$

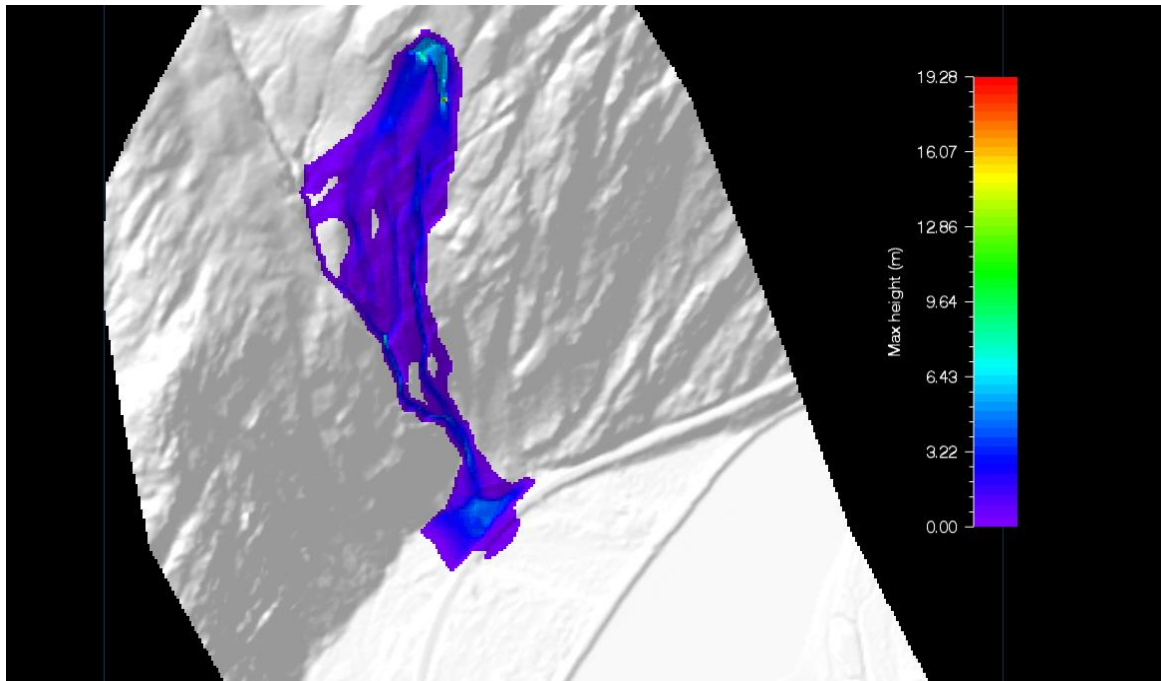


$\xi = 800$

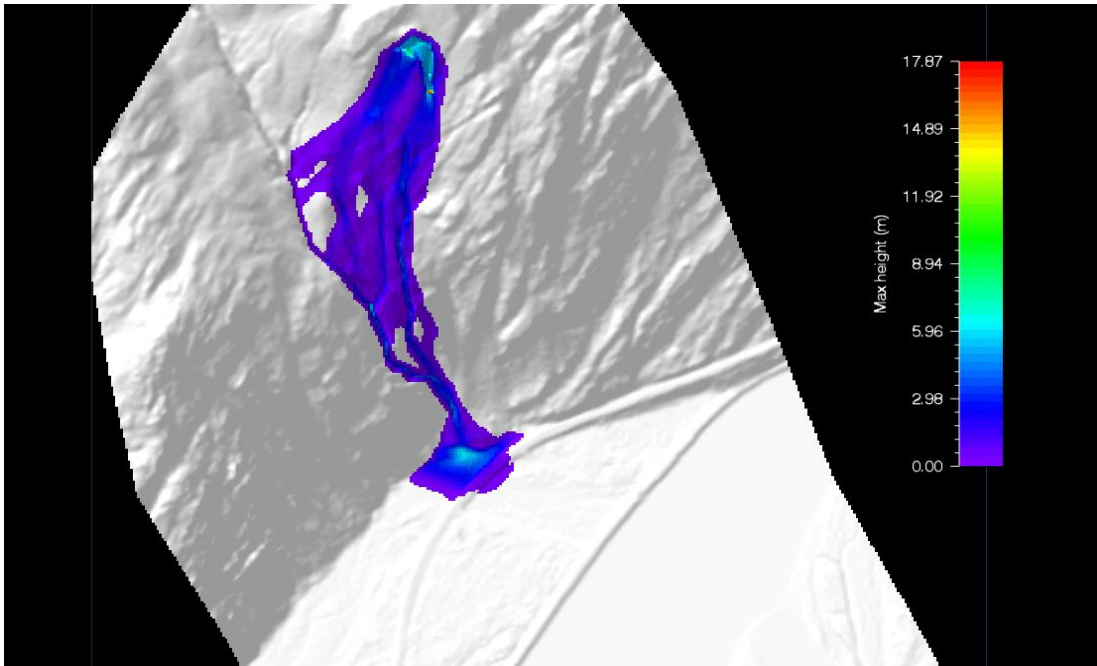
*Varying Dry Coulomb-type Friction Coefficient*



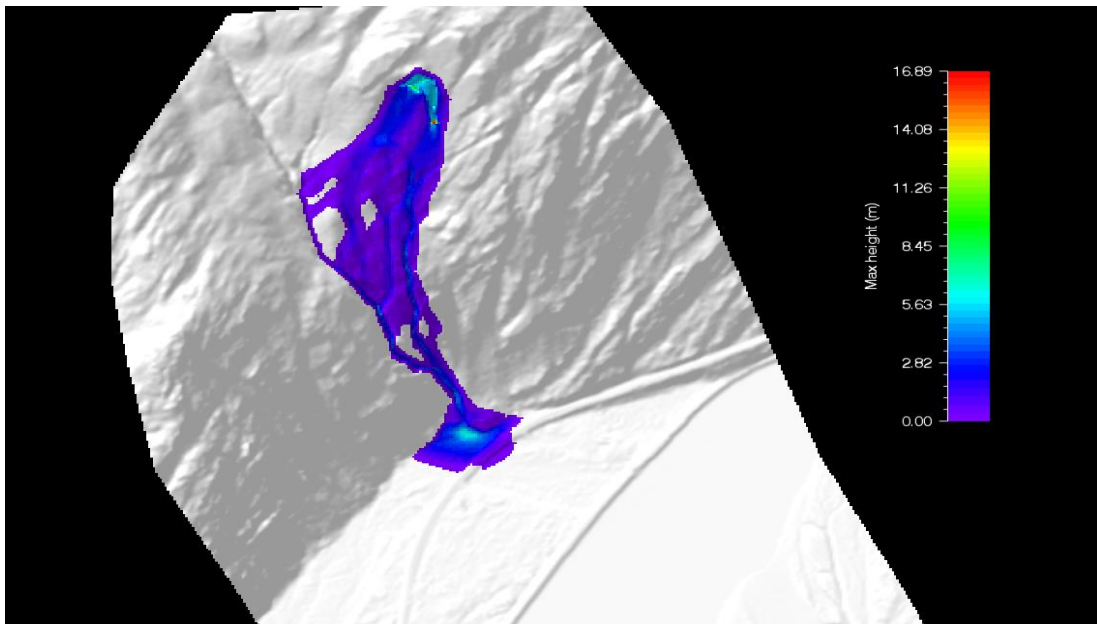
$\mu = 0.05$



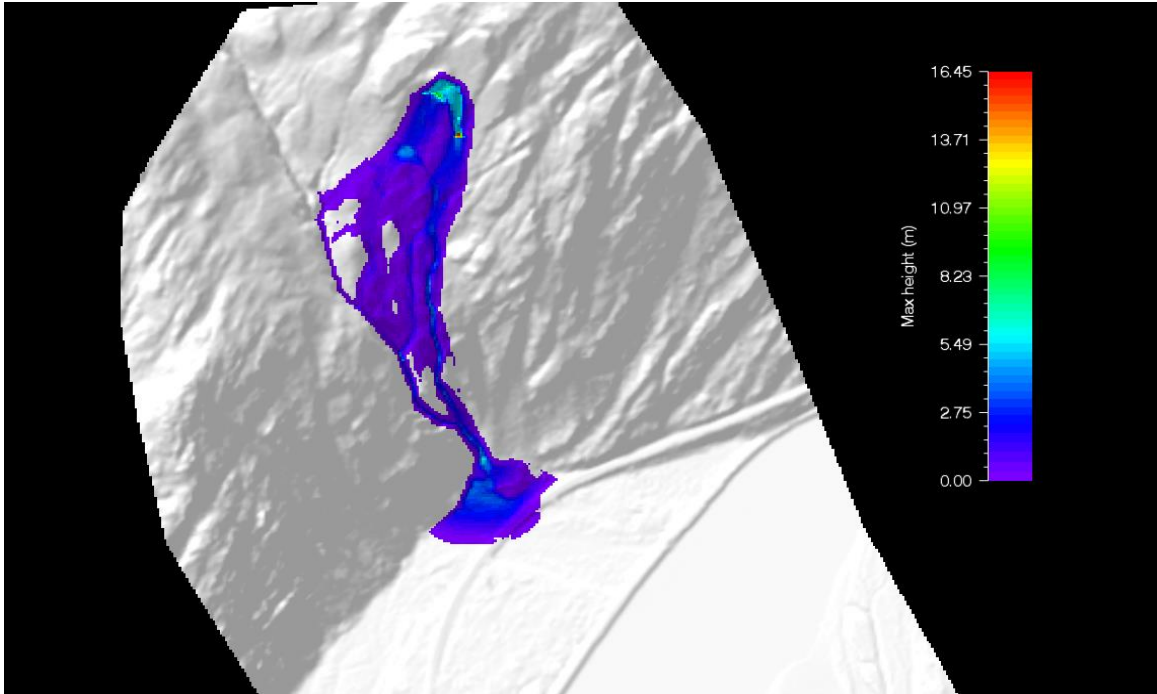
$\mu = 0.08$



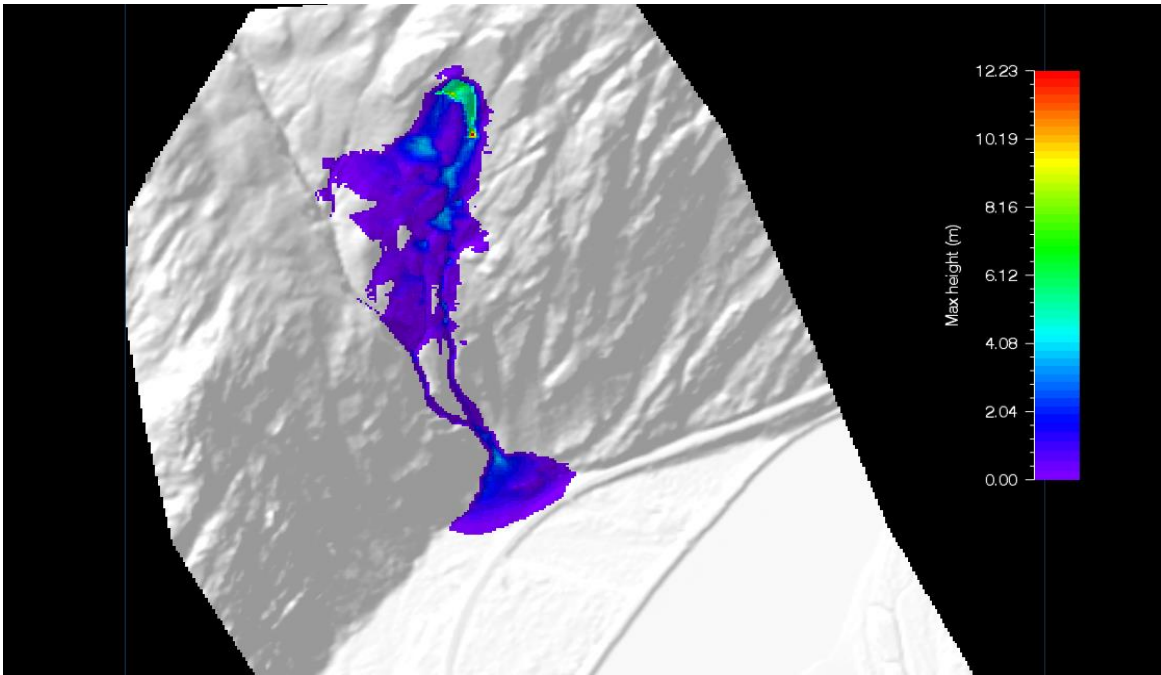
$\mu = 0.15$



$\mu = 0.2$



$\mu = 0.3$



$\mu = 0.5$